The Pennsylvania State University

The Graduate School

College of Medicine

UNDERSTANDING OSTEOGENIC NODULE FORMATION FROM SINGLE EMBRYONIC STEM CELL-DERIVED PROGENITORS

A Thesis in

Genetics

by

Nicole L. Woll

Submitted in Partial Fulfillment
of the Requirements
for the Degree of

Doctor of Philosophy

May 2007

The thesis of Nicole L. Woll was reviewed and approved* by the following:

Sarah K. Bronson
Associate Professor of Cellular and Molecular Physiology
Co-Chair, Intercollege Graduate Degree Program in Genetics
Thesis Advisor
Chair of Committee

Mala R. Chinoy
Professor of Surgery
Director, Lung Development Research Program

Henry J. Donahue
Baker Professor and Vice Chair for Research
Department of Orthopaedics and Rehabilitation
Professor of Cellular and Molecular Physiology
Director, Graduate Program in Cellular and Molecular Biology

Ralph L. Keil
Associate Professor of Biochemistry and Molecular Biology

*Signatures are on file in the Graduate School

ABSTRACT

The process of bone formation can be observed *in vitro* in the form of a mineralized nodule. Mesenchymal stem cells (MSCs), the immediate precursors to osteoprogenitors, are found in the marrow, and likely in numerous other sites throughout the organism. Differentiation of these progenitors, when placed into culture under appropriate conditions, proceeds through characteristic stages of commitment, proliferation, matrix secretion, and mineral deposition during a period of 3-4 weeks. We have developed an embryonic stem cell (ESC)-derived osteogenic culture system. ESCs are allowed to form embryoid bodies (EBs) that are then disrupted after two days and plated as single cells at densities as low as 25 cells/cm^2. By eight days post plating, a significant percentage of the colonies have morphology characteristic of other types of osteogenic cultures. By three weeks in culture, these colonies go on to form layered nodules. Generally 60% of the colonies are layered, mineralized nodules.

This thesis provides three lines of evidence for osteogenesis in these ESC-derived cultures: (i) cell and colony morphology as revealed by phase contrast microscopy, (ii) mineralization of extracellular matrix as revealed by von Kossa staining, and (iii) QRT-PCR analysis of cDNA from entire plates and individual colonies revealing expression of genes characteristic of, and specific for, osteoblasts. For QRT-PCR analysis, we have isolated RNA from entire plates and individual colonies at different stages of the differentiation process to investigate the expression of genes characteristic of the osteoblast lineage, as well as genes characteristic of other lineages and stem/progenitor cells. Analysis of gene expression in the first week revealed that brachyury, *Twist-2*,

Runx2, and *Sox-9* are up-regulated by day 4 of the osteogenic culture, with osterix expression increasing by day 7. *Runx2*, osterix, type I collagen, and *Bglap1*, all important for osteogenesis, are transcriptionally up-regulated by day 14 and continue to increase in expression out to 21 days. QRT-PCR analysis of amplified RNA from individual colonies indicates that it is the morphologically osteogenic colonies that are expressing mRNA characteristic of the osteoblast lineage and allows us to further categorize colonies into hematopoietic, osteogenic, adipogenic, myogenic or a mixture of mesenchymal lineages.

The goal of this project has been to define the timing and molecular basis of commitment in ESC-derived osteogenic cultures. We hypothesize that there is a critical decision point involving mesenchymal lineages that occurs somewhere before day 3 of the osteogenic culture. In order to investigate the commitment of progenitor cells to the osteogenic lineage, we have developed methods permitting overexpression and knockdown of *Runx2* mRNA. Runx2 is a transcription factor necessary for bone formation and is postulated to be the transcriptional switch of osteoblast differentiation. Three methods of inducing *Runx2* expression have been utilized: (i) up-regulation of *Runx2* by bone morphogenetic protein 2 (BMP-2), (ii) constitutive overexpression of *Runx2* constructs, and (iii) tetracycline-inducible overexpression of *Runx2* constructs. For the knockdown of *Runx2* mRNA expression, we have utilized both a constitutive and tetracycline-inducible short hairpin RNA (shRNA) system, which employs components of the pSUPERIOR RNAi System™. The overexpression studies suggest that before cells commit to the osteogenic lineage, overexpression of *Runx2* is detrimental to the osteogenic lineage. The loss-of-functions studies suggest that there is a critical time point

between the ESC and day 2 embryoid body (D2EB), in which induction of shRNA for *Runx2* is also detrimental to osteogenesis.

This method of initiating osteogenesis from murine ESC cultures, where individual EB-derived progenitors are plated at a low density such that the potential and differentiation of a single cell can be determined, is the only described method that allows for the observation and manipulation of the commitment stage of mesengenesis from single murine embryonic progenitors. It also shows great promise for unraveling the mechanisms of commitment to the osteogenic lineage, as well as exploring the therapeutic potential of cells of this lineage.

TABLE OF CONTENTS

LIST OF TABLES

LIST OF FIGURES

LIST OF ABBREVIATIONS

m^7G cap	7-methylguanosine cap
ATF4	activating transcription factor 4
Amp	ampicillin
Agc1	aggrecan
aTc	anhydrotetracycline
BAC	bacterial artificial chromsome
Bglap1	bone gamma carboxyglutamate protein 1 (osteocalcin)
βGP	β-glycerophosphate
bHLH	basic helix-loop-helix
BMP-2	bone morphogenetic protein-2
bp	base pair
Bsp	bone sialoprotein
CCD	cleidocranial dysplasia
CD45	cluster of differentiation 45
CFU	colony forming unit
CMV	cytomegalovirus
CRT	cell replacement therapy
Col1a1	procollagen, type I, alpha 1 (type I collagen)
Col2a1	procollagen, type II, alpha 1 (type II collagen)
Col10a1	procollagen, type X, alpha 1 (type X collagen)
Dex	dexamethasone
DMEM	Dulbecco's Modified Eagle Medium
Dmp1	dentin matrix protein 1
DMSO	dimethyl sulfoxide
Dox	doxycycline
dsRNA	double-stranded RNA
EB	embryoid body
EC	embryonic carcinoma
EDTA	ethylenediaminetetraacetic acid

eIF-4E	eukaryotic initiation factor 4E
ESC	embryonic stem cell
FBS	fetal bovine serum
FGF	fibroblast growth factor
Foxd3	forkhead box D3
GFP	green fluorescent protein
HAT	hypoxanthine-aminopterin-thymidine
hESC	human embryonic stem cell
HLA	human leukocyte antigen
HMG	high mobility group
Hprt	hypoxanthine phosphoribosyltransferase
ICM	inner cell mass
Id	inhibitor of differentiation
Ihh	indian hedgehog
IMEM	Iscove's Modified Eagle Medium
IVS	intervening sequence
JAK	janus-associated tyrosine kinases
kb	kilo base pair
LacZ	β-galactosidase
LB	Luria Bertania
LCR	locus control region
LIF	leukemia inhibitory factor
LIFR	LIF receptor
Lpl	lipoprotein lipase
miRNA	micro RNA
MSC	mesenchymal stem cell or marrow stromal cell
Myh11	smooth muscle myosin 11
NF-κB	nuclear factor κB
Oct-4	octamer binding transcription factor 4
OI	osteogenesis imperfecta
oim	osteogenesis imperfecta mouse

P body	processing body
PBS	phosphate buffered saline
PCR	polymerase chain reaction
Pecam1	platelet endothelial cell adhesion molecule
PEV	position effect variegation
poly A	polyadenylation signal sequence
PTGS	posttranscriptional gene silencing
Ptprc	protein tyrosine phosphatase receptor type C (CD45)
QRT-PCR	quantitative real time – polymerase chain reaction
RANK	receptor activator of nuclear factor κB
RANKL	receptor activator of nuclear factor κB ligand
RISC	RNA-induced silencing complex
RNAi	RNA interference
Rpl7	ribosomal protein L7
RT	reverse transcription
rtTA	reverse tetracycline-responsive transcriptional activator
Runx2	runt related transcription factor 2
SCNT	somatic cell nuclear transfer
shRNA	short hairpin RNA
siRNA	small interfering RNA
Sox	SRY-related HMG box
Sp7	trans-acting transcription factor 7
SRY	sex determining region of Chr Y
SSEA	stage specific embryonic antigens
STAT	signal transducer and activator of transcription
TAE	Tris-acetate-EDTA buffer
TBE	Tris-borate-EDTA buffer
TBBMC	total body bone mineral content
Tet	tetracycline
tetO	tetracycline operon
$TetO_2$	tetracycline operator 2

TetR	tetracycline repressor
TGF-β	transforming growth factor β
TGS	transcriptional gene silencing
TRE	tetracycline responsive element
Vegfa	vascular endothelial growth factor
YAC	yeast artificial chromosome
YFP	yellow fluorescent protein

ACKNOWLEDGEMENTS

I would like to take this opportunity to thank several people who have been instrumental in my graduate career. First, I would like to thank my thesis advisor, Sarah Bronson, for her dedication, support, and encouragement of my graduate work over the past six years. Not only has she helped me develop as a scientist but she has also been a great friend.

I also need to thank the past and present members of the Bronson laboratory. I especially need to thank Jean DeMarco who has made lab an extremely fun place to come everyday and for thinking about science with me, on the rare occasions we decided to do that. I would also like to thank Jason Heaney and Kim Dunham for all their help and support throughout my first several years in the lab; as well as Ashley Rettew who helped out tremendously with the QRT-PCR analysis.

I would like to acknowledge the members of my thesis committee, Mala Chinoy, Hank Donahue, and Ralph Keil, I appreciate all of their time and suggestions throughout my graduate work. Jim Hopper was also a member of my thesis committee until my fifth year when he relocated to Ohio State University but I also want to thank him for his input and support of my research. I also need to thank Chris Niyibizi for his help with the BMP-2 experiments, as well as, Mel Leiby for her careful contributions to the editing of my thesis. Also, a big thank you to the past and present members of the Functional Genomics Core Facilty, Rob Brucklacher, Kevin Finnerty, Dan Krissinger, and Terry Rager, for all their help and support with QRT-PCR. Thank you to the Graduate, Genetics and Physiology office staff for all their efforts and help throughout the past several years.

Finally, I would most like to thank my family for their unconditional love, constant support and encouragement throughout all the ups and downs of graduate school. And especially my husband, Matt, who has given me an incredible amount of support and encouragement not only during graduate school but since I have known him. Without all of you this would not have been possible.

CHAPTER 1

INTRODUCTION

1.1 Development of the Skeleton

1.1.1 Cell Types Found in Bone

The skeleton is the internal support system of all higher vertebrates. It is a complex living tissue in which the extracellular matrix is mineralized. The two tissues that form the skeleton are cartilage and bone. Bone is composed of an organic matrix, of which type I collagen constitutes approximately 95%; the remaining 5% is composed of proteoglycans and numerous noncollagenous proteins (1). Morphologically, there are two types of bone: cortical (compact) and cancellous (spongy). The cortical bone consists of densely packed collagen fibrils, while cancellous bone is loosely organized with a porous matrix. The structural make up of each bone type relates to its function. Cortical bone functions in mechanical and protective roles, and cancellous bone functions in metabolic roles (1). Cartilage and bone each have their own specific cell types: the chondrocyte in cartilage and the osteoblast, osteoclast, osteocyte, and bone lining cells in bone. Each of these cell types has its own differentiation pathways, physiological functions, and associated pathological conditions (2). The osteoblasts, osteoclasts, and bone lining cells are all found on the surface of bone while the osteocytes are found embedded within the mineralized matrix. Osteoblasts, osteocytes, and bone lining cells are derived from a mesenchymal origin, while osteoclasts arise from a hematopoietic origin. Of these cell types the osteoblasts and osteoclasts, which function in bone

formation and resorption, respectively, are the two distinct cell types of bone (3); however, osteocytes and the bone lining cells are both critical components of bone as well.

Osteoblasts are the mature cells of bone and are responsible for the production of the bone matrix (bone formation), as well as regulating the activity of the osteoclast. At the end of the bone forming phase the osteoblast can undergo one of four different fates: (i) become embedded in the bone matrix as an osteocyte, (ii) transform into an inactive osteoblast and line the surface of bone, (iii) undergo apoptosis, or (iv) transdifferentiate into a chondrogenic lineage cell (reviewed in (4)). The morphological characteristics of the osteoblast include a large nucleus, enlarged Golgi apparatus, and a well developed endoplasmic reticulum. The osteoblast secretes type I collagen and the remaining noncollagenous proteins of bone and is highly abundant in alkaline phosphatase. The collagen serves as a template for the initiation of mineralization within the bone. The osteoblast has been referred to as a sophisticated fibroblast because it is morphologically very similar and both cell types express the same genes with the exception of a couple of osteoblast-specific genes (1,3,5).

Osteoclasts are multinucleated cells responsible for the resorption of bone, and yet at the same time play a critical role in the normal development of bone. As reviewed by Li et al. and Marks et al. (1,6), osteoclasts are derived from hematopoietic progenitor cells in the bone marrow, which are deposited at sites of bone resorption where they proliferate and differentiate into osteoclasts. This process is regulated by three independent signal transduction pathways, the cAMP-mediated pathway, the gp130-mediated pathway, and the 1α25(OH2)D3-receptor-mediated pathway. The

differentiation of osteoclasts is regulated by osteoblasts, stromal cells, and bone. Osteoclast precursors express receptor activator of nuclear factor κB (NF-κB) (RANK) and upon binding to its ligand (RANKL), which is expressed by osteoblasts and stromal cells, initiate the differentiation of osteoclasts. Morphologically, osteoclasts are very large cells (about 50 – 100 μm in diameter), and contain anywhere from 6 – 100 nuclei. They have a high density of mitochondria, numerous lysosomes, and free ribosomes. Osteoclasts contain two plasma membrane areas that are in direct contact with the mineralized areas of bone: a ruffled border and a sealing zone or clear zone. The ruffled border is the area of the plasma membrane where resorption takes place, while the sealing zone is the area of the plasma membrane that surrounds the ruffled border and serves to attach the osteoclast to the bone matrix. Through bone resorption, the osteoclasts act to regulate extracellular calcium concentrations; in turn, the extracellular and intracellular calcium levels regulate osteoclast activity (1,6).

The osteocyte is the terminally differentiated or mature osteoblast that secretes non-mineralized bone matrix, the osteoid, and is found within the bone matrix. Even though, it is the most abundant cell type of bone, the understanding of the osteocyte is far behind that of the osteoblast and osteoclast. The mechanism of osteoblast to osteocyte transition is not well understood, although, several models have been proposed as to the manner in which osteoblasts become buried within the mineralized matrix (4). The osteocyte location within the bone suggests that they may play more of a role in bone development than once thought. They are spaced regularly throughout the bone matrix and found within individual lacunae, which are minute cavities within bone. Their morphology is stellate and they are connected by slender cell processes (7). The

osteocyte is derived from the osteoblast and transforms from a motile osteoblast to an embedded osteocyte in about three days. It is during this time that the rounded morphology of the osteoblast changes to a more stellate shape (7,8). They communicate with neighboring cells, osteoblasts, and bone lining cells through gap junctions (9-12), suggesting a role in supplying nutrients and signals to these other cells. It has also been suggested that the osteocyte modulates signals from mechanical loading by translating mechanical strain into biochemical signals. This in turn may dictate formation and resorption of bone, allowing for the body's proper response to mechanical loads (9).

The bone lining cells are inactive, flat, elongated cells that cover the surface of bone. The bone lining cells are part of neither bone formation nor resorption. The actual function of these cells is not well understood, but it has been suggested that they are both a precursor to the osteoblast (1) as well as a cell fate of the osteoblast (4,13). It has been suggested that bone lining cells secrete collagenase to remove an unmineralized collagen layer that covers the surface of bone and prevents osteoclasts from attaching (13). It has also been suggested that osteoclasts target a certain location on the surface of bone for resorption based on a signal given by bone lining cells that have received their cues from osteocytes (13).

1.1.2 Overview of Bone Formation

The bones of the mammalian skeleton have three distinct origins (paraxial mesoderm, lateral plate mesoderm, and neural crest) and undergo two distinct methods of bone formation (intramembranous and endochondral) (reviewed in (14)). Intramembranous bone formation occurs through a direct differentiation into osteoblasts,

while endochondral bone formation begins with a cartilage template. This is all part of the process of skeletogenesis, which occurs in four phases: migration of pre-skeletal cells to the site of future bone formation, the interaction of these cells with the epithelium, condensation, and differentiation to osteoblasts or chondroblasts (15). Figure 1.1 depicts both intramembranous and endochondral bone formation.

Several signaling molecules play important roles in the development of the skeleton, including members of the bone morphogenetic protein (BMP) family, the transforming growth factor β (TGF-β) superfamily, fibroblast growth factors (FGFs), members of the Wnt family of secreted factors, and members of the hedgehog family (16). The decision of mesenchymal cells to become osteoblasts or chondrocytes is regulated by canonical Wnt signaling. Wnt cytokines bind to Frizzled receptors and Lrp5/6 co-receptors preventing the degradation of β-catenin in the cytoplasm. β-catenin is therefore able to enter the cell nucleus and up-regulate or down-regulate specific transcription factors implicated in bone development. During intramembranous bone formation, there is a high level of β-catenin in mesenchymal cells, which induces the transcription of genes required for the differentiation of osteoblasts and inhibits transcription of genes necessary for the differentiation of chondrocytes (reviewed in (17)). The necessity of β-catenin in determining the osteogenic or chondrogenic cell fate of mesenchymal precursors was shown in studies in which β-catenin was inactivated in the limb and head mesenchymal cells. Osteoblast precursors that have inactivated β-catenin do not differentiate into osteoblasts but instead form chondrocytes (18). It was also shown that ectopic expression of β-catenin led to enhanced osteoblast formation and suppression of the chondrocyte lineage (19).

1.1.3 Intramembranous Bone Formation

Intramembranous bone formation occurs through a process in which mesenchymal cells condense and directly differentiate into osteoblasts. Bones formed intramembranously are mainly derived from ectodermal neural crest cells and give rise to the flat bones of the cranial vault, which include the cranial suture lines, some facial bones, and parts of the mandible and clavicle. Intramembranous bone formation also gives rise to the bone within the periosteum on the outer surface of long bones (14,15,17). Within the mesenchymal condensations where intramembranous bone formation occurs, there is a high density of blood vessels. As the bone forms and begins to grow, the formation and development of blood vessels, also known as angiogenesis (20), is an integral part of the process (Fig. 1.1A) (17).

1.1.4 Endochondral Bone Formation

Endochondral bone formation occurs through a process in which a cartilage template is formed from mesenchymal condensations and then replaced by bone. Bones formed through endochondral formation are mainly derived from paraxial mesoderm and lateral plate mesoderm, which give rise to the axial and appendicular skeleton, respectively (14). During the process of endochondral bone formation, mesenchymal cells condense where a future skeleton is to form and begin to take its future shape. The cells in the center of the condensation differentiate into chondrocytes and begin to express markers of cartilage such as type II collagen, type IX collagen, type XI collagen, aggrecan, chondromodulin-1, and matrilin-3. The cells on the outer edges of the condensation differentiate into fibroblast-like perichondrial cells while the chondrocytes

in the center of the condensation stop proliferating and become hypertrophic (enlarge). These cells then mineralize the surrounding matrix and undergo apoptosis as vascularized tissue invades. The vascularized tissue brings osteoblasts that deposit bone matrix onto the cartilaginous matrix that has been degraded, and this forms the primary spongiosa, which then forms trabecular bone. The perichondrial cells on the outer edges of the condensation differentiate into osteoblasts and form the bone collar, which gives rise to the cortical bone (Fig.1.1B) (reviewed in (14)). The interactions of the cartilage, perichondrium, and invading vasculature are controlled by secreted and intercellular factors, many of which have already been identified and probably some which are yet to be discovered (14).

1.1.5 Transcriptional Control of Bone Formation

One of the most critical transcription factors induced during osteogenic differentiation is *Runx2* (runt related transcription factor 2), also known as *Cbfa1* or *Osf2*. *Runx2* is a member of the Runt domain family of transcription factors that activate or repress the transcription of genes by binding to the DNA sequence TGPyGGTPy. It is required for mesenchymal condensations, osteoblast differentiation from mesenchymal stem cells, chondrocyte hypertrophy, and vascular invasion of developing skeletons (21). Ducy and Karsenty first identified an osteoblast-specific cis-acting element, termed OSE2, in the promoter of the osteocalcin gene (*Bglap1*), the most abundant noncollagenous protein of bone found exclusively in osteoblasts (22-25). This element was named Osf2/Cbfa1 and later named Runx2. In 1997, Cell published three articles that support the role of Runx2 in osteogenesis (26-28). Ducy et al. showed that the

expression of *Runx2* occurs early during skeletal development and that it is restricted to cells of the mesenchymal condensations and the osteoblast lineage, regardless of embryonic origin or mechanism of bone formation (intramembranous or endochondral) (27). It was also shown that there were OSE2-like elements in the promoter of several other genes and that Runx2 affects the expression of these genes expressed in osteoblasts, including osteocalcin (*Bglap1*), type I collagen (*Col1a1*), bone sialoprotein (*Bsp*) and osteopontin (27). Otto et al. generated *Runx2*-deficient mice and showed that homozygous mutant mice die after birth due to respiratory failure. Analysis of the skeletons through Alcian blue and Alizarin red staining, which stain for cartilage and calcified tissue (bone), respectively, showed an almost complete lack of mineralized bone but unaffected cartilage formation. The heterozygous mice display hypoplasia of the clavicles and a delay in development of intramembranous bones. These defects are also observed in a heritable human skeletal disorder known as cleidocranial dysplasia (CCD) (26). In the same issue of Cell, Komori et al. also showed that mice with a homozygous deletion of *Runx2* die just after birth due to respiratory failure. They also showed that homozygous mutant mice completely lacked bone formation in the skeleton as well as vascular or mesenchymal invasion of the cartilage (28). These three articles (26-28) provided indisputable evidence that *Runx2* is an essential transcription factor required for the differentiation of the osteoblast lineage in both intramembranous and endochondral bone formation, but whether or not *Runx2* is sufficient to drive osteogenic differentiation remains to be determined.

Since Runx2 plays such a pivatol role in osteogenesis, it is worth examining some of the structural and functional features of this gene (reviewed by Shroeder et al. (21)).

The Runx2 gene encodes several different transcripts that arise from two promoters and alternative splicing. The two promoters, termed P1 (distal) and P2 (proximal), initiate expression of the two major isoforms of *Runx2*, type II and type I, respectively. The type I isoform gives rise to a product of 513 amino acid residues that begins with the protein sequence MRIPV. This isoform has been shown to be expressed in nonosseous mesenchymal tissues and in osteoblast precursors at a consistent level throughout osteoblast differentiation (29). The type II isoform gives rise to a product of 528 amino acid residues that begins with the protein sequence MASNS. The expression of the type II transcript was shown to increase during differentiation of primary osteoblasts and is induced in osteoprogenitors and in premyoblast cells C2C12 in response to bone morphogenetic protein 2 (BMP-2), a polypeptide that plays a role in the development of bone and cartilage (29). In transgenic mice expressing *lacZ* under the control of the P1 promoter, type II isoform expression was detected in mesenchymal condensations and mature chondrocytes and restricted to the axial skeleton (30). Mice engineered to contain a targeted deletion of the *Runx2* II isoform, showed defects in endochondral bone formation but not to the extent found in *Runx2* null mice (31). These experiments suggest that *Runx2* isoform I is sufficient for early osteogenesis and intramembranous bone formation while *Runx2* isoform II is necessary for complete osteoblast maturation and endochondral bone formation (21). Interestingly, *Runx2* has also been shown to autoregulate in part by negative feedback of its own promoter to stringently regulate bone formation (32).

The only other osteoblast specific transcription factor shown to be downstream of *Runx2* is osterix (*Sp7*). This novel zinc finger-containing transcription factor belongs to

the Sp/XKLF family and was identified in 2002 by Nakashima et al. (33). Transfection of osterix into C2C12 myoblasts resulted in an induction of osteocalcin and type I collagen, and in C3H10T1/2 mesenchymal cells there was an induction of osteocalcin RNA, demonstrating that osterix could induce typical osteoblast genes (33). In stably transfected NIH3T3 fibroblasts, osterix was able to induce expression of osteopontin but not other bone-related markers, including type I collagen, alkaline phosphatase, osteocalcin, and osteonectin (34). This suggests that osterix is not sufficient to direct osteogenic lineage commitment in all cell lines. In osterix null mice, normal cartilage developed but there was a complete lack of bone formation in intramembranous and endochondral skeletal elements, and they died shortly after birth of respiratory failure, similar to *Runx2* knockout mice (33). The heterozygous mutant mice were normal and fertile. There is expression of *Runx2* in the osterix null mouse as well as hypertrophic chondrocytes, but osterix is not detected in *Runx2* deficient mice, suggesting that osterix is downstream of *Runx2* expression in the pathway of osteogenesis (16,33).

While the *Runx2* and osterix deficient mice are similar in that neither have osteoblast differentiation or intramembranous or endochondral bone formation, they do have some phenotypic differences. The *Runx2* null mice have a thin layer of mesenchyme in the periosteum, while the osterix null mice have an abundant mesenchyme. *Runx2* null mice do not display invasion of the cartilage matrix by osteoclasts and hypertrophic chondrocyte differentiation is inhibited, while osterix null mice do have invasion by osteoclasts and no inhibition of hypertrophic chondrocytes (16). These phenotypic characteristics of osterix as well as the fact that cells in the mesenchyme of osterix null mice express genes characteristic of chondrocytes (*Sox-9*,

Sox5, *Col2a1* and *Ihh*) suggests that osterix null cells may undergo a cell fate change (16). This also leads to the notion that osteoblasts and chondrocytes are derived from the same bipotential progenitor (16).

Sox-9 is one of the key transcription factors that may play a role in the commitment of cells to the osteoblast or chondrocyte lineages and has recently been shown to be a marker of an osteo-chondroprogenitor. Sox-9 is a high mobility group (HMG) domain transcription factor and is a member of the family of proteins that includes the mammalian Y-linked testis-determining factor SRY (35). *Sox-9* expression is found in mesenchymal condensations before and during chondrogenesis and in differentiated chondrocytes but not in hypertrophic chondrocytes. It is also found in other tissues as well, including the central nervous system, otocysts, heart, testis, and vibrissae (35,36). The expression of *Sox-9* coincides with the expression of type II collagen (*Col2a1*), a known marker of chondrocyte differentiation, in chondrocytic cells suggesting a critical role for Sox-9 in chondrogenesis (37). *Sox-9* heterozygous mutant mice die perinatally from a phenotype that closely resembles the severe skeletal dysmorphology syndrome campomelic dysplasia (38). *Sox-9* was shown to be a regulator of the chondrocyte lineage and required for cartilage formation in *Sox-9* null ESCs (39). Chimeric mice generated with the *Sox-9* null ESCs showed no contribution of the null ESCs to cartilage formation and could not express chondrocyte-specific markers, implicating *Sox-9* as an initiator of chondrogenesis (39). Interestingly, use of the Cre-loxP system to inactivate *Sox-9* expression before chondrogenic mesenchymal condensations have formed results in the absence of cartilage and the osteoblast lineage, as well as *Runx2* expression. This suggests that *Sox-9* is needed to establish osteo-

chondroprogenitor cells that can produce both chondrocytes and osteoblasts (40). Most recently this hypothesis was proven using mice in which a β-galactosidase (LacZ) reporter was activated by a Cre recombinase gene inserted into the 3′ untranslated region of the Sox-9 gene. Cell fate mapping revealed that *Sox-9* expressing limb bud mesenchymal cells gave rise to both chondrocytes and osteoblasts and showed that *Sox-9* is expressed before *Runx2* in the developing skeleton (41).

Twist-1 and Twist-2, previously known as Twist and Dermo-1, respectively, are two members of the basic helix-loop-helix (bHLH) family of transcription factors that are involved in bone formation. *Twist-1* null mice are embryonic lethal and have cranial neural tube defects. These mice also have defects in head mesenchyme, somites, and limb buds (42). *Twist-2* null mice show enhanced proinflammatory cytokine gene expression in multiple tissues. *Twist-1* and *Twist-2* compound heterozygotes recapitulate this phenotype, suggesting redundancy and dose dependence of these genes (43). *Twist-1* heterozygous mice exhibit skull and limb defects including craniosynostosis, which presents as increased bone formation in the cranial sutures (44). This same phenotype is seen in Saethre-Chotzen patients who are also heterozygous for *Twist-1* (44-46). This suggests that the Twist proteins are playing an inhibitory role in osteoblast differentiation by blocking Runx2 (47). This hypothesis by Karsenty et al. was proposed and proven in studies that showed the Twist proteins transiently inhibited Runx2 function during skeletogenesis. It was shown that *Twist-1* and *Twist-2* are expressed in *Runx2* expressing cells during early development, but osteoblast specific gene expression was not seen until the expression of *Twist-1* and *Twist-2* decreased. *Twist-1* was also shown to inhibit osteoblast differentiation without affecting *Runx2* expression, suggesting that the

inhibitory role of Twist proteins was on Runx2 function and not *Runx2* expression. This was proven by interaction studies of Twist-1 and Runx2, which showed that the Twist box of Twist proteins could bind to the Runx2 DNA binding domain (Runt domain) and inhibit its transactivation abilities (47).

There are other transcription factors that have been shown to function during bone formation, such as activating transcription factor 4 (ATF4). The targeted disruption of ATF4, also known as c-AMP response element protein 2, RAXREB67, mTR67, or C/ATF, was shown to result in perinatal lethality, dwarfism, and severe osteoporosis (48,49). However, Runx2, osterix, Sox-9, Twist-1, and Twist-2, have stood out as key players during osteogenesis both *in vitro* and *in vivo* and will be investigated in this thesis. Their expression patterns and loss-of-function and gain-of-function phenotypes are summarized in Table 1.1. Table 1.2 highlights other transcription factors that regulate bone formation.

1.2 Embryonic Stem Cells (ESCs)

1.2.1 Origins of ESCs

During mammalian development, the first differentiation event occurs when the outer morula cells compact to form the extraembryonic epithelial layer, or trophectoderm, which is required for uterine implantation. The inner part of the morula develops into the inner cell mass (ICM) of the blastocyst and contains the progenitor cells of the embryo proper. The ICM, prior to implantation, splits into two cell lineages: the epiblast (primitive/embryonic ectoderm), which will eventually form the three somatic germ layers (endoderm, ectoderm, and mesoderm) and primordial germ cells, and the hypoblast (primitive/embryonic endoderm), which will generate the two extraembryonic lineages, the visceral and parietal endoderm (Figure 1.2) (50,51). Embryonic stem cell (ESC) lines are derived from the ICM and are considered the "immortal" *ex vivo* counterpart of early embryo stem cells (52). The derivation of pluripotent cells from the mouse embryo was first established in 1981 by Evans and Kaufman, followed by groundwork accomplished on embryonic carcinoma (EC) cells (51,53,54). Up until this point it was known that pluripotent cells in the mouse embryo could form chimaeric animals as well as teratocarcinomas. Evans and Kaufman were able to establish pluripotent cell lines isolated directly from the mouse blastocyst and further differentiate these cells into tumors either *in vitro* or *in vivo*, while maintaining normal karyotypes (53). These cells were maintained by co-culture with mouse embryonic feeder cells. They, along with other colleagues, went on to demonstrate that these cell lines were capable of forming functional germ-line chimaeras (55).

In 1997, a generic technique for establishing ESC lines from the mouse with 100% efficiency was described (56). The following year, human blastocyst-derived pluripotent cell lines were isolated, resulting in the first derivation of human embryonic stem cells (hESC) (57). These cell lines had normal karyotypes and expressed markers characteristic of primate embryonic stem cells. The authors proposed the essential characteristics of hESCs, based on mouse ESCs and primate ESCs, including (i) derivation from the preimplantation or periimplantation embryo, (ii) prolonged proliferation in the absence of differentiation, and (iii) stable developmental potential to form derivatives of all three embryonic germ layers even after prolonged culture (57,58). This finding dramatically increased the interest in ESCs and their use in cell based therapies; however, due to ethical and political reasons, the use of hESCs is limited both by availability and the ability to implement the cells. For example, hESCs cannot be tested for their ability to contribute to the germ line in chimaeras, which still leaves murine ESCs and nonhuman primate ESCs as valuable tools for the study of tissue differentiation *in vitro*, as well as proof of concept for use in cell based therapies for future use in humans.

While murine ESCs are able to shed light on hESCs and their potential therapeutic applications due to their similarities, there are also differences between these two types of ESCs. They are morphologically distinct in that murine ESCs are tight, rounded clumps in which individual cells cannot be determined, while hESCs form flatter, less compact colonies. Both ESCs express several common markers such as Oct-4 and Nanog but differ in expression of stage-specific embryonic antigens (SSEA), specifically SSEA-1, 3 and, 4. hESCs express SSEA-3 and 4 when undifferentiated and

SSEA-1 as they differentiate, the reverse of what is seen in murine ESCs. Murine ESCs and hESCs also differ in their dependence on leukemia inhibitory factor (LIF). hESCs do not require LIF, a key factor in maintaining self-renewal of murine ESC cultures, but instead require a feeder layer of cells in the presence of basic fibroblast growth factor (bFGF) or conditioned medium (reviewed in (54) and (57)).

1.2.2 Properties of ESCs: Self-Renewal

There are two properties that generally define a "stem cell": the ability to self-renew without undergoing senescence and the ability to differentiate into all cell types of the developing embryo. These properties make stem cells distinct from progenitor or precursor cells, which are derived from stem cells but represent intermediates in the process of differentiation. When mouse ESCs were initially established, they were maintained by co-culture with mouse embryonic feeder cells. Subsequent studies identified LIF as one of the pivatol factors in maintaining mouse ESCs in an undifferentiated state (51,59-61). LIF can be provided by a feeder layer of embryonic fibroblasts and/or a recombinant protein. LIF engages in a heterodimeric receptor complex consisting of two related cytokine receptors, LIF receptor (LIFR) and gp130 (62). This complex activates associated Janus-associated tyrosine kinases (JAK) that phosphorylate the receptor chains. The signal transducer and activator of transcription (STAT) family of transcription factors bind receptor phosphotyrosines and are key substrates for JAKs. Phosphorylation of STATs promotes their dimerization, triggering their translocation to the nucleus and binding of target sites on DNA. In ESCs, LIF predominantly activates Stat3 (63). Stat3 acts as a transcription factor to activate target

genes, which include essential genes to maintain a pluripotent cell phenotype. It has also been shown that bone morphogenetic proteins (BMPs), in particular BMP-4, play a role in the maintenance of embryonic stem cell self-renewal in collaboration with Stat3 (64). It was shown that in the presence of BMP-4 and LIF, murine ESC cultures could maintain self-renewal and multilineage potential in the absence of feeders or serum. BMPs induce expression of Inhibitor of Differentiation (Id) genes via the SMAD pathway to maintain ESC self-renewal.

There are three key transcriptional regulators in the maintenance of self-renewal of ESCs: Oct-4, Sox-2, and Nanog (65). Oct-4 (octamer binding transcription factor 4) is a mammalian POU domain transcription factor expressed in early embryo germ cells (66-68). The precise level of *Oct-4* governs three cell fates (67,69). ES cells require a critical level of *Oct-4* to maintain stem cell renewal, but less than a two-fold increase causes differentiation into the primitive endoderm and mesoderm, whereas a reduction to less than 50% of the normal expression level triggers dedifferentiation into the trophectoderm. Therefore, it is thought that Oct-4 is a candidate for the master regulator of initiation, maintenance, and differentiation of pluripotent cells. Oct-4 is able to regulate gene expression by interacting with other factors such as Sox-2. Sox-2 is a member of the SOX (SRY-related HMG box) gene family that encodes transcription factors with a single HMG DNA-binding domain. *Sox-2* is required for the development of the epiblast and extraembryonic ectoderm, as shown by the targeted disruption of *Sox-2* (70). Although Sox-2 plays an important role in the maintenance of pluripotency, its expression is not restricted to pluripotent cells (65). The most recently identified transcription factor involved in the maintenance of self-renewal is Nanog. Nanog is a

divergent homeobox transcription factor expressed in the inner cells of a compacted morula and blastocyst and germ cells during early mouse development (71,72). The loss of function of *Nanog* causes cells to differentiate into the primitive endoderm, while the overexpression of *Nanog* promotes self-renewal independently of LIF (65,71,72). These studies indicate Oct-4, Sox-2, and Nanog as critical regulators in the maintenance of stem cell self-renewal and early cell fate decisions.

1.2.3 Properties of ESCs: Pluripotency

The ability of stem cells to differentiate into different cell types is described in terms of their potential or plasticity. Stem cells exhibit varying degrees of potential that range from totipotency to unipotentiality. Totipotent cells maintain the ability to develop into all cell types and are found in blastomeres of the early morula, but these cells have not been shown to proliferate indefinitely. Pluripotent cells are typically defined as cells destined for the inner cell mass (ICM) or the trophectoderm lineage and maintain the ability to differentiate into all cells of the embryonic germ layers. Multipotent cells usually refer to adult, or somatic, stem cells that are capable of self-renewal and have the ability to differentiate into multiple cell types of the same tissue or organ. Their role is to replenish or replace mature, damaged, or diseased cells (reviewed in (54)).

When stem cells are removed from the factors that maintain their pluripotency, they will begin to differentiate and, under appropriate conditions, generate cell lineages of the three embryonic germ layers, mesoderm, ectoderm and endoderm (51). There are three general approaches used to initiate ESC differentiation (reviewed in (51)). The first is to allow the cells to aggregate and form embryoid bodies (EBs) (73), the second is to

culture the ESCs directly on stromal cells (74), and the third is to differentiate ESCs on a monolayer of extracellular proteins (75). These three differentiation methods have been used to generate a wide spectrum of cell types from murine ESCs, including smooth muscle, adipocytes, osteoblasts, chondrocytes, keratinocytes, neurons, and oligodendrocytes, to name a few (Table 1.3) (52). Of particular interest is the differentiation of mouse ESCs into osteoblasts and this will be discussed in more detail in section 1.3.

1.2.4 Therapeutic Potential of ESCs

ESCs have begun to revolutionize the field of developmental biology as a tool to understand the molecular mechanisms occurring during the process of differentiation of cell lineages. The properties of ESCs make them an appropriate and attractive candidate for use in cell replacement therapy (CRT) of degenerative disorders, such as myocardial infarction, heart disease, Parkinson's disease, Alzheimer's, and bone related disorders. However, the use of CRT to restore respective organs to their normal function is still in its infancy, which further supports the need for more research and clinical trials. The idea of CRT, which is to replace abnormal cells in a tissue with cells of normal function, is anticipated to have a better efficiency than current methods for treating these disorders. If the proper stimuli can be added to stem cells to direct their differentiation into the desired cell lineage, they could be used in a therapy for almost any tissue (76). However, for this type of therapy to advance to the next level, more research needs to be done on both mouse and human ESC differentiation. Additionally, several issues need to be addressed. One issue or obstacle to overcome is to understand the type and number of

cells that need to be transplanted as different cell lineages may require a different stage of maturation as well as a different number of cells to be transplanted. Another critical issue is the possibility of tumor formation from undifferentiated ESCs being transplanted into the recipient. Understanding the stage of maturation needed for a specific application, as well as a technique to isolate this replacement cell, should help in reducing the number of undifferentiated ESCs that are transplanted. A third obstacle to overcome is the possibility of immune rejection once the cells are transplanted. One technique to overcome this obstacle is to use somatic cell nuclear transfer (SCNT) in which the cells used for transplantation are genetically identical to the patient. However, there are ethical limitations to this procedure because it requires the use of oocytes and blastula creation could lead to human reproductive cloning (51,76). Despite the problems that can be encountered with CRT the potential remains and research continues to move forward in pursuit of this therapy.

ESCs are also beginning to be used in the area of drug discovery and drug development. The use of ESCs has the potential to shorten the timeline for the identification of new therapeutics, as well as reduce the amount of *in vivo* testing that is required. The development of genetically modified mice has been extremely valuable because genes can be inactivated in these mice, and drug target function, selectivity, and toxicity can be determined based on the inactivated gene and its corresponding phenotype. As well as inactivation in mouse models, there is the technique of introducing reporters to identify specific populations of ESCs derived by their unique gene expression. These ESCs could then be used in screens to identify molecules or drugs that promote maturation or the function of a specific lineage. Also, many

genetically modified ESCs mimic the phenotype seen in human disorders or diseases and drug discovery tools can be used to develop drugs to treat those diseases (51,77). The therapeutic potential of ESCs in the treatment of degenerative disorders and diseases has generated a great deal of excitement in the field of stem cell research; however, the application of this technology is still in its infancy. This further supports the need for research of *in vitro* differentiation culture systems in both mouse and human ESCs.

1.3 Stem Cells and Osteoblast Formation

1.3.1 Mesenchymal Stem Cells (MSCs) and Osteoblast Formation

Mesenchymal stem cells, or marrow stromal cells, (MSCs) are multipotent adult stem cells found within the bone marrow that have the potential to differentiate into a number of mesenchymal cell types, including fibroblasts, chondrocytes, adipocytes, and osteoblasts (Figure 1.3). MSCs are also found in cord blood, placenta, amniotic fluid, heart, skeletal muscle, adipose tissue, synovial tissue, and pancreas, but the bone marrow is the best characterized source of MSCs (reviewed in (78)). The nomenclature for MSCs has changed considerably since their first identification. They have been referred to as connective tissue stem cells, stromal stem cells, and stromal fibroblastic stem cells, but the favored term is mesenchymal stem cells (79). In 1867, Julius Cohnheim studied wound repair in mammals and suggested that the cells appearing at the site of the wounds were coming from the bloodstream, and by inference, the bone marrow (referenced in (78,80); original article in German). Friedenstein et al. were the first to describe stromal cells in the bone marrow that had proliferative capacity *in vitro* and the ability to form bone when transplanted *in vivo* in diffusion chambers (78,79,81). They demonstrated that these cells could arise from single colony forming units, colony forming unit-fibroblast (CFU-F) (reviewed in (78,79)). Over the next several years, it was demonstrated that the cells isolated using Friedenstein's technique (discarding cells that were nonadherent) were capable of differentiating into several different cell types, including osteoblasts, chondroblasts, adipocytes, and even myoblasts (reviewed in (80)). However, there has been evidence to suggest that the CFU-F is heterogeneous in size, morphology, and

potential to differentiate into different lineages. As a result of this heterogeneity in MSCs, it has been difficult to directly identify these cells using surface markers. Some progress has been made, and several surface markers such as STR0-1, HOP-26 (CD63), CD49a, and SB10/CD166 have been suggested for human marrow stromal cells (82). However, there are no unique molecular probes able to unequivocally identify these cells. Therefore, the definition of an MSC is still largely based on their isolation from bone marrow, adherence to plastic in culture, and ability to differentiate into multiple mesodermal tissue lineages.

The *in vitro* differentiation of MSCs into osteoblasts has been studied extensively in many animal models, including mouse and human. The effects of several different hormones, vitamins, growth factors, and cytokines on MSC proliferation and differentiation have been studied, including estrogen, conditioned medium, and BMP-2 (78). In particular, the medium in which MSCs differentiate into osteoblasts has been shown to be optimal when dexamethasone (Dex), ascorbic acid, and β-glycerophosphate (βGP) are added. This process of differentiation has been categorized into three different events: (i) proliferation, (ii) deposition of the matrix, and (iii) mineralization; with characteristic gene expression changes occurring at each stage (79). These changes in expression, with regard to the stages of osteoblast proliferation and differentiation, are complex and depend upon the interrelationship between growth control and expression or suppression of tissue-specific genes (83). During the proliferation stage, histones and protooncogenes, such as c-fos and c-myc, as well as certain cyclins, including cyclins B and E, are up-regulated (79,83). Characteristic osteoblast-associated genes, including type I collagen, alkaline phosphatase, osteopontin, osteocalcin, and bone sialoprotein, are up-

regulated during the stages of matrix deposition, maturation, and mineralization (79,83). Jane Aubin and James Triffitt have summarized this progression of gene expression in a chapter in *Principles of Bone Biology*, and based on the expression patterns of different markers both *in vivo* and *in vitro*, they suggest that osteoblast differentiation progresses through seven transitional stages as opposed to the three stages listed above (79). The markers used to characterize this progression are grouped into transcription factors, surface markers, enzymes, collagenous and non-collagenous proteins, factors, receptors, and adhesion molecules. The seven stages they outline in Figure 2 of this chapter display decreasing proliferative capacity and increasing differentiation of MSCs and include a multipotential progenitor, immature osteoprogenitor, mature osteoprogenitor, preosteoblast, mature osteoblast, and osteocyte (79).

There is also the concept that there is heterogeneity in the expression patterns that characterize osteoblast development and differentiation (79). In this same chapter of *Principles of Bone Biology*, this heterogeneity is discussed. Some of the possibilities that may reflect these variations in gene expression include inherent differences in populations, i.e., different mixtures of more or less primitive progenitors and more mature cells. It is also possible that this heterogeneity is a reflection of developmental events in different osteoblasts. For example, different cells may be undergoing different stages in the progression of proliferation, matrix secretion, and mineralization. While the exact cause of this heterogeneity is not known, it is important to appreciate that this heterogeneity exists in osteogenesis both *in vitro* and *in vivo* (reviewed in (79)).

Since MSCs are multipotent and can be expanded in culture to increase their numbers, there has been a lot of interest in their use therapeutically. In particular, MSCs

have the potential to be used in tissue regeneration. Of specific interest is the use of MSCs in the treatment of an inherited bone disease called osteogenesis imperfecta (OI), or brittle-bone disease, in which the patient's bones are extremely fragile and break easily. The use of MSCs to treat this disease has been met with limited success and will be discussed in greater detail in the Chapter 6 Discussion. Briefly, there are some major limitations to the use of MSCs in the healing of bone defects. These include the need for a relatively high numbers of cells, that are found at a relatively low frequency in the bone marrow (reviewed in (78)), as well as a finite capacity for self-renewal (84). As a result, there is still the need to develop alternative cell sources for therapy, and the use of ESCs for the differentiation of osteoblasts may prove to be a useful therapeutic avenue.

1.3.2 ESCs and Osteoblast Formation: *In Vitro* Culture Systems (Mouse and Human)

In the 1980's researchers interested in the field of bone biology began to focus on isolating osteoblasts that would retain the specific function of bone forming cells in culture, specifically the ability to form a type I collagen matrix (85). The ability to mimic bone formation *in vitro* is now a valuable tool for understanding bone formation biochemically, hormonally, and transcriptionally. The process of bone formation can be observed *in vitro* in the form of a mineralized nodule. In one of the first *in vitro* culture systems able to support the formation of mineralized nodules, single-cell suspensions from enzymatic digestions of fetal rat calvaria (skull bone) were grown long-term in culture in the presence of ascorbic acid, β-glycerophosphate, and dexamethasone (86). In the presence of ascorbic acid, three dimensional nodules that were covered with

polygonal cells resembling osteoblasts that secreted and mineralized matrix in the presence of β-glycerophosphate were formed. The nodules resembled woven bone and they stained positive for alkaline phosphatase and type I collagen (86) (also discussed in (87)). The use of mineralized nodules as a model for bone formation *in vitro* allowed the field of bone biology to move toward understanding the factors that regulate the proliferation and differentiation of cells of the osteoblast lineage. Since the first evidence that the differentiation of functional osteoblasts could occur in culture, *in vitro* osteogenic culture systems have evolved to allow for a better understanding of the process of osteogenesis. Some of these culture systems will be discussed with regard to the methodology of differentiating ESCs into osteoblasts *in vitro* in mouse and human that has led to the culture system presented in this thesis.

In one of the first culture systems involving the differentiation of murine ESCs into osteoblasts, ESCs were allowed to form embryoid bodies (EBs) for five days in culture. After five days, the EBs were trypsinized and plated at a confluent density of 5 x 10^4 cells/well of a six well culture dish. The medium was supplemented with 50 μg/ml ascorbic acid and 50 mM β-glycerophosphate, as well as dexamethasone or retinoic acid. The cultures were also grown in the presence of antibiotics. With this method, confluent plates of mineralized bone nodules that consisted of aggregates of between 50 and 100 cells entrapped within an extracellular matrix were formed. Nodules were shown to stain with both von Kossa (mineral) and alizarin red (calcium), and express type I collagen and *Bglap1* (osteocalcin) after 21 days (88).

Another culture system employs the hanging drop method in which 750 cells were seeded onto the inner side of the lid of a Petri dish filled with phosphate buffered

saline (PBS). The cells condense to form EBs and are allowed to grow for three days before they are transferred to Petri dishes for an additional five days of growth. After five days, individual EBs were plated separately into 24 well culture plates. The medium was supplemented with 50 μg/ml ascorbic acid and 10 mM β-glycerophosphate, and in some cases, 1α,25-OH vitamin D_3. This method resulted in high efficiency, *in vitro* differentiation of murine ESCs into osteoblasts that showed expression of all major genes specific for mineralization (89).

Another osteogenic culture method was published in which EBs were formed using the hanging drop method. In this instance, 1×10^3 cells were aggregated per 10 μl of medium for two days and then pooled and cultured in suspension with retinoic acid for three days, followed by two days without retinoic acid. Whole EBs were then plated on gelatin-coated dishes with 50 μg/ml ascorbic acid, 10 mM β-glycerophosphate, 10 μM dexamethasone, as well as BMP-4. This method produced nodules that displayed characteristic morphology, mineralization, and gene expression of osteoblast differentiation. This methodology also revealed that different mesenchymal fates can be generated in the presence of different growth factors. For example, treatment with transforming growth factor-β (TGF-β) promotes chondrogenic differentiation (90).

With the isolation of hESCs in 1998, came the use of these cells in *in vitro* osteogenic culture systems as well. Different methodologies also exist for the differentiation of hESCs into osteoblasts and include different methods of EB formation, variable time in EB formation, as well as the absence of the EB step, differences in subsequent plating methods and densities, and differences in the use of supplemental medium (91-93). However, as stated earlier, the limitations to the availability and use of

hESCs, make murine ESCs a good model system for the study of osteogenesis *in vitro*. The method of initiating osteogenesis from murine ESC cultures described in this thesis, where individual EB-derived progenitors are plated at a low density such that the potential and differentiation of a single cell can be determined, is the only described method that allows for the observation and manipulation of the commitment stage of mesengenesis from single murine embryonic progenitors.

A. Intramembranous Bone Formation

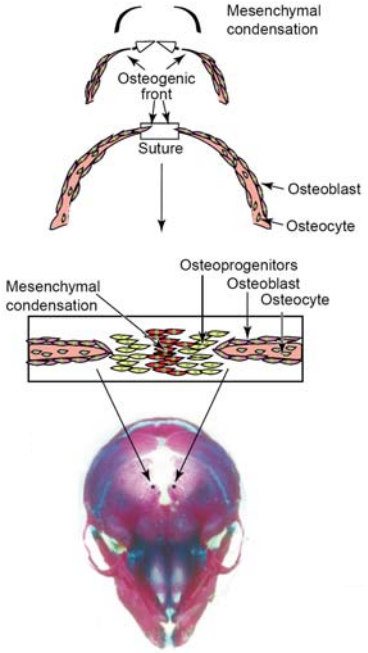

B. Endochondral Bone Formation

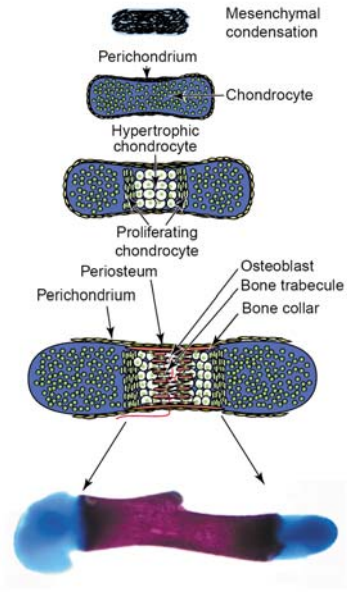

Figure 1.1: Intramembranous and endochondral bone formation. (Figure and legend adapted from source (16)). **(A.)** Craniofacial bones form through intramembranous bone formation which begins in mesenchymal condensations on the lateral side of the head. From the mesenchymal condensations, the cellular mass with osteogenic activity spreads upward toward the top of the skull. At the ends of the masses, a suture is formed where cells in the mesenchymal condensations differentiate into osteoprogenitor cells. Osteoprogenitor cells differentiate into osteoblasts, which differentiate into osteocytes. The skull in panel **(A.)** is a frontal view at E18.5 stained with alizarin red (mineral) and alcian blue (cartilage). **(B.)** Long bones form through endochondral bone formation, which also begins with the formation of mesenchymal condensations. Cells within the mesenchymal condensations form chondrocytes, whereas cells at the periphery form a perichondrium. Chondrocytes begin proliferating and differentiate into hypertrophic chondrocytes. Hypertrophic chondrocytes mineralize their own cartilaginous matrix, while at the same time, cells from the periosteum envelope the cartilaginous matrix, followed by invasion of vasculature and accompanying osteoclasts. The osteoclasts degrade the matrix and osteoblasts deposit a bone-specific matrix. The partially degraded, mineralized cartilage matrix forms a template for deposition of bone matrix by osteoblasts. The bottom picture in panel **(B.)** is a mouse humerous stained with alizarin red and alcian blue.

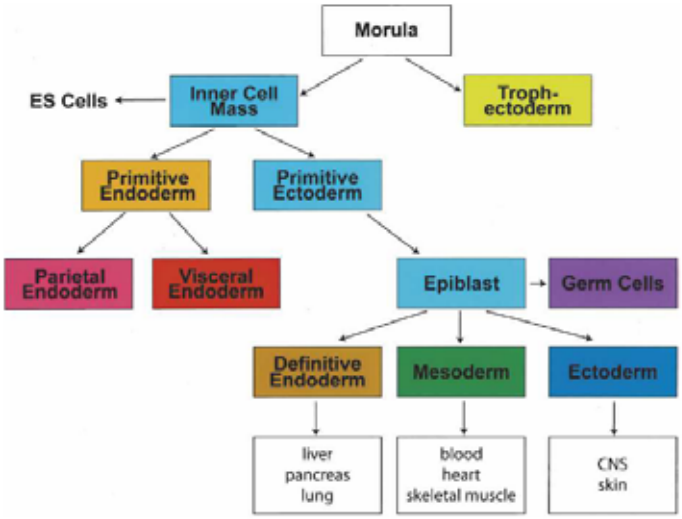

Figure 1.2: Early mouse development. Scheme of early mouse development showing the relationship of early cell populations to the primary germ layers and the origin of ESCs (source (51)).

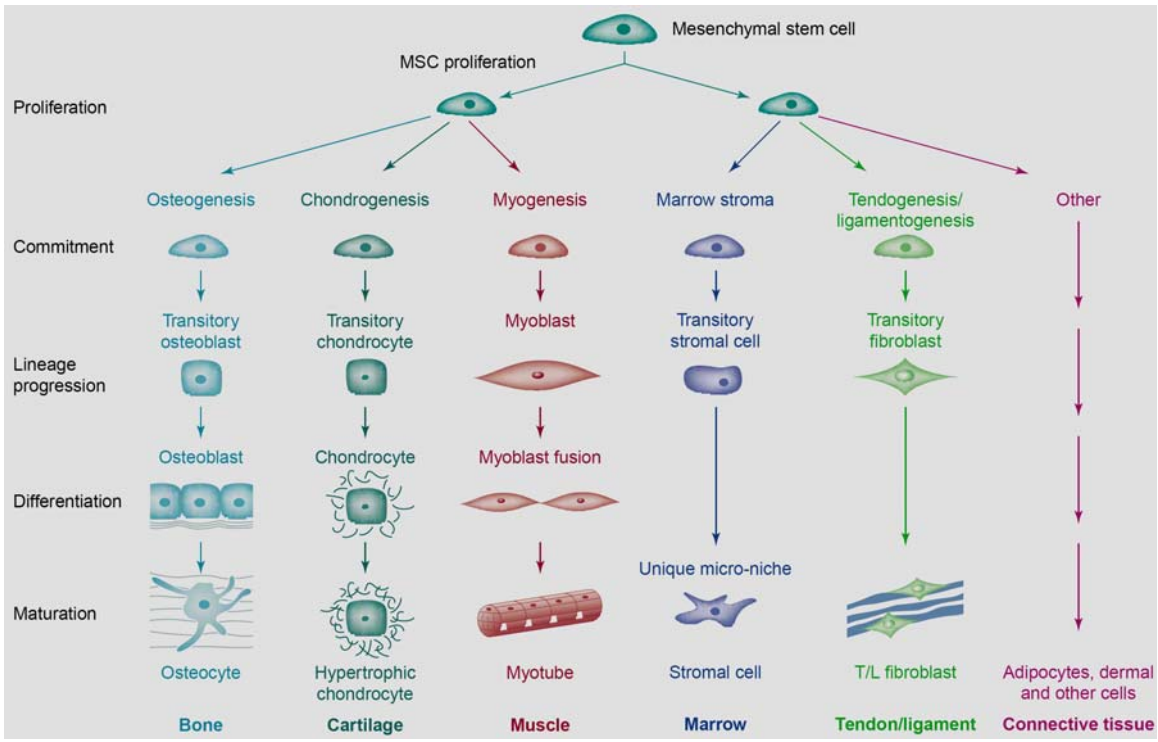

Figure 1.3: Potential of mesenchymal stem cells (source (94)).

Table 1.1 Transcription Factors Involved in Bone Formation. This list is not exhaustive.

Transcription Factors	Family	Expression Pattern	Loss-of-Function	Gain-of-Function
Runx2	Runt domain	Mesenchymal condensations, osteoblast lineage (27)	Embryonic lethal, Almost complete lack of mineralized bone, Unaffected cartilage (26,28)	Lineage specific, Rat MSCs-increase osteoblasts (95), NIH3T3, C3H10T1/2, and MC3T3-E1-induce osteoblast gene expression but MC3T3 unable to up-regulate mineralization (96), Restricted osteoblasts-blocks terminal differentiation (97,98)
Osterix	Sp/XKLF	Specifically in all developing bone (33)	Embryonic lethal, Complete lack of bone formation (intramembranous and endochondral), Normal cartilage (33)	Induction of osteoblast genes in myoblasts and mesenchymal cells (33) but not in fibroblast cells (with the exception of osteopontin) (34)
Sox-9	HMG domain, SRY	Mesenchymal condensations, Differentiated chondrocytes, central nervous system, otocysts, heart, testis, and vibrissae (35,36)	No cartilage formation, No expression of chondrocyte specific markers, No osteoblast formation (39,41)	In murine MSCs-enhances chondrogenesis (99), In murine ESCs-directs immediate chondrogenic commitment (100)
Twist-1	bHLH	Developing embryo, early bone development, central nervous system, cornea, alimentary system, brain, ear, retina (not exhaustive) (101)	Embryonic lethal, Cranial neural tube defects, Defects in head mesenchyme, somites, and limb buds (42), Premature osteoblast differentiation (47)	Increases periostin (a secreted protein found in early osteoblastic cells) expression (102), Inhibits osteoblast differentiation without affecting *Runx2* expression (47), Varying affects in different cell lines
Twist-2	bHLH	Developing embryo, early bone development, central nervous system, brain, ear, retina (not exhaustive) (101)	Enhanced proinflammatory cytokine gene expression (43), Premature osteoblast differentiation causing perinatal death (47)	In COS7 cells, decreased *Runx2* expression vector activity by 80% (47), Inhibits Runx2 function (47)

Table 1.2 Regulation of Osteoblast Differentiation by Other Transcription Factors

Transcription Factors	Family/ Classification	Loss-of-Function	Related Human Disease
Msx1	Homeobox protein	Delay in cranial bone formation and tooth development (103,104)	Similar to cleft palate and oligodontia (103)
Msx2	Homeobox protein	Delay in cranial bone formation and defects in endochondral bone formation, Defective teeth, hair follicle and mammary gland development (104,105)	Parietal foramina caused by haploinsufficiency (104,105)
Dlx5/Dlx6	Homeobox protein	Defects in craniofacial bones ($Dlx5^{-/-}$), Severe defects in craniofacial bones, and the calvarium, maxilla, and mandibula are not formed, Defects in endochondral bone formation as well ($Dlx5^{-/-}Dlx6^{-/-}$) (104)	Split-hand/split-foot malformation (SHFM), also called "lobster claw"
Krox-20	Zinc finger protein	Endochondral ossification disturbed, and trabecular bone is reduced (104,106)	
SP3	SP/Zinc finger protein	Perinatal lethality, Delay in intramembranous and endochondral ossification, In ESCs bone nodule formation is reduced (104,107)	
ATF4	CREB/Basic leucine zipper protein	Delay in ossification and osteopenia, Disturbance of type I collagen production, Interacts with Runx2 and enhances the expression and promoter activity of osteocalcin (48,104)	Coffin-Lowry syndrome (associated with $RSK2^{-/-}$) (48)

Table 1.3 Cell Types Produced from Mouse ESCs *in vitro* (source (52))

Cell Type	Reference
Yolk sac endoderm	(108)
Yolk sac mesoderm	(108)
Primitive hematopoietic	(108,109)
Definitive hematopoietic	(75,109,110)
Lymphoid precursor	(111)
Mast cell	(112)
Dendritic cell	(113)
Endothelial cell	(114,115)
Cardiomyocyte	(108,116)
Striated muscle	(117)
Smooth muscle	(115)
Adipocyte	(118)
Osteoblast	(88)
Chondrocyte	(119)
Keratinocyte	(115,120)
Neuron	(121,122)
Astrocyte	(123)
Oligodendrocyte	(124,125)

CHAPTER 2

MATERIALS AND METHODS

2.1 Characterization and Evaluation of the Osteogenic Culture System

2.1.1 Cell Lines and the Osteogenic Culture System

ESCs were grown on murine embryonic fibroblasts (feeders) in DMEM-H (Dulbecco's Modified Eagle Medium) (Life Technologies/Invitrogen) supplemented with 15% fetal bovine serum (FBS) (Atlanta Biologicals), 0.1 mM 2-mercaptoethanol (Sigma), 2 mM Glutamax (Invitrogen), and leukemia inhibitory factor (LIF) (Chemicon) conditioned supernatants (~1000 U/ml). ESCs were grown to sub-confluence, trypsinized, and split 1:3–1:10 to a nearly single cell suspension every two to three days. ESC cultures were maintained in humidified incubators at 37°C and 5% CO_2. No antibiotics were used in any of the cultures. These experiments were performed with the HM1 and BK4 cell lines, a rederivation or subclone of E14TG2a, respectively (126,127), although several other ESC lines perform similarly (128). ESC lines were stored in liquid nitrogen. Confluent plates of ESCs were trypsinized and frozen in a 5:4:1 ratio of FBS, ESC medium, and dimethyl sulfoxide (DMSO) (Sigma), respectively.

ESCs for osteogenic cultures were initiated within two passages of the thaw. The differentiation of ESCs into osteoblasts has been described previously (128,129). Briefly, 24 hours post-plating at a relatively high-density, the ESC colonies were flushed off the tissue culture plates with ESC medium and replated without LIF onto four 10 cm Petri dishes (bacterial grade plastic) to form embryoid bodies (EBs). The EBs were incubated

for two days at 37°C without additional feeding. After two days, the EBs were trypsinized to single cells, filtered through a 70 μm cell strainer (BD Falcon), and plated at 25 cells/cm^2 onto 10 cm tissue culture plates in osteoprogenitor medium [IMEM (Iscove's Modified Eagle Medium) (Life Technologies/Invitrogen) supplemented with 10% fetal bovine serum (Invitrogen), 0.1 mM 2-mercaptoethanol, 2 mM Glutamax, and 0.2 mM ascorbic acid (Sigma)]. After seven days, β-glycerophosphate (βGP) (Sigma) was added to the osteoprogenitor medium, at a final concentration of 2 mM, to aid in mineralization. The cultures were fed with osteoprogenitor medium every two to three days and allowed to differentiate for 21 days to form mature bone nodules. Figure 2.1A depicts a timeline of the osteogenic culture and Figure 2.1 B shows representative phase contrast images of the differentiation process.

2.1.2 Fixation and Staining of Osteogenic Cultures

Fixation and staining of osteogenic culture plates has been described previously (128,129). Plates were fixed in 10% neutral buffered formalin (Fisher) at room temperature for two hours. The plates were washed in distilled, deionized water (ddH_2O) and stained with 2.5% silver nitrate in ddH_2O for one hour on a UV light source (von Kossa stain). Plates were washed with ddH_2O and counterstained for fifteen seconds to one minute in methyl green (Vector Labs). The total number of colonies was counted in triplicate and the percentage of colonies that mineralized was determined. The analysis used to determine statistical significance was a Student's t-test.

2.1.3 RNA Isolation from Whole Plates and Individual Colonies

RNA from osteogenic culture whole plates was collected at various time points depending on the experiment. For characterization of osteogenic cultures, time points included ESC cultures, day 0 EBs through day 7 EBs (D0EB – D7EB), day 4 whole plates (WP4), day 7 whole plates (WP7), day 14 whole plates (WP14), and day 21 whole plates (WP21). RNA was prepared using TriReagent (Molecular Research Center, Inc.) according to the manufacturer's protocol. Briefly, 2 ml of TriReagent was added to a 10 cm osteogenic culture plate. The RNA was extracted from the homogenized cells with 200 μl chloroform and precipitated with isopropanol. The extracted RNA was washed with 70% ethanol and resuspended in 1 mM EDTA (ethylenediaminetetraacetic acid) to obtain approximately 1 μg/μl of RNA. Two plates were pooled for each sample to decrease the impact of heterogeneity. All reagents used in RNA isolation were RNase free.

RNA isolation from individual colonies was performed using the Qiagen RNeasy minikit. Individual colonies were isolated by mouth pipetting a small volume of lysis buffer onto the colony using a flame-pulled glass capillary, dislodging the colony, and pipetting it into buffer. The colonies were then placed directly into a Qiashredder column sitting in a 2 ml collection tube, and RNA was isolated according to the manufacturer's protocol. RNA from individual colonies did not yield a high enough concentration of RNA to be used in SYBR Green QRT-PCR. Therefore, the RNA from individual colonies was amplified using the Message Amp aRNA kit (Ambion). Prior to amplification, the RNA purity and integrity were checked using an Agilent 2100 Bioanalyzer.

2.1.4 Reverse Transcription (RT)

Two micorgrams of RNA were reversed transcribed with the RETROscript kit (Ambion) using an oligo (dT) primer and following the manufacturer's protocol. Briefly, total RNA, oligo (dT), and ddH_20 were incubated for three minutes at 78°C. The remaining RT components, 10X RT Buffer, dNTP mix, RNase Inhibitor, and MMLV-RT reverse transcriptase, were added and incubated for one hour at 42°C. The reaction was incubated at 92°C for ten minutes to inactivate the reverse transcriptase and stored at -20°C.

2.1.5 SYBR Green Quantitative Real Time Polymerase Chain Reaction (QRT-PCR)

QRT-PCR was performed with the ABI PRISM 7900HT and 7300 Sequence Detection Systems and the Quantitect SYBR Green PCR kit (Qiagen) following manufacturer's protocols. Serial dilutions of ESC, D0EB, or D2EB cDNA were used to generate standard curves for each primer set. Relative mRNA expression was normalized to ribosomal protein L7 (*Rpl7*) and displayed relative to D0EB, unless otherwise indicated. Assays were designed to detect only RNA such that one primer spanned an exon/exon boundary, allowing primer binding only when the intron was excised. An-RNA exclusive assay for Rpl7 could not be designed; however, *Rpl7* expression was so robust that any amount of product resulting from DNA contamination was negligible in comparison to product resulting from RNA. Assays for *Runx2*, osterix, *Dmp1* (in Figure 3.6), and *Agc1* were not specific for RNA. Because amplification products representing the 5′ end of the mRNA decrease with length, these assays were anchored as far 3′ in the

mRNA as possible, and as a result are not RNA specific. In these instances, we used RNA samples that had not been reverse transcribed as controls for DNA contamination and observed an insignificant amount of product. Duplicate or triplicate dilutions of 1:8 and 1:32 were analyzed for all cDNA. The amplification program included an initial denaturation step at 95°C for 15 minutes, followed by 50 cycles of 94°C for 15 seconds, 53°C for 30 seconds, and 72°C for 30 seconds; fluorescence was measured at the end of each extension step. To verify the specificity of the primers, a melting curve for each primer set was generated by heating the product to 95°C for 15 seconds, cooling it to 53°C, and then slowly heating it at 0.03°C/sec to 95°C; fluorescence was measured during the slow heating phase. (See Table 2.1 for a list of QRT-PCR primers used for characterizing and evaluating the osteogenic culture system.) The analysis used to determine statistical significance for the QRT-PCR data was a Student's t-test.

2.2 Overexpression of Runx2 in the Osteogenic Culture

2.2.1 Addition of Bone Morphogenetic Protein 2 (BMP-2) to the Osteogenic Culture

Human recombinant bone morphogenetic protein 2 (BMP-2) (a gift from the Genetics Institute used in collaboration with Christopher Niyibizi, Ph.D., The Pennsylvania State University College of Medicine) was added to the cultures at a concentration of 40 ng/μl. The medium was removed from the osteogenic culture plates and replaced with 1 ml of osteogenic culture medium (see section 2.1.1) supplemented with 2 μl of BMP-2 (40 ng/μl) for a final concentration of 80 ng/ml. The osteogenic cultures plates were placed in an incubator at 37°C for two hours. After two hours, 9 ml of osteogenic culture medium was added. This method was performed on two consecutive days of the osteogenic culture, starting with days 1 and 2 and continuing out to days 15 and 16. An unmanipulated plate was used as a control, as well as the removal and addition of medium to the plates in the absence of BMP-2. RNA was collected at various time points throughout the culture and plates were fixed and stained at day 21 with silver nitrate (mineral) and methyl green (counterstain) (see section 2.1.2).

2.2.2 Creation of Constitutive Overexpression of Runx2 cDNA Construct

The plasmid pKD3 (*Runx2* constitutive overexpression construct) was made by ligating four fragments: a human beta-actin promoter, *Runx2* cDNA, a polyadenylation signal sequence, and Hprt homology for single copy, targeted integration (130). This plasmid was made by Kimberly Dunham, a former member of the Bronson laboratory.

The human beta-actin promoter fragment was a 4.3 kb region of the pHβAPr-1 vector (131) cut out with EcoRI and SalI, in which the XhoI recognition site had been removed. A 3.2 kb fragment isolated from pCMV-Osf2 (a gift from Gerard Karsenty, M.D., Ph.D., Baylor College of Medicine) using EcoRI and XbaI, which contains the mouse *Runx2* cDNA (type I isoform), was ligated into pMTpA, a vector containing a polyadenylation signal sequence (poly A) from the metallothionein gene digested with EcoRI and SmaI. From this vector, a fragment containing the *Runx2* cDNA and poly A was isolated with SalI and SpeI. The human beta-actin promoter fragment, *Runx2* cDNA, and poly A were ligated into pBluescript II KS (+) (Stratagene). From this new vector, an XhoI/SpeI fragment was isolated containing the promoter, cDNA, and poly A. The sticky ends of this fragment were filled in with T4 DNA polymerase and 1 mM dNTP for 20 minutes at 12°C and heat inactivated for 15 minutes at 75°C. This fragment was then ligated with MluI linkers (New England Biolabs) and inserted into pMP8NEBΔLacZ, an MluI-linearized vector containing 5′ and 3′ homology to the Hprt locus, as well as a portion of the human HPRT. pMP8NEBΔLacZ was constructed from an 8 kb fragment of MP8SKB (130) cloned into pNEB193ΔLacZ (approximately 11 kb) (132). After linearization with PmeI, the vector was electroporated into the HM1 ESC line (see Fig. 4.8 for diagram of vector) for targeted integration at the Hprt locus.

2.2.3 Creation of Reverse Tetracycline-Responsive Transcriptional Activator (rtTA) Construct

The reverse tetracycline-responsive transcriptional activator (rtTA) was originally isolated from pTet-On (Clontech). A 1.5 kb fragment (with the BamHI recognition site removed) containing rtTA and an SV40 poly A was removed from pTet-On by partial digestion with EcoRI and HindIII and ligated to a 2.9 kb fragment of pBluescript II KS (+) created by digestion with EcoRI/HindIII. From this plasmid (rtTApbsII(+)KS), a 1.5 kb fragment containing rtTA and the SV40 poly A were removed by digestion with BamHI and XhoI and ligated to a 4.3 kb region of the pHβAPr-1 vector (131) created by digestion with EcoRI and BamHI, in which the XhoI site had been removed, as well as the 2.9 kb fragment of pBluescript II KS (+), both described above. The human beta-actin promoter, rtTA, and the SV40 poly A (6 kb fragment) were removed from this plasmid with XhoI and SpeI and ligated into pOSdupdel (a gift from Oliver Smithies, DPhil., The University of North Carolina at Chapel Hill) to include a loxP-flanked selectable marker, Neo^R, for random integration into the ESC genome and subsequent deletion of the marker (pKD2) (Fig. 4.11A). The proper creation of this vector was verified by restriction enzyme digestion with XhoI and PmeI (Fig. 4.11B). A 7.4 kb fragment containing the human beta-actin promoter, rtTA, SV40 poly A, and Neo^R was digested from pKD2 with SpeI and AseI. This fragment was electroporated into the HM1 ESC line and random integrants were selected by their G418 resistance. RT-PCR was used to verify the presence of rtTA in the ESC clones (Fig. 4.11C), and QRT-PCR was used to identify ESC clones expressing high levels of rtTA (Fig. 4.12). (See Table 2.2 for rtTA RT-PCR and QRT-PCR assays.)

2.2.4 Creation of Tetracycline-Inducible Overexpression of Runx2 cDNA Construct

pOsf2-mtpA was generated with a 3.2 kb *Runx2* cDNA fragment isolated from pCMV-Osf2 (as described above) and ligated into pMTpA (poly A) (described above) linearized with SmaI and EcoRI. The *Runx2* cDNA and poly A (3.5 kb) were isolated from pOsf2-mtpA after digestion with SalI and SpeI and ligated into SalI/SpeI-linearized pTET-Splice (Life Technologies) downstream of a tetracycline inducible promoter or tetracycline responsive element (TRE), creating pTET-Osf2pA (made by Kimberly Dunham). The tetracycline-inducible promoter, *Runx2* cDNA, and poly A (4 kb) were isolated from pTET-Osf2pA with XhoI and SpeI and were ligated with a 4.4 kb fragment isolated from pcDNA6/TR (Invitrogen) in order to achieve MluI sticky ends. The newly formed vector was digested with MluI to isolate the 4.3 kb fragment of interest and XmnI to break up the vector backbone. The 4.3 kb fragment was ligated into pMP8NEBΔLacZ (approximately 11 kb), an Hprt homology vector described in section 2.2.2 (Fig. 4.13A). The proper cloning of this vector was verified by restriction enzyme digestion with BamHI, XbaI, and SalI (Fig. 4.13B). The vector was linearized with PmeI and electroporated for targeted integration into an HM1 ESC line already containing a randomly integrated rtTA. RT-PCR analysis was used to verify the presence of the human HPRT (forward primer) and 3′ Hprt homology (reverse primer) in the ESC clone to be used in the osteogenic culture, indicating the targeted integration of the vector and rescued Hprt locus (Fig. 4.13C). (See Table 2.5 for primer sequences.)

2.2.5 Transgene Targeting to the Hprt Locus and Random Integration into Murine ESCs

Targeting of transgenes to the Hprt locus has been described previously (130,133). Briefly, properly identified constructs were linearized with PmeI and electroporated into the HM1 ESC line in the overexpression studies and the BK4 ESC line in the loss-of-function studies. ESC medium was used to bring the final concentration of DNA to 3 nM in 400 μl of medium. ESCs (1-4 x 10^7) were electroporated in a 2 mm cuvette with a BTX Electro Cell Manipulator ECM 600 set at 270 V, 50 μF, and 360 Ω. For random integration, ESCs and purified DNA fragments were electroporated as described above. Following electroporation, homologous recombinants were selected in medium supplemented with HAT (0.016 mg/ml of hypoxanthine, 0.01 mM aminopterin, and 0.0048 mg/ml of thymidine) and random integrants were selected in 0.2 mg/ml of G418 sulfate (Life Technologies) for 10 to 12 days. Individual colonies were isolated and expanded for osteogenic differentiation. ESCs containing a tetracycline-inducible construct were grown in tetracycline-system-approved fetal bovine serum (FBS) (Clontech), and doxycycline (0.1 μg/ml to 20 μg/ml) (Sigma) was added to the medium to induce transgene expression.

2.3 Knockdown of Expression of Transcription Factors in the Osteogenic Culture

2.3.1 Creation of the Tetracycline Repressor (TetR) Construct

The tetracycline repressor (TetR) was isolated from pcDNA6/TR (Invitrogen), a 6 kb vector that expresses the Tet repressor under the control of the human cytomegalovirus (CMV) immediate early promoter. A 2.3 kb fragment containing the CMV promoter, a globin intervening sequence (IVS), Tet repressor, and SV40 poly A was isolated from pcDNA6/TR using MluI. This fragment was blunt end ligated into HpaI-linearized pOSdupdel (see section 2.2.3) (Fig. 5.3A). pOSdupdel contains Neo^R, allowing G418 selection to be used to identify proper integrants. The proper cloning of this vector was verified by restriction enzyme digestion with NcoI (Fig. 5.3B). From the newly created vector, a 3.8 kb fragment containing the CMV promoter, globin IVS, Tet repressor, SV40 poly A, and Neo^R was isolated with SfiI and PciI; BstEII was also added to digest the backbone. The purified DNA fragment was randomly integrated after electroporation into the BK4 ESC line as previously described (see section 2.2.5). QRT-PCR was used to determine the expression of the Tet repressor in a subset of ESC clones (Fig. 5.4). (See Table 2.2 for TetR QRT-PCR assays.)

2.3.2 Creation of Tetracycline-Inducible Short Hairpin RNA (shRNA) Constructs

The loss-of-function siRNA constructs were based on the pSUPERIOR vector of the pSUPER RNAi System^{TM} (OligoEngine). The pSUPERIOR vector is used in combination with a pair of custom designed oligonucleotides that contain a unique 19 nucleotide sequence derived from the mRNA transcript to be suppressed. All target

sequences used for these studies were previously published. (See Table 2.3 for a list of target sequences and corresponding references.) The forward and reverse oligonucleotides, synthesized by OligoEngine, were resuspended at a concentration of 3 mg/ml with sterile, nuclease free H_20 and annealed by mixing 1 μl of each oligo (forward and reverse) with 48 μl annealing buffer (Buffer 3, New England Biolabs). The mixture was incubated for four minutes at 90°C and then for ten minutes at 70°C. The annealed oligos were then cooled slowly to 10°C (37°C for 15 – 20 minutes, then to 10°C or room temperature) before moving to 4°C.

The pSUPERIOR vector contains a polymerase III H1 RNA promoter with a sequence modification between the TATA box and transcriptional start site containing a tetracycline operator 2 site, which allows for the binding of two molecules of the Tet repressor. The pSUPERIOR vector was linearized with sequential digestions of HindIII and BglII. The purified, linearized pSUPERIOR vector was ligated with the annealed oligos. A negative control cloning reaction was performed with the linearized vector alone and no oligo insert. After ligation but prior to transformation, the plasmids were treated with BglII to reduce the level of background. (The BglII site is destroyed upon proper ligation of the plasmid and oligos, allowing for efficient screening of positive clones.) In the case of *Oct-4* siRNA, a 315 bp fragment containing the H1 promoter and inserted oligos was isolated with SmaI and HincII (blunt end enzymes). This 315 bp fragment was ligated to pSKB1 after digestion with EcoRI and blunting with T4 DNA polymerase. pSKB1 (containing 5′and 3′ Hprt homology) was constructed by inserting a linker, containing two additional restriction enzyme sites, PmeI and AscI, into the SacII/BamHI site of pMP8SKB (130). In the case of *Runx2* siRNA, a 350 bp fragment

containing the H1 promoter and inserted oligos was isolated after PCR amplification with primers containing EcoRI linker sites. (See Table 2.4 for RT-PCR primers). The purified fragment was then digested with EcoRI for sticky end ligation into pSKB1 linearized with EcoRI (see Fig. 5.6A for general diagram of vector). The proper cloning of these vectors was verified by restriction enzyme digestion with NcoI and HindIII (Fig. 5.6B, C). Each vector was sequenced to verify insertion of correct siRNA sequences. Properly ligated pSUPERIOR fragments and pSKB1 were linearized with PmeI and electroporated for targeted integration into a BK4 ESC line containing a randomly integrated Tet repressor as previously described (see section 2.3.1). RT-PCR analysis was used to verify the presence of the human HPRT (forward primer) and 3′ mouse Hprt homology (reverse primer) in the ESC clones to be used in the osteogenic culture, indicating the targeted integration of the vector and rescued Hprt locus (Fig. 5.6D, E). (See Table 2.5 for Hprt primer sequences.) For QRT-PCR analysis of *Oct-4* mRNA expression, after knockdown with siRNA, new primer sequences were anchored on either side of the target siRNA sequence. (See Table 2.6 for new Oct-4 primer sequences.)

2.3.3 Constitutive Expression of Runx2 Short Hairpin RNA (shRNA) in Murine ESCs

Properly ligated *Runx2* pSUPERIOR fragments and pSKB1 were linearized with PmeI and electroporated for targeted integration into a BK4 ESC line that did not contain a randomly integrated Tet repressor, allowing for constitutive expression of shRNA.

2.3.4 Polymerase Chain Reaction (PCR)

After a five minute incubation at 95°C, all PCR products were amplified for 30 cycles under the following conditions: 30 seconds at 95°C, 30 seconds at 58-63°C, and one minute at 72°C, followed by a final extension at 72°C for five minutes. PCR products were electrophoresed through a 1% agarose gel prepared in 1X TAE (Tris-acetate-EDTA buffer) or 1X TBE (Tris-borate-EDTA buffer) and visualized with ethidium bromide.

2.3.5 General Techniques for Cloning

All enzymes were obtained from New England Biolabs (NEB). Ligations were performed using T4 DNA Ligase, NEB Buffer 1, 10 mM ATP, and ddH_20 for 16 hours at 16°C and heat inactivated for 20 minutes at 65°C. Fragments and linearized vectors used in ligations were isolated from 1% agarose gels prepared in 1X TAE or 1X TBE and DNA was extracted using the Sephaglas™ Bandprep Kit (Amersham Pharmacia Biotech). Ligations were transformed into JM109 competent cells (Promega), recovered in SOC media (20 g/L bacto tryptone, 5 g/L bacto yeast extract, 0.5 g/L NaCl, 2.5 mM KCl, 10 mM $MgCl_2$, 20 mM glucose, pH 7.0) for one hour at 37°C and plated on LB (Luria Bertania) agar plates supplemented with 100 μg/ml ampicillin (LB/Amp) at 37°C. Colonies were isolated and grown in LB/Amp media at 37°C. After restriction enzyme verification of properly cloned vectors using small-scale DNA preparations, large-scale amounts of high quality DNA were prepared using the BioRad Quantum Prep Plasmid Maxiprep kit according to the manufacturer's protocol. After digestion fragments were electrophoresed through 1% agarose gels prepared in 1X TAE or 1X TBE and DNA was

extracted using Freeze and Squeeze columns (BioRad). Extracted fragment DNA and linearized vector DNA were purified with 70% ethanol and 5M NaCl, and resuspended in 1X TE (Tris-EDTA: 10 mM Tris-Cl, 1 mM EDTA) pH 7.2.

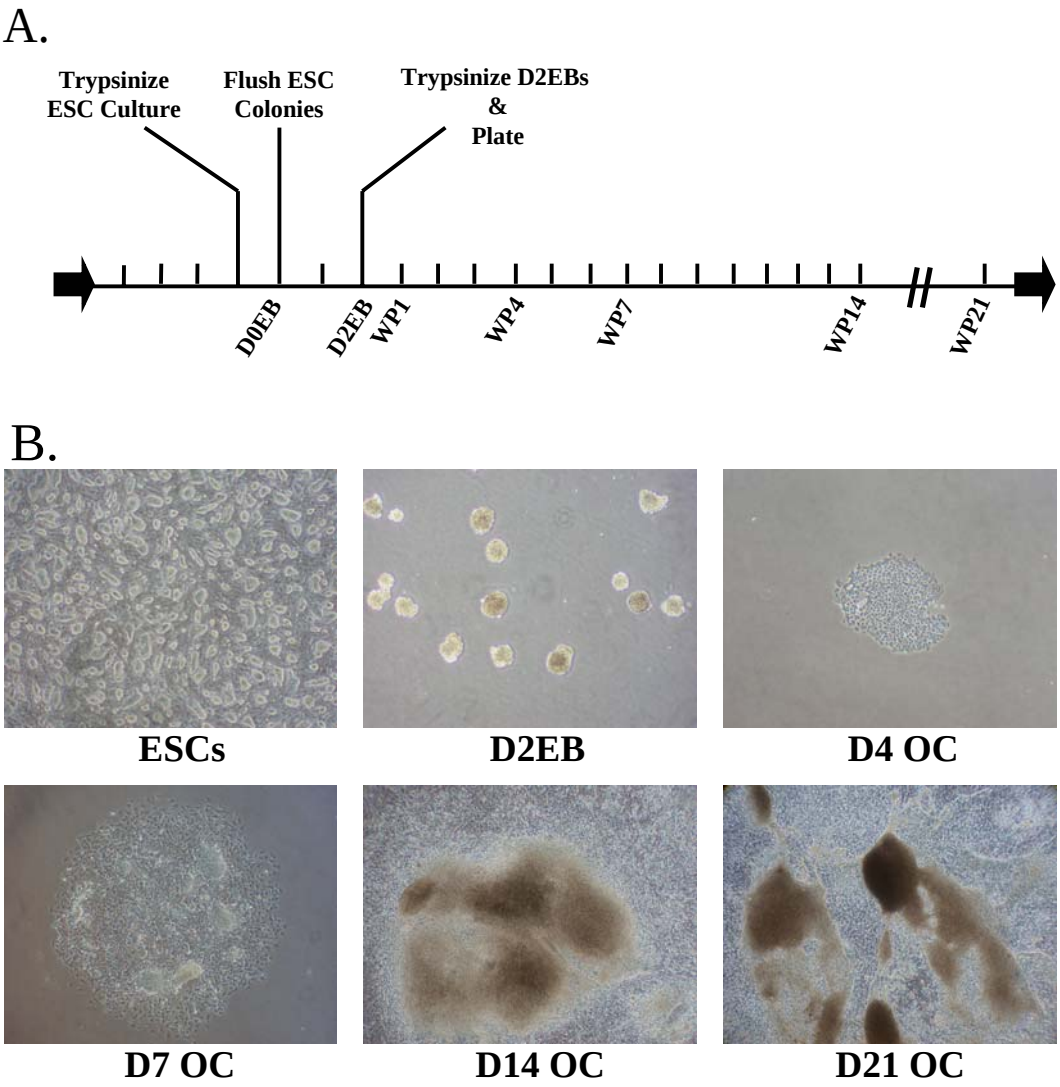

Figure 2.1: Timeline (**A**.) and phase contrast images (40x) (**B**.) of the differentiation of ESCs into osteogenic nodules. Tick marks represent days. D0EB = day 0 embryoid body, D2EB = day 2 embryoid body, WP1 = whole plate day 1 of the osteogenic culture, WP4 = whole plate day 4, WP7 = whole plate day 7, WP21 = whole plate day 21, D4 OC = day 4 osteogenic colony, D7 OC = day 7 osteogenic colony, D14 OC = day 14 osteogenic colony, D21 OC = day 21 osteogenic colony.

Table 2.1 QRT-PCR Primer Sequences for Characterization and Evaluation of the Osteogenic Culture System

Gene	Forward Primer 5' → 3'	Reverse Primer 5' → 3'	Size (bp)
Rpl7	CCCTGAAGACACTTCGAAAGG	GCTTTCCTTGCCATCCTAGC	121
Oct-4	CGAGGAGTCCCAGGACATGA	AAGCGACAGATGGTGGTCTG	162
Brachyury	CTCCAACCTATGCGGACAAT	GGCGTTATGACTCACAGGCA	116
Nestin	AGATCGCTCAGATCCTGGAA	CCTCCAGCAGAGTCCTGTATT	93
Foxd3	TGATGCAGAGCTTCGGAGCC	GCCGTAGGGTCCTGCGC	69
Sox-9	ATCTTCAAGGCGCTGCAAGC	CTGAGATTGCCCAGAGTGCT	89
Twist-1	CCGGAGACCTAGATGTCATTGT	GTTATCCAGCTCCAGAGTCTCT	72
Twist-2	GCTACGTGGCTCACGAGCGT	TGCAGGTGGGTCCTGGCTTG	134
Runx2 (Fig.3.5)	GGAACCAAGAAGGCACAGACA	AATGCGCCCTAAATCACTGAG	82
Runx2 (Fig.3.6)	CAGACCAGCAGCACTCCATAT	ATAGCGTGCTGCCATTCGAG	134
Osterix (Fig.3.5)	CTGCTTGAGGAAGAAGCTCA	TGGCTTCTTTGTGCCTCCTT	129
Osterix (Fig.3.6)	GAGAGCCCACCTAACAGGAG	TTCTCGTGGCTTCTAGGCAC	152
Col1a1	CCGGAAGAATACGTATCACC	ACCAGGAGGACCAGGAAGTC	147
Bglap1	CTACCTTGGAGCCTCAGTCC	TTAGGGCAGCACAGGTCCTA	160
Dmp1	GCTACATTGCTTTGGCTCCT	AGCTCCAGGCTTTGCTACTG	152
Lpl	AGGGCTCTGCCTGAGTTGTA	AATGGAACACTTTGTAGGGC	131
Myh11	AGGTGGAGGACATGGCAGAG	GAGTAGGTATAGATGAGGCC	97
CD45	TGAAGTGTCCCTACTTGCCT	CTTGTCCGGACGATCTGCTT	97
Agc1	TGCGGTACCAGTGCACTGAG	GTCTGTGCAGGTGATTCGAG	101
Col2a1	CATCGCCTACCTGGACGAAG	CAGTGTGTTTCGTGCAGCCA	140
Col10a1	CATAAAGGGCCCACTTGCTA	CCTCTTACTGGAATCCCTTTACTC	81
Pecam1	GTCTTCCACTCCGGGAAGTA	TTGGATACGCCATGCACCTT	95
Vegfa	AACGTACTTGCAGATGTGACAAG	TCCGGTGAGAGGTCTGGTT	92

Table 2.2 Primer Sequences for RT-PCR and QRT-PCR of rtTA and TetR

Target Sequence	Forward Primer 5′ → 3′	Reverse Primer 5′ → 3′	Size
rtTA	GGACGAGCTCCACTTAGACG	AGGGCATCGGTAAACATCTG	186
TetR	GAACTTCAGGCTCCTGGGC	GGCTGCTCTACACCTAGCTTCTG	209

Table 2.3 Target Sequences for Inducible siRNA

Gene	Target Sequence	References
Oct-4	GTTTCTGAAGTGCCCGAAG	(134)
Runx2	GGTTCAACGATCTGAGATT	(135)
Twist-1	AAGCTGAGCAAGATTCAGACC	(136)

Table 2.4 RT-PCR Primer Sequences for Isolating pSUPERIOR Fragments

Gene	Forward Primer 5′ → 3′	Reverse Primer 5′ → 3′	Size (bp)
pSUPERIOR vector	GTAGAATTCGCCGCTCTAGA ACTAGT	CTAGAATTCGAGGTCGACG GTATC	350 (with oligo inserts)

Table 2.5 RT-PCR Primer Sequences for Detection of the Rescued Hprt locus

Gene	Forward Primer 5′ → 3′	Reverse Primer 5′ → 3′	Size (bp)
Hprt	CTCCTCCTGAGCAGTCAGCC	CATCGCTAATCACGACGC	71

Table 2.6 QRT-PCR Primer Sequences for Oct-4 (Chapter 5)

Gene	Forward Primer 5′ → 3′	Reverse Primer 5′ → 3′	Size (bp)
Oct-4	ACCTTCAGGAGATATGCAAA TCG	TGCTGTAGGGAGGGCTTCG	130

CHAPTER 3

CHARACTERIZATION OF *IN VITRO* DIFFERENTIATION OF MURINE EMBRYONIC STEM CELLS INTO OSTEOGENIC NODULES (THE OSTEOGENIC CULTURE SYSTEM)

3.1 Introduction

The bone tissue of vertebrate skeletons is comprised of several cell types. Of these, the osteoblast secretes and mineralizes the bone matrix during both intramembranous and endochondral bone development, as well as during bone repair and remodeling in adults (1,16,137). Mesenchymal condensations in the embryo and mesenchymal stem cells, or marrow stromal cells, (MSCs), in the adult organism are the immediate progenitors of the osteoblast lineage. Differentiation of these progenitors proceeds through characteristic stages of commitment, proliferation, matrix secretion, and mineral deposition and results in a resting osteoblast in the periosteum, an osteocyte embedded within the matrix, or apoptosis of the terminally differentiated cell. The process of bone formation can be approximated *in vitro* in the form of a layered, mineralized nodule. The nodules consist of cuboidal osteoblasts on the surface and osteocytes, with long cellular processes, embedded within the bone matrix (138,139). Many laboratories have differentiated osteoprogenitors or MSCs from fetal or neonatal calvaria or from bone marrow *in vitro* (86,87). While several factors, including bone morphogenetic proteins, parathyroid hormone, and glucocorticoids, have been shown to influence the number and function of osteoblasts both *in vivo* and *in vitro* (140,141), the

signals that directly mediate differentiation of mesenchymal progenitors into osteoblasts are not well understood.

Typically, expression of specific genes delineates the stages of osteoblast development (79,139). *Runx2* (runt related transcription factor 2), also referred to as *Cbfa1* or *Osf2*, encodes a transcription factor that is the earliest marker of, and necessary for, osteogenesis (27,139). Osterix, also referred to as *Sp7*, encodes an osteoblast-specific transcription factor required for the differentiation of osteoprogenitors into mature osteoblasts (33). Alkaline phosphatase attaches to the extracellular surface of cell membranes and may play a role in matrix mineralization. Although a well-regarded marker of osteogenesis, alkaline phosphatase expression is nonspecific and found in several tissues (142). *Runx2* is critical throughout osteogenesis, promoting transcription of the gene for type I collagen (*Col1a1*) from relatively early in differentiation and expression of the gene for osteocalcin (*Bglap1*) in mature osteoblasts.

Embryonic stem cells (ESCs) have the potential to differentiate into nearly all cell lineages (52,53,56,143). The differentiation potential of murine ESCs can be preserved long-term in the presence of leukemia inhibitory factor (LIF) and fetal bovine serum (FBS) (52,64). ESC colonies can be flushed from a feeder layer, and in the absence of LIF and with forced suspension, embryoid bodies (EBs) will form and differentiation is initiated (108). We have utilized this method to generate single MSC-like progenitors for the initiation of osteogenic colonies capable of forming mineralized nodules *in vitro* (128,129).

Osteogenic cultures using murine (88-90,144) and human ESCs (91-93) have been described. These methods typically involve examining osteogenesis in whole

adherent EBs or in confluent cultures of EB-derived cells. Our method of initiating osteogenesis from ESC cultures, where individual EB-derived progenitors are plated at a low density such that the potential and differentiation of a single cell can be determined, is the only described method that allows for the observation and manipulation of the commitment stage of mesengenesis from single murine embryonic progenitors (128,129). The ability to track osteogenesis over time in these cultures will allow us to identify appropriate genes and generate reporters for intermediate cell stages. Isolation of cells expressing such reporters may also allow for enrichment, or even purification, of therapeutically valuable cells. This capability would enable treatment of severe fractures and diseases such as osteogenesis imperfecta and in principal can be applied to other lineages and disease therapies (76). The osteogenic cultures may also be useful for drug target identification and validation, as well as development of novel therapeutics (77).

3.2 Results

3.2.1 Osteogenic Differentiation of Murine Embryonic Stem-Cell Derived Progenitors

After trypsinization of day 2 embryoid bodies (D2EBs), single cells were plated at 25 cells/cm^2 in osteogenic medium containing ascorbic acid and β-glycerophosphate, additives documented to improve matrix structure and mineral deposition, respectively (86,87). In this osteogenic culture system, ECM deposition and mineralization are initiated approximately 7 days post-plating; by 21 days post-plating, mineralization of the nodule is extensive. Typically, 2 x 10^3 cells/10 cm dish will yield 20-40 colony forming units (CFUs) with approximately 60%-80% of these colonies layered and mineralized, yielding a frequency of CFU-osteogenic (CFU-O) of approximately 1 in 100 EB-derived cells (Fig. 3.1A). Figure 3.1B shows a digital image of a 10 cm dish at day 21 after fixation and staining with silver nitrate/methyl green. Figure 3.1C is a phase contrast image of an osteogenic colony at day 7. This figure shows the initiation of layering and mineral deposition evident in the center of these colonies as early as day 7 of the osteogenic culture.

Figure 3.2 reveals total colony forming units and percentage of colonies with mineralization after osteogenic culture plating of D0EB, D2EB, D4EB, and D6EBs. Total colonies are plotted per 1 x 10^3 cells plated. Total colonies were significantly ($p<0.05$) decreased as the day in EB formation increased, while the percentage of colonies with mineralization did not change. This suggests that as the day in EB formation increases, the osteogenic potential of the precursor cells decreases or the

potential changes. The highest number of morphologically osteogenic colonies after one week is achieved with progenitors derived from D2EBs.

3.2.2 Gene Expression During Embryoid Body (EB) Formation and Early Time Points in the Osteogenic Culture

QRT-PCR analysis was conducted on several transcription factors implicated in osteogenesis (each will be discussed in further detail in section 3.2.3), during sequential days of embryoid body formation and during early time points in the osteogenic culture. RNA was isolated on day 1 (D1EB) through day 7 (D7EB) of embryoid body formation, as well as day 4 (WP4) and day 7 (WP7) of the osteogenic culture. Figure 3.3 and 3.4 allow for comparison of early gene expression in the osteogenic culture with days in EB formation. This comparison provides insight into the fate of progenitor cells in the EBs if they were not disrupted and plated for the osteogenic culture. While there is a slight up-regulation of brachyury in the D2EB, there is a more prominent up-regulation in the D6EB followed by a rapid down-regulation in the D7EB (Fig. 3.3). *Twist-2*, *Sox-9*, and *Runx2* were all up-regulated in the D4EBs and continued to increase to at least the D7EBs (Fig. 3.3). Osterix expression was not up-regulated at any time point during EB formation (Fig. 3.3). The mRNA expression of brachyury, *Twist-2*, *Sox-9*, and *Runx2* were all up-regulated by day 4 of the osteogenic culture (Fig. 3.4), while osterix was not up-regulated until day 14 (Fig. 3.5B) or between day 7 and 14. The expression of *Twist-2*, *Sox-9*, and *Runx2* in day EBs and early time points of the osteogenic culture suggest a somewhat parallel pathway, with some notable differences. The expression of *Sox-9* was more prominent than *Twist-2* in the EBs, but the reverse was true in the osteogenic

culture. Also, the up-regulation of *Runx2* was more prominent in the EBs than in the osteogenic culture. This suggests that the osteogenic differentiation is accelerated in the EBs compared to the osteogenic culture perhaps because in the EBs the cell/cell interactions have not been disrupted. Also, there is evidence that chondrogenesis occurs in later day EBs, which may explain the increased *Sox-9* levels (119,145).

3.2.3 Gene Expression During Later Time Points in the Osteogenic Culture

QRT-PCR analysis at various time points throughout the ESC-derived osteogenic culture revealed a gene expression pattern characteristic of the osteoblast lineage (Fig. 3.5). RNA was isolated at the following time points: immediately after flushing colonies from the ESC culture (D0EB), after two days of EB formation (D2EB), entire plates after two weeks of the osteogenic culture (WP14), and entire plates after three weeks of the osteogenic culture (WP21). Figure 3.5 depicts specific genes displayed as common log plots detailing their progression throughout the osteogenic culture. *Oct-4*, also known as *Pou5f1*, encodes a marker of pluripotent stem cells, and its expression is necessary for maintaining ESC potential and self-renewal capacity (146,147). *Oct-4* was expressed in the D0EB but decreased in the D2EB and was not significantly present in later stages of the osteogenic culture (Fig. 3.5A). Expression of brachyury, a *T* box transcription factor that plays a role in the formation and organization of the mesoderm (148), was up-regulated in the D2EB and down-regulated as time in culture progressed (Fig. 3.5A). The expression pattern of these two transcription factors in the osteogenic culture is consistent with the timing of their expression in embryonic development and distinguishes the D0EB, D2EB, and later time points in culture. Nestin (*Nes*) expression is a marker of

neuroepithelial stem cells (149) and is sharply down-regulated as stem cells transition into neurons. Nestin expression has also been identified in myoprogenitors but not in mature muscle cells (150). In the osteogenic culture, nestin expression was up-regulated over 200-fold in the D2EB, and as differentiation proceeded its expression began to decline. However, by 21 days in culture, nestin expression was still increased 100-fold in comparison to the D0EB, suggesting the persistence of neuroepithelial progenitors. The possibility that *Nes* expression was indicative of the presence of progenitors for the neural crest lineage in these cultures led us to assay for the expression of *Foxd3*. *Foxd3*, forkhead box D3 (also known as *Genesis* or *Hfh2*), is a winged-helix transcription factor expressed embryonically and known to promote a neural crest cell fate (151-153). *Foxd3* message was increased only 2-fold in the D2EB and returned to baseline expression by days 14 and 21 of the osteogenic culture, a result consistent with the absence of significant neural crest maturation in these cultures.

Figure 3.5B presents expression data for several transcription factors implicated in osteogenic differentiation. *Sox-9* is expressed early in mesenchymal condensations, specifically those destined to undergo endochondral osteogenesis (35,154). *Sox-9* was highly up-regulated by day 14 in the osteogenic culture, displaying approximately a 50-fold increase in expression when compared to the D0EB; this level of expression was maintained to at least 21 days. The Twist proteins, Twist-1 and Twist-2, are basic helix-loop-helix (bHLH)-containing transcription factors implicated in osteoblast differentiation (47). The expression of *Twist-1* and *Twist-2* was highly up-regulated by 14 days in culture, and although both decreased in expression by 21 days, they were still highly up-regulated, approximately 100-and 500-fold, respectively, in comparison to

D0EB (Fig. 3.5B). *Runx2* expression is initiated in mesenchymal condensations, and mice homozygous for a null allele of *Runx2* have no detectable osteoblasts and no bone at birth (21,26-28). There was a low level of *Runx2* expression in D0EB samples, similar to many of the transcription factors, a decrease in the D2EB samples, and a considerable induction by 14 days in culture. In addition to a role in commitment of mesenchymal progenitors to the osteogenic lineage, *Runx2* is also critical for mature osteoblast function. Ducy et al. identified Runx2 binding sites in the osteoblast-specific genes encoding osteocalcin, bone sialoprotein, and osteopontin, as well as type I collagen (27). Robust *Runx2* expression persists out to 21 days in culture (Fig. 3.5B). Osterix, transcriptionally the most osteoblast-specific factor, is a novel zinc finger-containing transcription factor expressed in all developing bones and is required for osteoblast differentiation (33). Overall, osterix expression was up-regulated by day 14 of the osteogenic culture, and its expression persisted to at least day 21 (Fig. 3.5B). Osterix is expressed several days later than *Runx2* developmentally, and this delay in expression was also seen in our osteogenic cultures (Fig 3.4).

While transcription factors are critical for the differentiation of ESCs into osteoblasts, mature markers can also be used to identify the presence of the osteoblast lineage. Type I collagen, *Col1a1*, is the most abundant extracellular protein of bone, constituting approximately 95% of the organic matrix (1,155). While type I collagen is not exclusive to bone, it is essential for proper bone growth and development. The brittle bone disorder osteogenesis imperfecta (OI) is caused almost exclusively by mutations in the COL1A1 and COL2A2 genes that encode polypeptides of type I collagen. Osteocalcin, encoded by *Bglap1*, is the most abundant noncollagenous protein of bone

and is found exclusively in osteoblasts (22-24). *Col1a1* and *Bglap1* were up-regulated approximately 2000-fold by 21 days in culture (Fig. 3.5C). In fact, the abrupt increase in *Bglap1* message between 14 and 21 days of culture is the most pronounced distinction between these two time points.

The D2EB cells seeded in the osteogenic cultures are capable of forming tissues from all of the classically defined lineages: ectoderm, endoderm, mesoderm, and gametes. Osteogenic medium, via the fetal bovine serum, is expected to contain the osteogenesis-promoting growth factor bone morphogenetic protein; it also contains additives to support robust osteogenic nodule formation (64). However, it is not surprising that evidence for other cell types was found, particularly those that represent lineages with progenitors capable of colony formation on an adherent surface and no defined medium requirements beyond those typically found in serum. Three other mesoderm-derived lineages were found in the cultures: adipogenic, myogenic, and hematopoietic. Figures 3.5C and D illustrate this point via data from QRT-PCR assays designed to assess gene expression characteristic of mature cells from these lineages. *Lpl* (lipoprotein lipase) expression is a marker for adipose cells (156), *Myh11* (myosin heavy polypeptide 11) expression is a marker for smooth muscle, and *CD45*, more recently referred to as *Ptprc* (protein tyrosine phosphatase receptor type C), expression is a marker for hematopoietic cells (157). All three of these markers were up-regulated at least 100-fold by 21 days in culture (Fig. 3.5C, D).

Expression of several other genes was investigated to identify other lineages and cell types that may be present in the osteogenic culture, including relatively specific markers *Col10a1* and *Pecam1*, as well as the nonspecific marker *Vegfa* (Fig. 3.5D). The

gene for type X collagen (*Col10a1*) is expressed specifically in hypertrophic chondrocytes (158). In the osteogenic culture, its expression was up-regulated approximately 10-fold by 21 days in culture. This increase in expression of *Col10a1* by 21 days (10-fold) was small in comparison to the induction of *Col1a1* expression (2000-fold, Fig. 3.5C). Vascular endothelial growth factor A (VegfA) is a critical regulator of angiogenesis during development. *Vegfa* expression was increased a little less than 10-fold by day 21 of the osteogenic culture. Despite this finding, mRNA for *Pecam1* (platelet/endothelial cell adhesion molecule 1), located on the borders of endothelial cells, platelets, and white blood cells (159,160), did not change significantly from D0EB to WP21.

3.2.4 Gene Expression in Individual Colonies

Individually isolated colonies from day 21 of the osteogenic culture were used to begin to categorize the potential and/or commitment of the D2EB-derived progenitors (Fig. 3.6). RNA was amplified from eight individually isolated colonies in order to obtain sufficient RNA for QRT-PCR. Figure 3.6A displays phase contrast images of the eight individually isolated colonies analyzed by QRT-PCR. These eight colonies are a representative subset of the colonies present in a given osteogenic culture at 21 days. The images reveal the morphological differences between colonies at day 21, especially with regard to matrix secretion and mineral deposition. Figure 3.6B displays QRT-PCR data representing the relative mRNA levels for several genes at 21 days for all eight colonies. Table 3.1 summarizes the phenotype of each individual colony based on RNA and morphology. QRT-PCR analysis of individual colonies from different osteogenic

cultures has been conducted and similar results have been found. We examined expression of genes for two transcription factors necessary for osteogenesis, *Runx2* and osterix; two markers of the mature osteoblast, *Col1a1* and *Bglap1*; one marker of the terminally differentiated osteoblast (the osteocyte), *Dmp1* (dentin matrix protein 1) (161); three markers of chondrogenesis or mature chondrocytes, *Agc1* (aggrecan) (162), *Col2a1*, and *Col10a1*; and mature markers of adipogenesis (*Lpl*), myogenesis (*Myh11*), and hematopoiesis (*CD45*). Expression of *Col1a1* was found in all eight of the colonies. While *Col1a1* is not specific for osteogenesis, it is a key component of the bone matrix. Its expression was increased over 50-fold in osteogenic colonies C1, C2, and C3 (data not shown). Transcripts for *CD45* were not present in any of the colonies (data not shown). Transcripts for *Agc1*, *Col2a1*, and *Col10a1* were not present at a significant level in any of the eight colonies, with the exception of transcripts for *Col2a1*, which were expressed at low levels (approximately a 15-fold increase over D0EB) in C3, C5, and C6 (data not shown). It should be noted that the assay for *Col2a1* expression was not designed to differentiate between the two different isoforms, IIA (chondrogenic precursors) or IIB (differentiated chondrocytes) (163).

Colony 1 (C1) was both layered and mineralized, with mineral deposits present in the center of the colony (Fig. 3.6A). At 21 days in culture, C1 displayed expression of *Runx2*, *Bglap1*, *Dmp1*, *Lpl*, and *Myh11* (Fig. 3.6B). This gene expression pattern clearly defines C1 as a mature, mixed colony containing osteogenic and adipogenic, as well as myogenic cells. Colony 2 (C2) was both layered and mineralized, appearing morphologically similar to C1 (Fig. 3.6A). C2 also expressed *Runx2*, *Bglap1*, *Dmp1*, *Lpl*, and *Myh11* (Fig. 3.6B). While C2 did not display the robust *Bglap1* expression of C1, it

did express a high level of *Dmp1*, suggesting significant osteocytic differentiation. Colony 3 (C3) was also layered and mineralized (Fig. 3.6A). Similar to C1 and C2, C3 expressed *Runx2*, *Bglap1*, *Dmp1*, *Lpl*, and *Myh11*. In addition to these genes, osterix expression was also present, showing that while it was a mature, mixed colony, there were also early osteogenic cells still present at 21 days (Fig. 3.6B). Colony 4 (C4) presented morphology more characteristic of a pure osteogenic colony. There was layering and mineralization in the center of the colony with a monolayer of proliferating cells around the periphery. In addition to appearing purely osteogenic, the colony also seemed to be at an earlier differentiation stage than C1, C2, or C3 based on the observation that the layering and mineralization were more localized to the center of the colony and the mineralization was not as robust (Fig. 3.6A). The gene expression appeared to correlate with this observation as well; C4 expressed *Runx2*, osterix, and *Col1a1*, all present during early osteogenesis, with no expression of the mature osteoblast markers *Bglap1* and *Dmp1*, or *Myh11* and *Lpl*. (Fig. 3.6B).

Colony 5 (C5) showed a few small areas of mineral deposition but was not layered and only expressed *Col1a1* and *Lpl*, suggesting it was an adipogenic colony. Under higher magnification, the upper right hand corner of the colony contained lipid droplets (data not shown), further characterizing C5 as adipogenic (Fig. 3.6A, B). Colony 6 (C6) was layered and mineralized but did not look like osteogenic colonies C1-C4. The layering and mineralization were not centrally located and were not as uniform (Fig. 3.6A). C6 expressed *Lpl* and *Myh11*. The colony did not display significant *Bglap1* or *Dmp1* message, but did contain *Runx2* and *Col1a1*, suggesting that along with adipogenesis and myogenesis, early osteogenesis may have been occurring (Fig. 3.6B).

Colony 7 (C7) was both layered and mineralized; however, it only expressed *Col1a1* and *Lpl* (Fig. 3.6A, B). In terms of gene expression it was similar to C5, but morphologically it was distinguishable. Colony 8 (C8) was a monolayer and exhibited no mineralization (Fig. 3.6A). The only gene expressed in this colony was *Col1a1* (Fig. 3.6B). The morphology and gene expression of C8 were not characteristic of osteogenesis, adipogenesis, or myogenesis, nor did it have classical fibroblast morphology. These results indicate that the osteogenic colony forming units are diverse and include unipotential and multipotential progenitors with various combinations of mature mesenchymal lineages. Analysis of individual colonies has allowed for phenotyping beyond the morphological characteristics revealed by phase contrast microscopy and, by inference, provides insight into the individual progenitors that seed these colonies.

3.3 Discussion

This chapter provides three lines of evidence for osteogenesis in these ESC-derived cultures: (i) cell and colony morphology as revealed by phase contrast microscopy, (ii) mineralization of extracellular matrix as revealed by von Kossa staining, and (iii) QRT-PCR analysis of cDNA from entire plates and individual colonies revealing expression of genes characteristic of, and specific for, osteoblasts.

Our laboratory has created a working model of osteogenesis that tracks the ESC through differentiation to a terminally differentiated osteoblast or osteocyte (Fig. 3.7). The figure depicts expected cell types and relevant gene expression markers as well as lineages that have not been tested or are not present in the osteogenic culture due to the absence of mature marker expression (i.e. cartilage). QRT-PCR analysis has allowed for tracking of the ESC through a mesodermal cell, bipotential progenitor, osteoprogenitor, mature osteoblast, and finally to a terminally differentiated osteocyte. We propose an MSC intermediate as well; however, the lack of an MSC marker in the murine system does not allow for definitive identification of this cell. The working model also depicts other mesodermal lineages, such as adipogenesis and myogenesis that have been identified in the osteogenic culture with mature lineage markers. It is also important to note that there are two possible pathways to the mesenchymal lineage: mesodermal and ectodermal, which will be discussed below.

The gene expression data provides strong evidence for osteogenesis in these cultures, opens the door for genetic manipulations that may enhance osteogenesis, and reveals genes whose pronounced transcriptional induction would make extremely useful

reporters for further experimentation directed at understanding the decision points and functional capacity of mesenchymal progenitors. *Sox-9, Twist-1/2, Runx2,* and osterix are all expressed in these cultures. *Sox-9* is considered to be an initiator of chondrogenesis as chimeric mice generated with *Sox-9*-null ESCs show no contribution of the *Sox-9* null ESCs into cartilage (39). However, the conditional loss of *Sox-9* prior to its expression in limb bud condensations results in the absence of osteogenesis and the lack of *Runx2* expression, thus supporting the existence of an osteochondral progenitor in the condensation that is marked by the expression of *Sox-9* (40). The absence of a significant increase in proteoglycans as revealed by alcian blue staining (cartilage) (S.K. Bronson, unpublished) and the modest increase in *Col10a1* expression we see in these cultures does not support the presence of chondrogenesis. *In vitro* chondrogenesis typically requires whole EBs, cell pellets or micromasses, and the addition of TGF-β, further decreasing the likelihood that *Sox-9* expression is due to chondrogenic differentiation (145,164). We favor the conclusion that cells resembling an osteochondroprogenitor are present in the cultures (Fig. 3.5B).

Twist-1 was identified in a subset of mesodermal cells essential for the formation of the cranial neural tube in vertebrates and is required for the closure of the neural tube during mouse development (42,165). *Twist-2,* also known as *Dermo1,* is expressed early in mesenchymal condensations (166) and opposes Runx2 later during osteogenesis (47). Karsenty et al. propose and provide support for the idea that *Twist-1* and *Twist-2* expression keep early Runx2 function in check, explaining a lack of osteoblastic gene expression during the initial period of *Runx2* expression in embryonic development (47).

The persistence of the Twists in the culture system may provide an opportunity to promote osteogenesis in these cultures by interfering with *Twist* expression.

QRT-PCR analysis of cDNA from individual colonies hinted at a staggered maturation process, illustrated by the incomplete overlap of expression patterns for markers of osteoprogenitors, osteoblasts, and osteocytes (osterix, *Bglap1*, and *Dmp1*, respectively). Colony 4 exhibited osterix expression with little *Bglap1* or *Dmp1* expression, while colony 3 exhibited expression of all three markers. Colony 1 exhibited expression of *Bglap1* and *Dmp1*, and colony 2 exhibited low expression of *Bglap1* but high expression of *Dmp1*. The apparent staggering of colony maturation in these cultures is not surprising given the heterogenous population of stem cells that are likely to be present in the D2EB. We suspect that later progenitors are likely to be more lineage-specific while earlier progenitors are more likely to have multilineage potential (Fig. 3.2).

The analysis of individual colonies also demonstrated the presence of multilineage colonies. As the plating method is designed to exclude initiation of colonies by more than one cell, we conclude that multilineage colonies were initiated by multipotential progenitors. The differentiation of single cells in the osteogenic culture can be visualized by phase contrast microscopy. The incomplete overlap of mature markers expressed in multilineage colonies in this experiment, and in others we have performed, suggests the presence of different types of multipotential progenitors, and a non-linear progression from multilineage to unilineage potential. With regard to the relative contribution of each of these lineages to colony formation and to the development of individual colonies, we observed that the messages for *Col1a1* and *Bglap1* were up-regulated 2000-fold by 21 days in culture while the messages for

markers of other lineages, including adipogenic and myogenic, were up-regulated on the order of 100-fold. However, we have no information regarding the relative abundance of these messages in the mature cell types or of the percentage of cells representing each lineage in a given colony.

We are beginning to develop a picture of the microenvironment in which *in vitro* osteogenesis takes place. We see appreciable expression of *Vegfa*. The increases in *Vegfa* are even more interesting in the context of no significant change in expression of *Pecam1* from the D0EB stage to the WP21 state, suggesting a complete absence of vasculogenesis. In light of the fact that VegfA has been implicated in skeletogenesis, including both chondrocyte maturation and the regulation of osteoblast activity, the presence of *Vegfa* in these cultures may suggest an opportunity for enhancing osteogenesis through exogenous supplementation of this growth factor (167).

One particularly interesting and unresolved question regarding osteogenesis in these cultures is the nature of the progenitors that lie between the ESC and the committed osteoprogenitor. At least two different possibilities exist. The first avenue would be differentiation of the ESC into a mesodermal progenitor similar to that which precedes the condensations in the developing limb bud and other skeletal sites *in vivo*. A second avenue would be differentiation of the ESC into an ectodermal (neuroepithelial) progenitor that proliferates and then goes through a “transition” to mesenchyme, similar to the neural crest-derived osteogenesis seen *in vivo*. With regard to timing, we suspect either of these paths might be revealed by a change in gene expression in the D2EB. In light of the boost in brachyury and nestin expression in the D2EBs, it seems likely that both of these paths might be represented in the ESC-derived osteogenic cultures.

Kawaguchi et al., using a related ESC-based osteogenic system, observed enhanced osteogenesis after the addition of retinoic acid to the EB cultures (90). Retinoic acid is typically used to achieve maximum neurogenesis in ESC-derived differentiation cultures, but in this context may be serving to promote ectoderm/neural crest formation. This is likely to be a fruitful area of future experimentation as either mesoderm or neuroepithelial-derived progenitors or their committed progeny may be very useful in stem cell-based osteogenic therapies.

This method of initiating osteogenesis from ESC cultures is the only described method that allows for the observation and manipulation of the commitment stage of mesengenesis from single embryonic stem cell-derived progenitors. Other methods of initiating osteogenesis involve the deposition of entire EBs (89,168) or very high densities of cells (88) and are limited to measures of differentiation capacity. Further, we find relatively high levels of mesenchymal progenitors, ~1/100, in the absence of exogenous steroidogenic hormones, peptide growth factors, or cytokines. Through the use of this osteogenic culture system, there is the potential to more closely investigate the commitment of mesenchymal progenitors to the osteogenic lineage. This would promote an understanding of the basic biology of factors critical for this transition to occur and would permit pharmacological manipulation of the process. Finally, understanding commitment is a critical step in using any type of stem cell therapeutically. ESCs have been shown to form teratomas when transplanted *in vivo*, but the proliferative capacity of mature osteoblasts is negligible. These two factors render an intermediate cell population essential for therapeutic purposes. Our results provide reasonable evidence to suggest that an intermediate cell population within the ESC-derived osteogenic culture exists that

maintains the desired therapeutic qualities of significant proliferative capacity and restricted lineage potential.

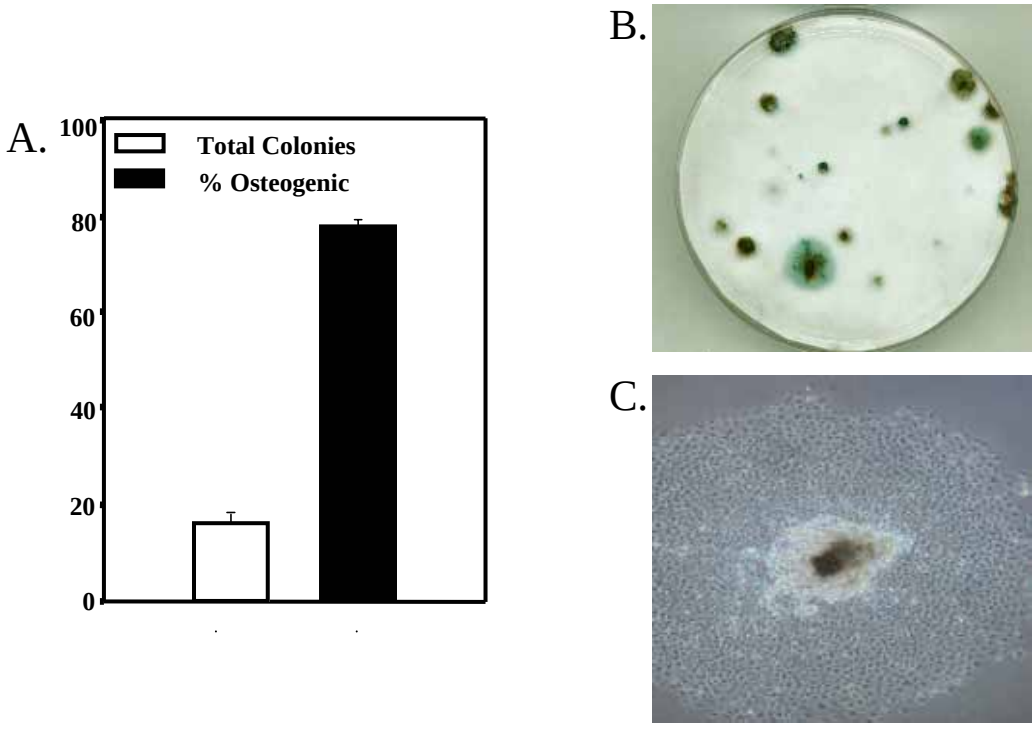

Figure 3.1: Osteogenic differentiation of murine embryonic stem cell-derived progenitors. (**A.**) Total colony forming units (17 +/- 1.73) and percentage of colonies (78.4% +/- 1.02%) with mineralization after 21 days in culture. (**B.**) Osteogenic cultures stained at day 21 with silver nitrate/methyl green. (**C.**) Phase contrast image (40x) of an ESC-derived osteogenic colony 7 days post-plating. The opaque area in the center of the colony indicates enhanced matrix secretion, while the darker central area represents early mineral deposition. This figure is representative of ten experiments that fall within the criteria listed in the results section.

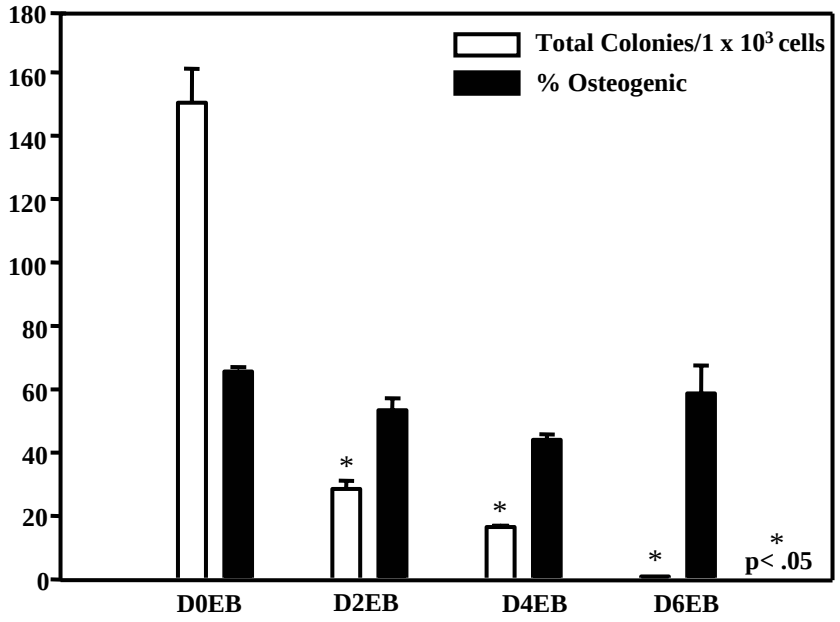

Figure 3.2: Total colony forming units and percentage of colonies with mineralization after osteogenic culture plating of day 0 (D0EB), day 2 (D2EB), day 4 (D4EB), and day 6 (D6EB) embryoid bodies. Total colonies are plotted per 1 x 10^3 cells plated. D0EB: total colonies (151.67 +/- 10.83) and percent osteogenic (66.33% +/- 1.36%), D2EB: total colonies (29.00 +/- 2.52) and percent osteogenic (54.00% +/- 6.54%), D4EB: total colonies (16.83 +/- .83) and percent osteogenic (44.57% +/- 1.80%), D6EB: total colonies (1.17 +/- .04) and percent osteogenic (59.30% +/- 8.94%). Asterisk represents significant difference when compared to D0EB Total Colonies.

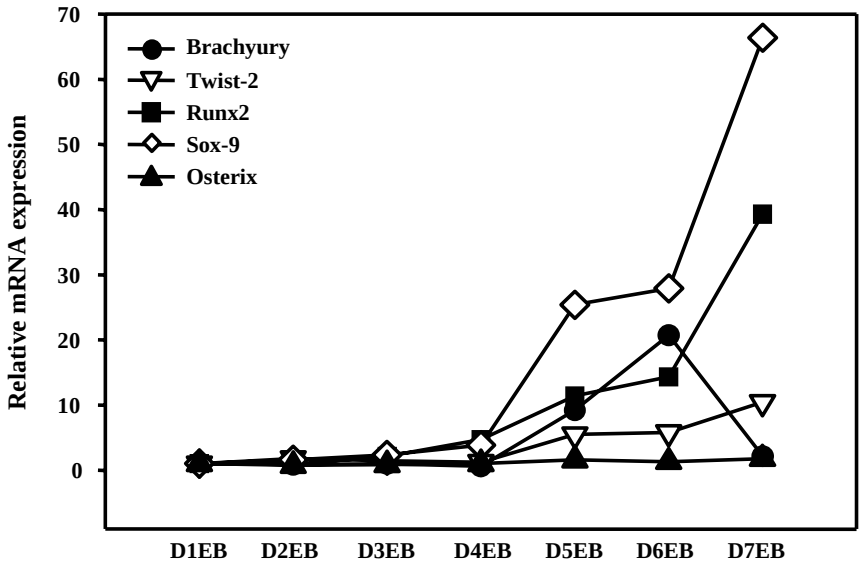

Figure 3.3: QRT-PCR analysis of transcription factors in embryoid bodies from sequential days of formation. Each assay was run in duplicate at two different template concentrations. Relative mRNA expression was normalized to ribosomal protein L7 (*Rpl7*) and displayed relative to D1EB (day 1 embryoid body).

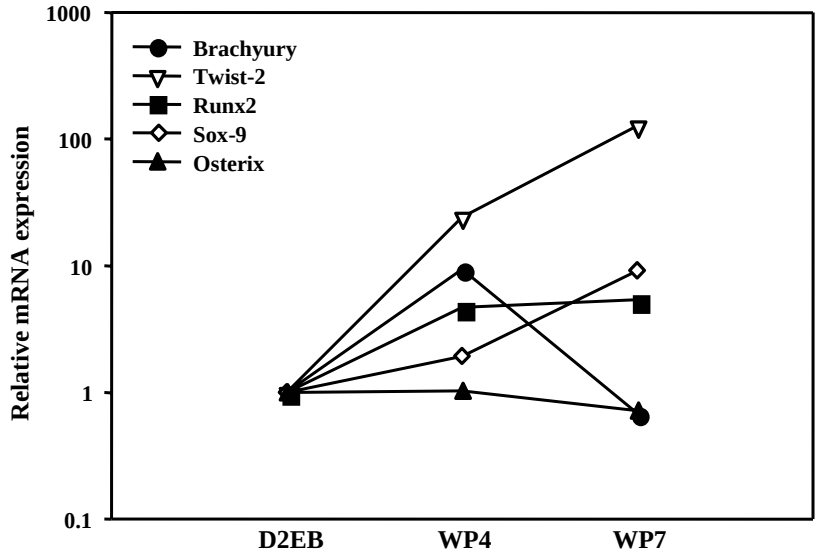

Figure 3.4: QRT-PCR analysis of transcription factors during early osteogenic cultures. Each assay was run in duplicate at two different template concentrations. Relative mRNA expression was normalized to ribosomal protein L7 (*Rpl7*), displayed relative to D2EB, and presented as a common log plot. D2EB = day 2 embryoid body, WP4 = whole plate day 4, WP7 = whole plate day 7

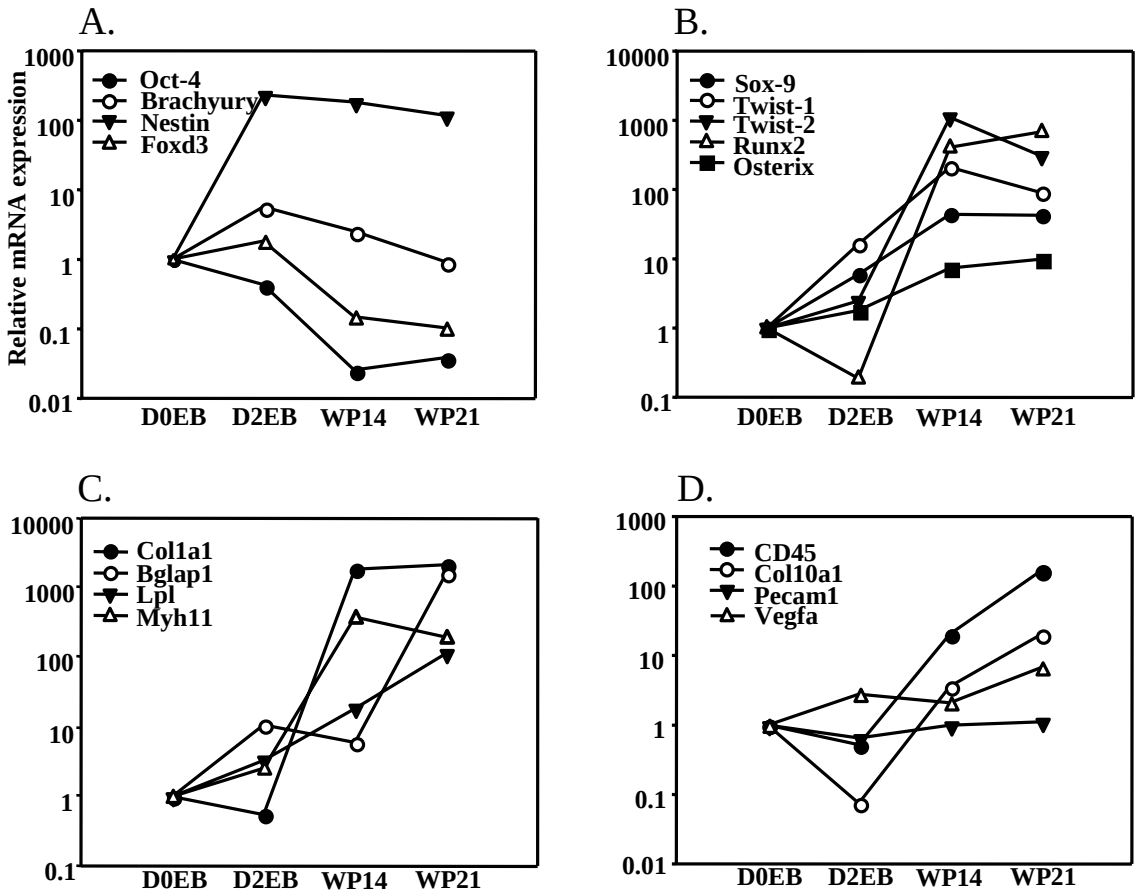

Figure 3.5: QRT-PCR analysis of ESC-derived osteogenic cultures. Each assay was run in duplicate at two different template concentrations. Relative mRNA expression was normalized to ribosomal protein L7 (*Rpl7*), displayed relative to D0EB, and presented as a common log plot. D0EB = day 0 embryoid body, D2EB = day 2 embryoid body, WP14 = whole plate day 14, WP21 = whole plate day 21. The data presented in this figure were obtained from a single osteogenic culture experiment, although two additional experiments provided the same results. Subsets of genes were also repeated in numerous additional osteogenic culture experiments. Groupings of **A.**, **B.**, **C.**, and **D.** will be discussed in Results section 3.2.3. QRT-PCR data has been published (169).

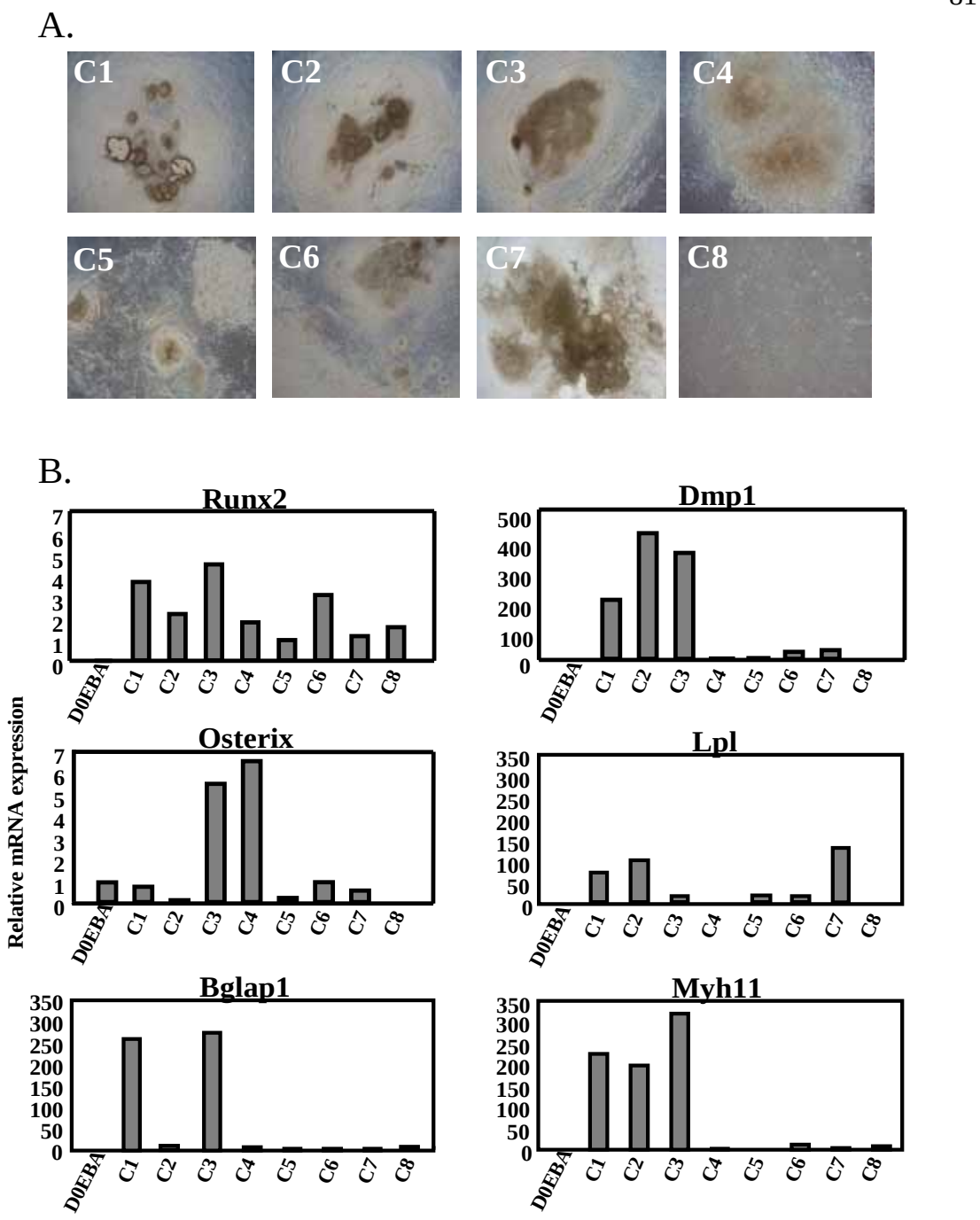

Figure 3.6: Phase contrast microscopy and QRT-PCR analysis of individual colonies. (**A.**) Phase contrast images (40x) of individual osteogenic colonies at day 21. (**B.**) QRT-PCR analysis of gene expression in individual osteogenic colonies at day 21. All RNA samples were amplified. Each assay was run in duplicate or quadruplicate at two different template concentrations. Relative mRNA expression was normalized to ribosomal protein L7 (*Rpl7*) and displayed relative to D0EBA, with the exception of *Runx2*, which was normalized to C5 due to limiting *Runx2* expression in the D0EB sample. D0EBA = D0EB amplified, C1 = colony 1, etc. Phase contrast images and QRT-PCR data have been published (169).

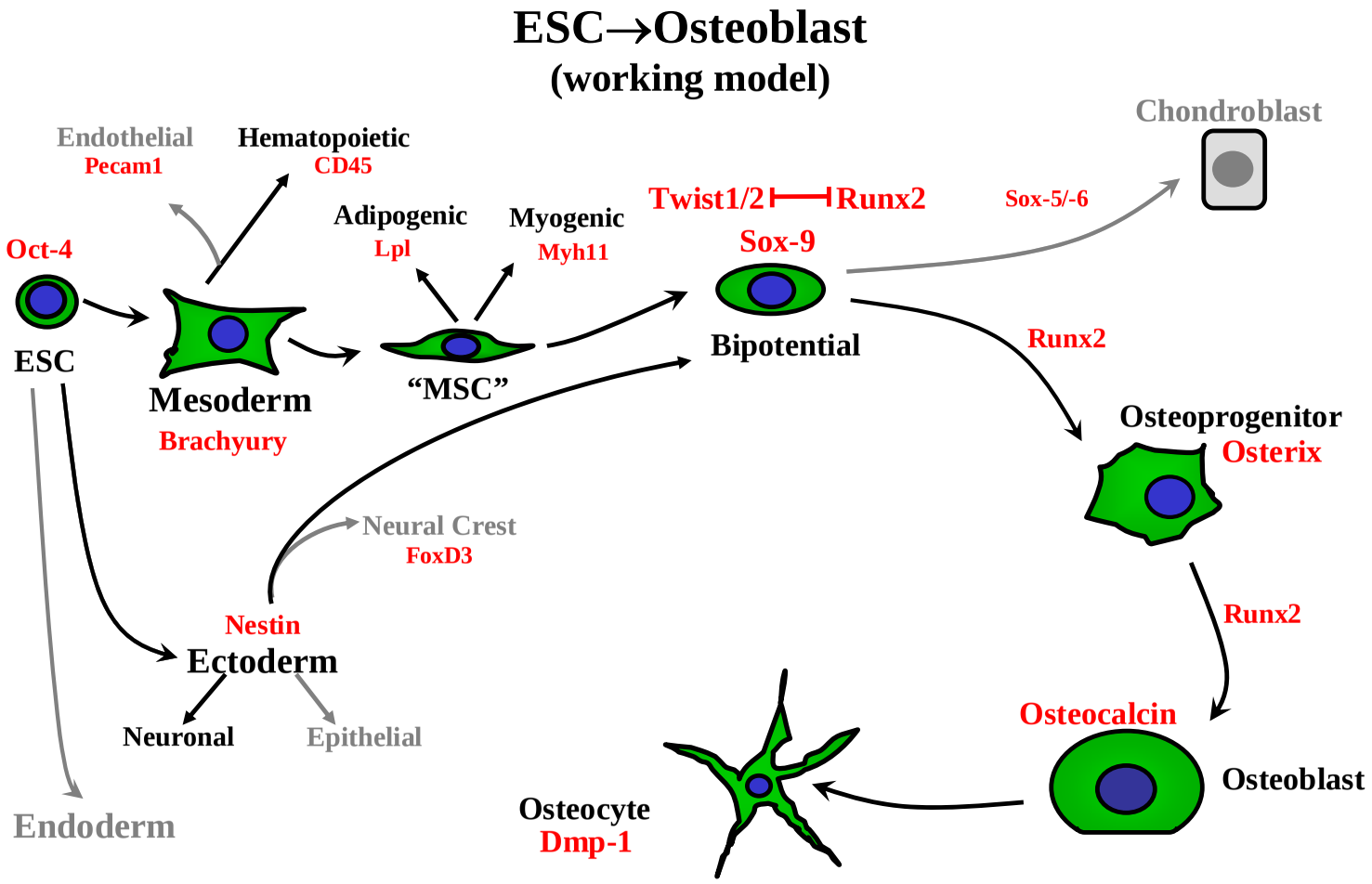

Figure 3.7: Overview of ESCs to osteoblast differentiation. Expected cell types are in black font and relevant gene expression markers are in red font. Lineages in gray have either not been tested (i.e. endoderm) or are suggested to be absent due to an absence of mature markers (i.e. cartilage). (source Bronson laboratory)

Table 3.1 Phenotype of Individual Colonies Based on RNA and Morphology

Colony #	Osteogenic			Myogenic	Adipogenic	Other
	Early	Mature	Late			
1		X		X	X	
2			X	X	X	
3	X	X	X	X	X	
4	X					
5					X	
6	X			X	X	
7					X	
8						X

CHAPTER 4

CONSTITUTIVE AND INDUCIBLE OVEREXPRESSION OF RUNX2 IN THE OSTEOGENIC CULTURE SYSTEM

4.1 Introduction

Understanding the commitment of the ESC-derived progenitors to the osteogenic lineage is a critical step in being able to use these cells therapeutically. In the *in vitro* osteogenic culture system described and characterized in Chapter 3, the starting cell populations are ESCs, which have the potential to develop into all cell types of the developing embryo, including osteoblasts. After the differentiation of these cells during three weeks in culture, the resulting cell population is more restricted, consisting mainly of mature mesodermal cells, including adipocytes, smooth muscle, and osteoblasts (typically 60% mineralize). Neither of these time points is an ideal population for therapeutic purposes. However, as these ESC-derived progenitor cells begin to differentiate, we hypothesize that a critical decision point involving the mesenchymal lineages occurs where these cells commit, in particular, to the osteogenic lineage. Identifying the commitment stage of osteogenesis in these cultures will allow for a better understanding of this lineage, as well as serving as a starting point for identifying progenitors that have a therapeutic capacity. One technique available for understanding the commitment of progenitor cells to the osteogenic lineage is overexpression of critical factors, specifically the overexpression of *Runx2*, a transcription factor known to be essential for osteogenesis. In order to manipulate osteogenesis in the culture system, we

have utilized three methods of increasing *Runx2* expression: (i) up-regulation of *Runx2* by bone morphogenetic protein 2 (BMP-2), (ii) constitutive overexpression of *Runx2* constructs, and (iii) tetracycline-inducible overexpression of *Runx2* constructs.

4.1.1 Bone Morphogenetic Protein 2 (BMP-2)

BMPs are multi-functional growth factors that belong to the transforming growth factor β (TGF-β) superfamily. This characterization is based on primary amino acid sequence homology, including the conservation of seven cysteine residues between the TGF-βs and BMPs (170,171). The activity of BMPs was first discovered by their ability to induce bone formation in the 1960s by Marshall R. Urist (172). They were identified by their presence in bone-inductive extracts of demineralized bone (discussed in (171)). However, the actual identification of specific proteins did not occur until the 1980s when BMP-2 (BMP-2A), BMP-4 (BMP-2B), and BMP-3 (osteogenin) were identified (reviewed in (170)) (173,174). The BMPs have been found to signal through serine/threonine kinase receptors, which include type I and type II subtypes. The type I receptors consist of type IA and IB BMP receptors and type IA activin receptor. The type II receptors consist of type II BMP receptor and type II and IIB activin receptors. The binding to BMP receptors activates their serine/threonine kinase activity, which in turn phosphorylates receptor specific Smads (reviewed in (170)). There are currently approximately twenty BMP family members that have been identified and characterized, and among these, BMP-2, -4, and -7 have been shown to be bone-inducing agents. In particular, BMP-2 was identified from protein extracts of bovine bone, and subsequently, a human cDNA clone was isolated that was shown to induce the formation of cartilage *in*

vivo (173). Human recombinant BMP-2 was also shown to form new bone in a rat ectopic assay system (171,175).

BMPs play a role in the development of several different systems, including heart, nervous tissue, cartilage, and bone. In particular, BMP-2, as stated above, has been shown to induce bone formation and *Runx2* mRNA expression in several different cell lines and model systems. It was shown in the mesenchymal precursor cell line C2C12 that BMP-2 blocked myogenic differentiation and transiently induced expression of *Runx2*, as well as type I collagen and alkaline phosphatase. The expression of *Runx2* was then down-regulated upon expression of the mature osteoblast markers osteopontin and osteocalcin. However, in transfection studies, BMP-2 suppressed osteocalcin promoter activity in C2C12 cells but not in osteoblastic ROS 17/2.8 cells. This suggested that BMP-2 could transiently induce *Runx2* expression and transdifferentiate a myoblastic cell to a potentially osteogenic cell but was not sufficient for osteoblast differentiation (176). Later studies in this same line (C2C12) verified these results and indicated that while *Runx2* was a target of BMP-2, an additional effector, BMP-specific Smad protein, was required for osteoblastic specific gene expression (177). Conversely, it was shown in C3H10T1/2 mesenchymal cells and primary cultures of marrow stromal cells that BMP-2 was required for *Runx2*-mediated induction of the osteoblast phenotype. The cells were transduced with a *Runx2* adenovirus and treated with BMP-blocking antibodies or its natural antagonist, Noggin. This inhibition of BMP-2 signaling disrupted the ability of Runx2 to activate an osteocalcin gene promoter-luciferase reporter in C3H10T1/2 cells, suggesting the absence of osteoblast differentiation (178).

In the studies above, it was shown that BMP-2 signaling can up-regulate osteoblast transcription factors, specifically *Runx2*, and osteoblast gene expression; however, a study with cycloheximide, a *de novo* protein synthesis inhibitor, blocked the BMP-2-induced expression of *Runx2*, suggesting *Runx2* is not the direct target of BMP-2 in the signaling cascade (179,180). Also mentioned above is the need for a BMP-specific Smad protein in osteoblastic specific gene expression, which further suggests intermediates in this pathway. It was shown that this intermediate was Dlx5, a bone-inducing homeodomain transcription factor that is expressed at later stages of osteoblast differentiation (179-181). *Dlx5*-deficient mice have a severe craniofacial abnormality with delayed cranial ossification and abnormal osteogenesis (180,182). *Dlx5* was found to be co-expressed with *BMP-2* (183), and *Dlx5* transcription was induced by BMP-2 treatment and unaffected by cycloheximide (179,180). This shows that *Dlx5* is downstream of BMP-2 signaling and suggests its role as the intermediate between BMP-2 and *Runx2* up-regulation. The inhibition of *Dlx5* by antisense expression vectors blocked the expression of *Runx2*, and *Dlx5* overexpression induced *Runx2* expression in the absence of *BMP-2*, further supporting this hypothesis (180). However, there is some confusion with regards to the exact role of these transcription factors in osteogenesis because *Dlx5* is expressed during later stages of osteoblast differentiation and Runx2 function has been suggested as the mediator of osteogenic commitment. In a review of BMP-2 induced osteogenic differentiation, several ideas to explain this apparent disparity were discussed (180). One possibility is that the hierarchy of expression of these transcription factors is different. In skeletal development, *Runx2* could be upstream of *Dlx5*, but in BMP-2 induced osteogenesis, *Dlx5* could be an upstream regulator of *Runx2*,

as well as osterix. This review suggests that BMP-2 may not be the initial inducer of *Runx2* expression during embryonic skeletogenesis and that perhaps other factors, such as fibroblast growth factors (FGFs), can induce expression of *Runx2*, impacting the commitment to osteogenic differentiation without involving Dlx5. And consequently, BMP-2 and Dlx5 mediated transcription are activated in later stages of differentiation and mineralization after *Runx2* expression has already been up-regulated (reviewed in (180)). Therefore, the impact of BMP-2 on the osteogenic culture system introduced in this thesis is worth investigating.

4.1.2 Effect of Runx2 Overexpression on Bone Formation

It is known from knockout studies conducted in mice that *Runx2* is required for osteoblast differentiation, but studies involving the overexpression of *Runx2* have proven to be somewhat more complicated to interpret. In rat mesenchymal stem cells, constructs were engineered to constitutively express *Runx2* and were introduced using retroviral gene delivery (184). The overexpression of *Runx2* in these cells significantly up-regulated osteoblastic differentiation and mineralization both *in vitro* and *in vivo* in an ectopic, nonosseous subcutaneous site. This same group showed that the overexpression of *Runx2* up-regulated osteoblast-specific genes, such as type I collagen and osteocalcin, as well as increasing alkaline phosphatase activity and mineralization (95). It was also previously shown that *Runx2* overexpression had the ability to induce osteoblast-specific gene expression but mineralization was cell-type-dependent (96). In NIH3T3 and C3H10T1/2 fibroblast cells and MC3T3-E1 immature osteoblast-like cells, the overexpression of *Runx2* induced expression of osteoblast-specific genes, but NIH3T3

and C3H10T1/2 cells were not able to produce significant mineralization while MC3T3-E1 cells showed robust up-regulation of matrix mineralization. In contrast to these overexpression studies, the overexpression of *Runx2* in lineage restricted osteoblasts blocked terminal differentiation and increased bone resorption (97,98). Transgenic mice were generated that overexpressed *Runx2* in osteoblasts using a type I collagen promoter, and this resulted in osteopenia, or a reduction in bone mass. Neonatal osteoblasts were found to accumulate while terminally differentiated osteoblasts were decreased suggesting that overexpression of *Runx2* was inhibitory at late stages of osteoblast development (97). Subsequent studies in mesenchymal stem cell transgenic lines suggested that overexpression of *Runx2* didn't increase bone formation but increased osteoclast differentiation *in vitro*, thus increasing bone resorption (98). *Runx2* overexpression was also shown to enhance osteoblastic differentiation and mineralization in adipose-derived stem cells both *in vitro* and *in vivo* when delivered by an adenovirus vector (185). These studies suggest that the expression of *Runx2* in bone formation relies heavily on the timing of expression and is cell type-dependent (21).

4.1.3 Tetracycline-Inducible Expression Systems

The regulation of *Runx2* in stimulating osteogenesis is critical for both gaining a better understanding of the process of bone formation and for developing safe and controlled methods for gene therapy. The overexpression of certain factors known to impact osteogenic growth and differentiation can be an instrumental tool when thinking therapeutically; however, the unregulated overexpression of these factors can lead to

abnormal bone formation. Recently, studies have been conducted in which the expression of *Runx2* is regulated in a tetracycline-inducible manner (186).

The tetracycline-regulatable system is one of the most widely used systems for controlling gene expression (187). This is mainly because it has so many advantages, such as the use of cell type-specific promoters to regulate target gene expression, its non-toxicity to mammalian cells, and its lack of pleiotropic consequences on other cellular metabolic pathways (187). Tetracycline and its analogue doxycycline are rapidly metabolized and do not interfere with native proteins (187). The first tetracycline-inducible system was described by Gossen and Bujard (188). They used the control elements of the tetracycline resistance operon encoded in Tn10 of *Escherichia coli* (*E. coli*) to create the regulatory system. The tetracycline-controlled transactivator (tTA) was created by the fusion of the *E. coli* tetracycline repressor (TetR) and the activating domain of virion protein 16 of the herpes simplex virus, which converts TetR from a transcriptional repressor to an activator. In the absence of tetracycline, tTA will bind to the tet operon (tetO) and activate transcription of the gene that is downstream. The tetracycline responsive element (TRE) consists of seven tandom tetO sequences upstream of a promoter, typically the CMV promoter. In the presence of tetracycline, tetracycline will bind to tTA, which blocks its ability to bind to tetO thus, preventing the activation of the downstream gene (186,188). This system is referred to as the Tet-OFF system (Fig. 4.1A). The Tet-ON system is based on mutations to the Tet-OFF system (187). Again, Gossen and colleagues induced a mutation of four amino acid exchanges in the original TetR that is bound to the VP16 domain, which resulted in the opposite function. The mutant was termed rtTA for reverse tetracycline-responsive transcriptional activator

(187,189). In this system rtTA is activated in the presence of tetracycline and activates the TRE, thus activating the downstream gene; in the absence of tetracycline, expression is switched off (Fig. 4.1B). It has been shown that the Tet-OFF system is more effective in regulating transgene expression than the Tet-ON system because the rtTA has some degree of affinity for tetO sequences in the absence of tetracycline, resulting in basal activity (187,190).

The Runx2 tetracycline-inducible system mentioned above is a Tet-OFF system that was delivered by a retrovirus to primary skeletal myoblasts (186). It was shown that the osteogenic effect of *Runx2* could be regulated by a tetracycline-responsive system both *in vitro* and *in vivo*. In the presence of anhydrotetracycline (aTc), *Runx2* mRNA and protein expression decreased in a dose-dependent manner. The expression of osteocalcin, bone sialoprotein, osteopontin, and osterix also decreased in the presence of aTc. Conversely, the expression of myogenin and troponin T, markers associated with myoblastic differentiation, increased in the presence of aTc, also in a dose-dependent manner. This expression pattern correlated with a decrease in alkaline phosphatase activity as well as calcium content in the presence of aTc and in the absence of aTc, von Kossa staining showing significant phosphate deposits. The osteoblastic differentiation could be temporally regulated by adding and removing aTc from the culture media. *In vivo*, cells were seeded onto collagen scaffolds and implanted intramuscularly in the hind limbs of syngeneic mice. Drinking water was supplemented with sucrose or aTc and mineralization was regulated as seen in the *in vitro* experiments (186). This study showed that the tetracycline-inducible regulation of *Runx2* could stimulate osteogenesis in myoblastic cells.

4.1.4 Random Integration of Transgenes

The constructs used in Chapters 4 and 5 were introduced into murine embryonic stem cells by either random integration or targeted integration through homologous recombination at the Hprt locus. Random integration can result in variable expression of the transgene based on the site of integration and/or the copy number. Conversely, random integration at certain sites can result in alterations to the host genome that lead to differences in phenotypes not associated with the integrated sequences. In terms of the site of integration, there can be position-dependent or independent transgene expression. In position-dependent transgene expression, the effects can either be grouped as stable position effects or silencing position effects, also known as position effect variegation (PEV). Stable position effects result in differences in expression between the transgene and the endogenous locus or transgenes integrated at other sites. These effects are the result of enhancer, promoter, or silencer elements near the site of integration. When a transgene contains sufficient regulatory elements (such as bacterial artificial chromosomes (BACs) or yeast artificial chromosomes (YACs)), the effect of regulatory elements at the site of integration is usually overridden. However, in smaller transgenes, the control mechanisms may not be dominant enough to overcome these position effects (191).

PEV is the variation in expression caused by the inactivation of a gene through its abnormal juxtaposition to heterochromatin (192). The inactivation can vary from cell to cell and result in mosaicism or variegation of the phenotype. The first description of PEV was in 1930 by Hermann Muller and described in *Drosophila* mutants (193,194). The mutants were generated by X-ray irradiation and showed mosaic expression of the

white gene, which is responsible for red eye color. This variable expression was shown to be associated with a chromosomal translocation of the *white* gene close to pericentric heterochromatin. This silencing effect gave rise to red and white patches of the *Drosophila* eye (194).

While larger transgenes, such as BACs and YACs, may contain sufficient regulatory elements to override position effects, there are also regulatory elements termed locus control regions (LCRs) that can overcome these position effects and lead to position-independent expression of the transgene (195). LCRs have the ability to direct tissue specific and copy-number dependent expression at high levels regardless of their chromosomal site of integration. The first LCR was identified in the β-globin gene and subsequently in the human CD2 gene (194,196,197). It was found that regions 5′ and 3′ to the β-globin locus contained DNase I hypersensitive sites that allowed for the tissue-specific and copy number-dependent expression of a transgene regardless of its integration site (196). A similar DNase I hypersensitive site was found in the 3′ flanking region of the human CD2 gene and also conferred tissue-specific and copy number-dependent expression (197). These regions confer position-independent expression by conferring an open chromatin domain (195).

While the site of integration can have an effect on the transgenes expression, the number of copies of the transgene that are inserted can also impact expression levels. It would seem that the more copies of a transgene that are integrated, the higher the gene expression; however, this is not usually the case. In fact, there is typically not a linear relationship between copy number and expression level of a transgene due to the site of integration. When a transgene is integrated it typically inserts in a concatameric array at

a single position. These multiple tandom repeats can lead to a decrease in the level of expression per copy as copy number increases. It has also been shown that a reduction in copy number results in an increase in expression of the transgene (198). As well as position effects and copy number-dependent effects, random integration can also lead to insertional mutagenesis. Insertional mutagenesis is the insertion of the transgene into either the coding sequence or regulatory elements of an endogenous gene, resulting in abnormal gene function.

4.1.5 Targeted Integration of Transgenes Through Homologous Recombination at the Hprt Locus

Another method for integrating a transgene into embryonic stem cells (ESCs) is the targeted integration of a single-copy to a chosen-site. Not only is this another method for integration, but it also has many advantages over random integration, including the ability to control position of insertion, copy number, and exclusion of insertional mutagenesis (130). Some of the constructs or transgenes used in Chapters 4 and 5 were integrated using this technique, which utilizes homologous recombination for site-specific integration. The chosen site used in this method is the hypoxanthine phosphoribosyltransferase (Hprt) locus, which is located on the X chromosome and codes for a housekeeping gene that is ubiquitously expressed and located in a region of open chromatin (199). The embryonic stem cell lines used in this thesis (a rederivation or subclone of E14TG2a (126,127)) have a partial deletion in the Hprt locus, which can be restored by inclusion of sequences that complement the deletion in the targeting vector. The targeting vector contains complementary sequences 5′ and 3′ to the Hprt deletion that

flank the transgene to be integrated. The complementary sequences 3′ to the transgene contain a portion of the human HPRT as well as mouse Hprt. Through homologous recombination, the targeting vector is recombined into the Hprt locus, rescuing the Hprt deletion and integrating the transgene. Correctly targeted transgenes can then be selected by growth in hypoxanthine-aminopterin-thymidine (HAT) medium (130,133). This technique results in the integration of the transgene in a single-copy to a chosen site in the ESCs. Figure 4.2 depicts the general method for targeting transgenes to the Hprt locus in ESCs.

4.2 Results

4.2.1 Effect of Bone Morphogenetic Protein 2 (BMP-2) on the Osteogenic Culture

Human recombinant BMP-2 was added to the osteogenic cultures to investigate the impact on total colony formation, as well as mRNA expression of *Runx2* and other related osteogenic factors. Figure 4.3 shows the total number of colonies and the percentage of colonies with mineralization at 21 days of the osteogenic culture after treatment with BMP-2 on days 1 and 2. BMP-2 was added at a concentration of 40 ng/μl. The medium was removed from the osteogenic culture plates and supplemented with 2 μl of BMP-2 in 1 ml of osteogenic culture medium for a final concentration of 80 ng/ml. After two hours, 9 ml of osteogenic culture medium was added. This process was repeated for two consecutive days of the osteogenic culture. Addition of BMP-2 to the osteogenic culture at days 1 and 2 resulted in a significant ($p<0.05$) decrease in total colonies when compared to the number of total colonies of plates that did not receive BMP-2, approximately 36 colonies in comparison to 145, respectively. The percentage of colonies that displayed layering and mineralization upon staining with silver nitrate (% osteogenic) did not change significantly when BMP-2 was added, suggesting that BMP-2 has a negative impact on overall colony formation but not mineralization when added during early time points of the osteogenic culture.

In the experiment shown in Figure 4.4, BMP-2 was added on two consecutive days of the culture, starting with days 1 and 2 and continuing until days 8 and 9; BMP-2 was also added on days 15 and 16. Similar to the results shown in Figure 4.3, there was a significant ($p<0.05$) decrease in total colonies at day 21 when BMP-2 was added to the

osteogenic culture at days 1 and 2, as well as at days 2 and 3, when compared to the no manipulation control. (The no manipulation control was added to this experiment in order to control for the removal and addition of medium to the plates.) After day 3, BMP-2 addition did not have a significant impact on the total number of colonies when compared to the no manipulation plates (Fig. 4.4A). There was no significant difference in the total number of colonies when BMP-2 was not added to the osteogenic culture in comparison to no manipulation plates at any time points, indicating the medium changes had no effect on the osteogenic culture. The effect of medium removal was also tested in a third experiment with no appreciable differences observed (data not shown). The percentage of colonies that mineralized did not change significantly when BMP-2 was present or absent when compared to the no manipulation plates (Fig. 4.4B), further suggesting that addition of BMP-2 to the osteogenic culture during early time points, specifically before day 3, has a negative impact on colony formation.

BMP-2 has been shown to induce *Runx2* mRNA expression in different cell lines and model systems (176). Figure 4.5 shows the results of QRT-PCR analysis of *Runx2* mRNA expression at days 3, 6, and 9 of the osteogenic culture when BMP-2 was added at days 1 and 2; 4 and 5; and 5 and 6. There was an up-regulation of *Runx2* mRNA expression at day 3 of the osteogenic culture when BMP-2 was added at days 1 and 2 when compared to plates that did not receive BMP-2 (No BMP-2) (Fig. 4.5A). There was also an up-regulation of *Runx2* mRNA expression at day 6 of the osteogenic culture when BMP-2 was added at days 4 and 5 in comparison to No BMP-2 plates. However, at day 6, the up-regulation of *Runx2* mRNA expression that was seen at day 3 from addition of BMP-2 on days 1 and 2 was not observed, suggesting the up-regulation of *Runx2*

mRNA by BMP-2 to be transient (Fig. 4.5B). The up-regulation of *Runx2* was also observed at day 9 of the osteogenic culture when BMP-2 was added on days 4 and 5 and 5 and 6 but not on days 1 and 2, in comparison to No BMP-2 plates (Fig. 4.5C).

Since BMP-2 was shown to impact the cultures when added before day 3, the mRNA expression of other factors known to be up-regulated during these time points (Chapter 3) was investigated (Fig. 4.6). As can be seen in Figure 4.6A, the mRNA expression of *Oct-4* was shown by QRT-PCR to be significantly ($p<0.05$) down-regulated when BMP-2 was added to the cultures on days 1 and 2 in comparison to No BMP-2 plates. *Oct-4* is a transcription factor necessary for self-renewal and maintenance of pluripotency in ESCs (146,147), suggesting the addition of BMP-2 to the cultures induces differentiation. The expression of brachyury, a transcription factor that plays a role in the formation and organization of the mesoderm (148), was also significantly ($p<0.05$) down-regulated when BMP-2 was added to the cultures on days 1 and 2 in comparison to No BMP-2 plates, further suggesting an early induction of differentiation in these plates (Fig. 4.6B). Nestin was also significantly ($p<0.05$) down-regulated when BMP-2 was added to the cultures on days 1 and 2 in comparison with No BMP-2 plates (Fig. 4.6C). Nestin is a marker of neuroepithelial stem cells and myoprogenitors, further suggesting what was hypothesized with *Oct-4* and brachyury. Figure 4.6D shows the mRNA expression of *Twist-2* when BMP-2 was added to cultures on days 1 and 2. Although there is a trend toward down-regulation of *Twist-2* when BMP-2 was added, the decrease does not reach statistical significance. Twist-2 is a transcription factor implicated in bone development and has been shown to regulate the function of Runx2 (47). While *Twist-2* is expressed in *Runx2* expressing cells, the function of Runx2 is not

seen until *Twist-2* expression is decreased (47). This suggests that the down-regulation of *Twist-2* coincides with the up-regulation of *Runx2* expression. The down-regulation of these factors on day 3 of the osteogenic culture when BMP-2 was added on days 1 and 2 suggests a premature differentiation of progenitor cells at this time point.

The possible early induction of differentiation led to the investigation of mature lineage markers on day 21 of the osteogenic culture when BMP-2 was added on days 1 and 2, and 5 and 6 (Fig. 4.7). In comparison to No BMP-2 plates, the expression of *Bglap1*, a marker of bone formation (22-24) was significantly ($p<0.05$) down-regulated at day 21 when BMP-2 was added to cultures on days 1 and 2 but not on days 5 and 6, in comparison to No BMP-2 plates (Fig.4.7A). This suggests that the addition of BMP-2 before day 3 of the osteogenic culture is detrimental to the osteogenic potential of the cells. This down-regulation was also seen with *Myh11* expression, a marker of smooth muscle, when BMP-2 was added on days 1 and 2, as well as days 5 and 6 (Fig.4.7B). However, the same impact was not seen with *Lpl* expression, a marker for adipose cells (Fig. 4.7C). While BMP-2 has been shown to transiently induce *Runx2* expression in the osteogenic culture, there appears to be a negative impact on total colony forming units and osteogenic and myogenic gene expression by 21 days when BMP-2 has been added before day 3. This decrease in osteogenic potential may be caused by the apparent early induction of differentiation observed by the down-regulation of factors necessary for the maintenance of progenitor cells. This premature push for differentiation may be occurring before some progenitor cells are ready to commit to a lineage and in turn they lose their proliferative capacity, thus the decrease in number of total colonies and the loss of osteogenic gene expression.

4.2.2 Constitutive Overexpression of Runx2 in the Osteogenic Culture

To further investigate the up-regulation of *Runx2* in the osteogenic cultures, constitutive overexpression of *Runx2* constructs were used. Figure 4.8 shows a diagram of the construct, illustrating the components of the transgene, as well as those necessary for the targeted integration of the construct to the Hprt locus. The constitutive overexpression of the *Runx2* construct was cloned, verified, and targeted to the Hprt locus of ESCs by Kimberly Dunham, a former member of the Bronson laboratory. The construct contains *Runx2* cDNA downstream of the human beta-actin promoter, as well as 5′ Hprt homology upstream and 3′ Hprt homology downstream of the promoter and cDNA. This allows for the targeted integration of the human beta-actin promoter constitutively expressing *Runx2* cDNA in a single-copy to the Hprt locus.

Three ESC clones that survived HAT selection were used to investigate the impact of constitutive *Runx2* overexpression on the total colony forming units and the percentage of colonies that are able to mineralize in the osteogenic culture system (Fig. 4.9). By day 21 of the osteogenic culture, the three clones constitutively overexpressing *Runx2* showed a significant ($p<0.05$) decrease in total colony forming units when compared to the parental ESC line that did not have a targeted construct. These three clones also showed a decrease in mineralization (% osteogenic) when compared to the parental ESC line, although the decrease was significant ($p<0.05$) only in clone 2.

The expression of *Runx2* was investigated by QRT-PCR in the day 0 embryoid body (D0EB) and in the whole plate at day 21 (WP21) of the osteogenic culture (Fig. 4.10A). In the D0EB, the expression of *Runx2* was up-regulated at least 600-fold in clones 1, 2, and 3 in comparison to the parental ESC line. While the up-regulation of

Runx2 was significant ($p<0.1$) only in clones 1 and 2, the expression of *Runx2* amongst clones 1, 2, and 3 was not significantly different. This showed that *Runx2* was in fact being overexpressed in the clones containing the hβa-*Runx2* construct. At day 21 of the osteogenic culture, the expression of *Runx2* was up-regulated approximately 90-fold in the parental ESC line compared to the D0EB, which is typical of the osteogenic culture (Fig. 3.5B). The expression of *Runx2* in clones 1, 2, and 3 at day 21 was overexpressed at least 500-fold, but in comparison to the parental ESC line, only clones 1 and 2 were significantly ($p<0.1$) overexpressed. Again, there was no significant difference between *Runx2* expression of clones 1, 2, and 3 at day 21. This showed that *Runx2* was being overexpressed in all three clones throughout the osteogenic culture.

The impact of *Runx2* overexpression on mature lineage markers was then investigated (Fig. 4.10B). The expression of *Bglap1*, *Myh11*, and *Lpl* were not up-regulated in the D0EB of the parental ESC line or any of the clones. At day 21, all three lineage markers were up-regulated in the parental ESC line, which is typical of the osteogenic culture (Fig. 3.5C). However, in the three clones, *Bglap1* and *Myh11* expression were significantly ($p<0.1$) down-regulated in comparison to the parental ESC line at day 21. *Lpl* was significantly ($p<0.1$) down-regulated in clones 1 and 3 but not in clone 2 in comparison to the parental ESC line at day 21. These experiments suggest that the overexpression of *Runx2* throughout the osteogenic culture is detrimental to total colony forming units and mineralization and the potential of precursor cells for the osteogenic, myogenic, and to some degree, adipogenic lineages. These results support the BMP-2 experiments, suggesting that the overexpression of *Runx2* during early time points is inhibitory to the osteogenic lineage. These experiments illustrate the need for an

inducible overexpression system in the osteogenic culture because perhaps, as seen in other systems (21), the timing of *Runx2* expression is critical for osteogenesis.

4.2.3 Tetracycline-Inducible Overexpression of Runx2 in the Osteogenic Culture

The inducible system utilized to investigate the overexpression of *Runx2* in the osteogenic culture is a Tet-On system and, therefore, regulated by tetracycline addition. The tetracycline-inducible overexpression of *Runx2* consists of two separate constructs, the rtTA and the inducible *Runx2* cDNA. The rtTA construct (pKD2) contains the human beta-actin promoter upstream of a reverse tetracycline-responsive transcriptional activator (rtTA), making the expression of rtTA constitutive. This construct also contains the Neo^R gene so that G418 resistance can be used to identify ESCs that have stably integrated the construct (Fig. 4.11A). Figure 4.11B displays an agarose gel of the rtTA construct DNA digested with the restriction endonucleases XhoI and PmeI, verifying the proper cloning of the construct. The 7.4 kb fragment obtained from this digestion was then isolated, purified, and electroporated into the HM1 ESC line. After random integration, RT-PCR was conducted to test for the presence of the rtTA in a subset of ESC clones that were G418-resistant (Fig. 4.11C). (The negative control is cDNA from a D0EB which does not contain the rtTA, and the positive control is the parental plasmid pKD2.) All 16 clones tested produced a product of the correct base pair size. These clones, as well as several others, were then tested by QRT-PCR for the expression level of rtTA (Fig. 4.12). The upper panel in Figure 4.12 shows the first subset of clones tested, and the clone numbers correspond to those in Figure 4.11. Of this subset, clone 3 expressed rtTA at the highest level. This clone was then compared to another subset of

clones, shown in the lower panel of Figure 4.12. Of all clones tested for the expression of rtTA, clone 3 displayed the highest expression. The clone expressing rtTA at the highest level is desired because in this system, it would seem logical to assume that the more rtTA present, the more molecules for tetracycline to bind to and activate the TRE, thus increasing transcription of the downstream gene (Fig. 4.1B). Therefore, ESC clone 3 was used for the targeted integration of the second construct utilized in this system.

The second construct necessary for this system to function contains a *Runx2* cDNA downstream of a TRE that contains a tetracycline-inducible promoter. The cDNA used in this construct is the same cDNA used in the constitutive overexpression of *Runx2* constructs. This construct also contains 5′ Hprt homology upstream and 3′ Hprt homology downstream of the TRE-*Runx2* cDNA for targeted integration at the Hprt locus (Fig. 4.13A). The proper construction of this construct was verified by restriction enzyme digestion with BamHI, XbaI, and SalI (Fig. 4.13B). Once verification of cloning was complete, the vector was linearized, purified, and electroporated. This construct was targeted in a single-copy to the Hprt locus of the previously identified, rtTA-containing clone 3 (Figures 4.11 and 4.12). ESCs that survived HAT selection were then tested for the presence of the rescued Hprt locus by RT-PCR analysis with primers designed to detect the human HPRT and downstream 3′ Hprt homology (See Table 2.5 for primer sequences). Figure 5.13C shows the RT-PCR analysis for the clone used in the following experiments to study the overexpression of *Runx2* in the ESCs, as well as throughout the osteogenic culture. The left panel of Figure 5.13C shows the agarose gel of the positive and negative controls for the primer pair and the right panel shows the agarose gel indicating the expected band size in the clone.

Figure 4.14 reveals the results of QRT-PCR analysis of *Runx2* mRNA expression in an ESC line containing the randomly integrated rtTA and the targeted, inducible *Runx2* cDNA construct. Analysis was conducted at 96 hours after the ESCs received treatment with doxycycline at increasing concentrations. The ESCs were trypsinized at 48 hours and continued receiving the same concentration for a total of 96 hours. *Runx2* expression appeared to increase in a dose-dependent manner at 0, 5, and 10 μg/ml. Doxycycline concentrations of 20 μg/ml were toxic to the ESCs after the 48 hour trypsinization. From this experiment, the concentration of doxycycline used in the osteogenic culture was 10 μg/ml because it seemed to result in the greatest induction of *Runx2* expression without being cytotoxic.

This same ESC line was then differentiated using the osteogenic culture system. In this osteogenic experiment, tetracycline was added to the ESCs and maintained throughout the osteogenic culture. Therefore, *Runx2* expression should be up-regulated throughout the entire osteogenic culture, similar to the constitutive overexpression of *Runx2* experiments. Figure 4.15A displays images of osteogenic culture plates at day 15 when 0 and 10 μg/ml of doxycycline were added to the cultures. The plates were too dense to count individual colonies, but the images show that when doxycycline was added to the cultures there was a decrease in mineralization in comparison with the no doxycycline plates, as seen by a lack of silver nitrate staining. The expression of *Runx2*, as revealed by QRT-PCR, was significantly ($p<0.06$) up-regulated at day 15 when compared to the no doxycycline control. This up-regulation of *Runx2* was not as dramatic as that seen in the constitutive overexpression experiments (Fig.4.10A), approximately 25-fold in comparison with at least 500-fold. The expression of *Bglap1*

was also analyzed by QRT-PCR to determine whether the decrease in mineralization correlated with a decrease in *Bglap1* expression. Figure 4.15C shows that the expression of *Bglap1* was significantly ($p<0.05$) decreased at day 15 when compared to the no doxycycline control. While *Bglap1* (osteogenesis) was decreased, the expression of *Lpl* (adipogenesis) was not significantly changed (Fig. 4.16). In these experiments the percent mineralization was decreased but the total number of colonies formed was not. Overall, these studies suggest that the timing, and perhaps the level, of *Runx2* expression in the osteogenic culture is critical to osteogenesis. Specifically, overexpression of *Runx2* is detrimental to osteogenesis before the cells have committed to this lineage. Therefore, the induction of *Runx2* expression at later time points when the precursor cells have committed to a lineage may increase osteogenesis.

4.3 Discussion

This chapter describes three methods to induce *Runx2* expression in the osteogenic culture. The first method is through the up-regulation of *Runx2* by BMP-2, the second is through the targeted integration of a constitutively overexpressing *Runx2* construct, and the third is through the use of a tetracycline-inducible overexpressing *Runx2* construct. The overexpression of *Runx2* in the osteogenic culture appears to impact osteogenesis in a time-dependent manner. The results also suggest that the level of *Runx2* overexpression impacts osteogenesis.

The expansive amount of literature available concerning BMP-2-induced osteogenesis (171,175-180) led us to investigate the impact of this growth factor in our osteogenic culture system (Fig. 4.3 – 4.7). The BMP-2 used in this experiment was received from Dr. Christopher Niyibizi of the Department of Orthopedics, The Pennsylvania State University College of Medicine. Although the Niyibizi laboratory has shown that BMP-2 can induce osteogenesis in bone marrow-derived MSC cultures and, in particular, in MSCs from an osteogenesis imperfecta mouse (oim) (200), our results indicate that BMP-2 is unable to induce an osteogenic phenotype in our culture system and actually has a negative impact on osteogenesis when added during early time points in culture.

When BMP-2 was added to the cultures, there was an acute up-regulation of *Runx2* mRNA expression (Fig. 4.5), which supports what has previously been reported in the literature (176). However, the only phenotype this correlated with was a reduction in the total number of osteogenic colonies (Figs. 4.3 and 4.4A). As shown by QRT-PCR

analysis of lineage-specific markers, addition of BMP-2 to the cultures before day 3 disrupted not only osteogenesis (Fig. 4.7A), but also myogenesis (Fig. 4.7B) and adipogenesis (Fig. 4.7C). While these results do not necessarily support what is known about BMP-2 in the literature, it is important to consider the culture system and the different phases the cells are in throughout the osteogenic culture period. During early time points of the osteogenic culture, the cells are rapidly proliferating and we suspect are beginning to commit to specific cell lineage fates. Perhaps the addition of BMP-2 before day 3 of the osteogenic culture is disrupting the proliferative capacity of the progenitor cells before they have committed to a specific lineage. Microscopically, it appears that the cells adhere to the tissue culture plates and begin to proliferate but are halted after BMP-2 addition before day 3, and in turn, do not form colonies (data not shown). Thus, a decrease in total colony number, correlating with a decrease in gene expression for markers of osteogenesis, myogenesis, and adipogenesis, might be expected. Following the same logic, once the cells have passed their proliferative phase and committed to a lineage, specifically the osteogenic lineage, addition of BMP-2 should be able to induce osteogenesis. However, no significant differences in mineralization were observed when BMP-2 was added in later days of the culture (Fig. 4.4B).

There are several possibilities as to why there was no induction of osteogenesis in response to BMP-2 addition at later time points. Perhaps, the concentration of BMP-2 was not sufficient to induce osteogenesis. Although the concentration used (80 ng/ml) was recommended by the Niyibizi laboratory, concentrations as high as 200 and 300 ng/ml have been reported in the literature (176,201). A second possibility is that the cells require a longer time period of BMP-2 induction. Our experiments expose the cells to

BMP-2 for two hour intervals on two consecutive days, but it has been suggested in the literature that a longer exposure time is necessary for mesenchymal induction (202). A third possibility is that the medium used for the osteogenic culture, in particular the FBS, or the endogenous production of BMP-2 was already saturated so that additional BMP-2 wasn't able to further induce osteogenesis. It may also be possible that other co-factors are necessary for BMP-2 induced osteogenesis, such as vitamin D_3 (202). All of these possibilities allow for the interpretation that the addition of BMP-2 before day 3 of the osteogenic culture is disruptive to the proliferative capacity and lineage potential of the cells, and that after this time point, BMP-2 is unable to induce osteogenesis. While we realize that the use of growth factors to gain a better understanding of the osteogenic culture and the stages the cells are going through is important, we were unable to find an affordable and reliable source of BMP-2 to continue these experiments.

Interestingly, increased *Runx2* expression caused by a constitutively overexpressing *Runx2* construct targeted to the Hprt locus of ESCs (Fig. 4.8, 4.9, and 4.10) produced data remarkably similar to that seen in the BMP-2 experiments. It might be expected that the constitutive overexpression of *Runx2* would be detrimental to the viability of the ESCs because *Runx2* drives differentiation, which is contrary to the maintenance of ESCs. However, this was not the case because ESCs were able to survive normal ESC and EB culture. It might then be expected that the overexpression of *Runx2* would have a positive effect on the induction of osteogenesis. In contrast to these predictions, but in support of the BMP-2 data, when *Runx2* was constitutively overexpressed in the osteogenic culture, there was a significant decrease in the total colony forming units and a reduction in mineralization (Fig. 4.9) that was accompanied

by a major decrease in mesenchymal gene expression (Fig. 4.10B). This further supports the notion that overexpression of *Runx2*, in particular during early time points when the cells are rapidly proliferating and before they have committed to a lineage, is detrimental to not only osteogenesis but myogenesis and adipogenesis as well.

The results of the BMP-2 and the *Runx2* constitutive overexpression studies suggested that an inducible overexpression system may be more ideal for this culture system. We hypothesized that if we could specifically overexpress *Runx2* after the cells committed to the osteogenic lineage, then we could induce and/or enhance osteogenesis in these cultures without disrupting their proliferative capacities. This type of experiment would also enable us to determine the time frame in which commitment occurs, a critical question that we predict would need to be addressed before these cells could be used therapeutically, as well as the question of whether Runx2 is necessary (26-28) and sufficient for osteogenesis.

The creation of an inducible overexpression of *Runx2* system in the ESCs has proven to be somewhat of a challenge. The original bi-transgenic construct was created by Kimberly Dunham, a former member of the Bronson laboratory, and contained a TRE-*Runx2* and hβa-rtTA, as well as Hprt homology for targeting. Preliminary experiments with this construct showed that while detectable levels of rtTA were observed, there was no increase in *Runx2* mRNA expression in the presence of the inducer, doxycycline. We hypothesized that the close proximity of the two constructs may be causing a problem for the proper expression of the transgenes. Therefore, the two constructs were separated and the hβa-rtTA was randomly integrated into the ESC genome while the TRE-*Runx2* was targeted to the Hprt locus. QRT-PCR analysis

revealed that in comparison to the targeted bi-transgenic construct containing hβa-rtTA, the randomly integrated rtTA construct had clones with higher rtTA expression (Fig. 4.17). This suggests that in the original bi-transgenic construct the expression of rtTA was somehow suppressed or decreased, thus inhibiting the effectiveness of the inducible system. Perhaps the close proximity of promoter elements led to competition for transcription factors or the introduction of hβa-rtTA in a single copy in the original construct provided too low of an expression level for the TRE to be properly induced. While the second possibility is valid, it is widely accepted that for a transgene to be copy number dependent it requires a locus control region (LCR) (196), which this construct does not have.

Upon targeted integration of the TRE-*Runx2* into an ESC clone expressing rtTA at the highest level detected (clone 3, Fig. 4.12) doxycycline was able to induce *Runx2* mRNA expression in ESCs at a level of 2- and 3-fold higher than no doxycycline controls at concentrations of 5 and 10 μg/ml, respectively (Fig. 4.14). This indicated that induction was occurring and the system was functional. The induction of *Runx2* throughout the osteogenic culture from the ESC to day 21 with 10 μg/ml doxycycline also seemed to impact osteogenesis, but in a somewhat different manner than that seen in the constitutive overexpression of *Runx2* experiments. We predicted that inducing *Runx2* expression throughout the osteogenic culture from the ESC to day 21 would mimic the constitutive results, but this was not entirely the case (Fig. 4.15). In the inducible experiments, there was a decrease in mineralization observed by silver nitrate staining (Fig. 4.15A) and *Bglap1* (mature osteogenic marker) expression (Fig. 4.15C) but no impact on the total number of colony forming units (Fig. 4.15A), in contrast to

constitutive overexpression experiments where the total number of colony forming units was decreased significantly while the mineralization was only decreased significantly in one clone (Fig. 4.9). The most pronounced difference between the two experiments was the level of *Runx2* expression. In the constitutive *Runx2* experiments, the level of *Runx2* was up-regulated at least 500-fold above the D0EB control (Fig. 4.10A), while in the inducible *Runx2* experiments, the level of expression was up-regulated, at the most, 25-fold above the D0EB control (Fig. 4.15B). These results suggest that the level of *Runx2* mRNA overexpression also plays a role in osteogenic cell fate.

In the inducible experiments, while the overexpression of *Runx2* from early time points throughout the culture was detrimental to the osteogenic culture, the level of *Runx2* overexpression seems to be more specific to the osteogenic lineage. The mineralization and expression of the mature osteogenic marker, *Bglap1*, was diminished at day 15, but the expression of *Lpl* was not significantly changed (Fig. 4.16). In the constitutive experiments, the high levels of *Runx2* overexpression were detrimental to total colony forming units and *Bglap1*, *Myh11*, and *Lpl* expression. This suggests that at high levels of *Runx2* overexpression, mesenchymal lineages in general were negatively impacted. In any case, *Runx2* overexpression, at low or high levels, before the cells have committed to the osteogenic lineage is detrimental to osteogenesis. The next step would be to induce *Runx2* mRNA expression at later time points throughout the osteogenic culture and investigate the osteogenic outcome by mineralized colony formation and gene expression analysis of whole plates as well as individual colonies. We hypothesize that if the cells have already committed to the osteogenic lineage, then induction of *Runx2* overexpression would increase osteogenesis evidenced by an increase in mineralization

and *Bglap1* expression. On a side note, the concentration of doxycycline used was the highest concentration used thus far on the osteogenic culture system and more controls would need to be done to rule out an effect of the doxycycline itself.

While there was an increase in *Runx2* mRNA expression after induction with doxycycline, as stated above, this increase was significantly lower than that seen with the constitutive construct. Although, a phenotype was detected at day 15, there was no increase in *Runx2* mRNA expression before this time point (Fig. 4.15B), suggesting some potential problems in achieving doxycycline-induced gene expression. Some design alternatives to address this issue would be to generate more hβa-rtTA ESC clones and screen for higher expressing random integrants. It may also be beneficial to shift to the rtTA2^{S}-M2, which has been shown to function at a 10-fold lower doxycycline concentration, be more stable, and have lower background expression in the absence of doxycycline (203), although background expression does not seem to be the problem. In terms of the overexpression of *Runx2* constructs, the experiments outlined in this chapter were conducted with one properly integrated ESC clone, chosen based on morphology and proper integration into the Hprt locus. Conducting experiments with other overexpression of *Runx2* ESC clones may provide more substantial doxycycline induction. Integrating the overexpression of *Runx2* constructs randomly as opposed to in a single copy may also provide an increase in doxycycline response. Although there are published reports of single-copy transgenes targeted to the Hprt locus, no inducible targeted transgenes have been published (133). We also recognize that there may be potential problems with the TRE promoter that regulates *Runx2* expression in this construct and propose an experiment that utilizes a reporter, such as green fluorescent

protein (GFP), to visualize the ability of the promoter to induce expression in ESCs and the osteogenic culture.

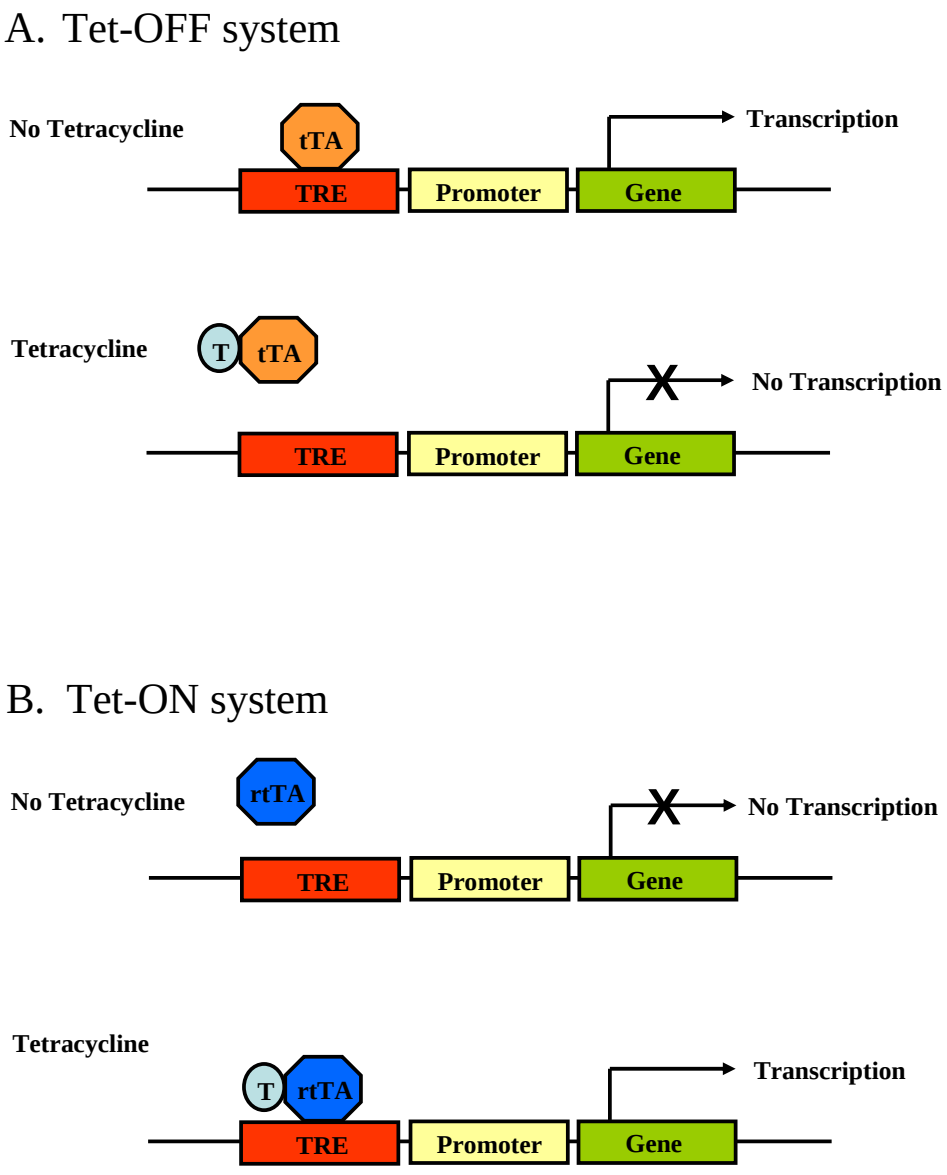

Figure 4.1: Tet-OFF and Tet-ON systems. (**A**.) Schematic of Tet-OFF system. In the absence of tetracycline, tTA binds to the TRE and activates transcription, while in the presence of tetracycline, tetracycline binds to tTA and blocks interaction of tTA with TRE, preventing transcription. (**B**.) Schematic of Tet-ON system. In the absence of tetracycline, rtTA is unable to bind to the TRE and unable to activate transcription, while in the presence of tetracycline, tetracycline binds to rtTA, allowing binding to the TRE and activation of transcription. tTA = tetracycline-controlled transactivator, TRE = tetracycline responsive element, T = tetracycline, rtTA = reverse tetracycline transcriptional activator

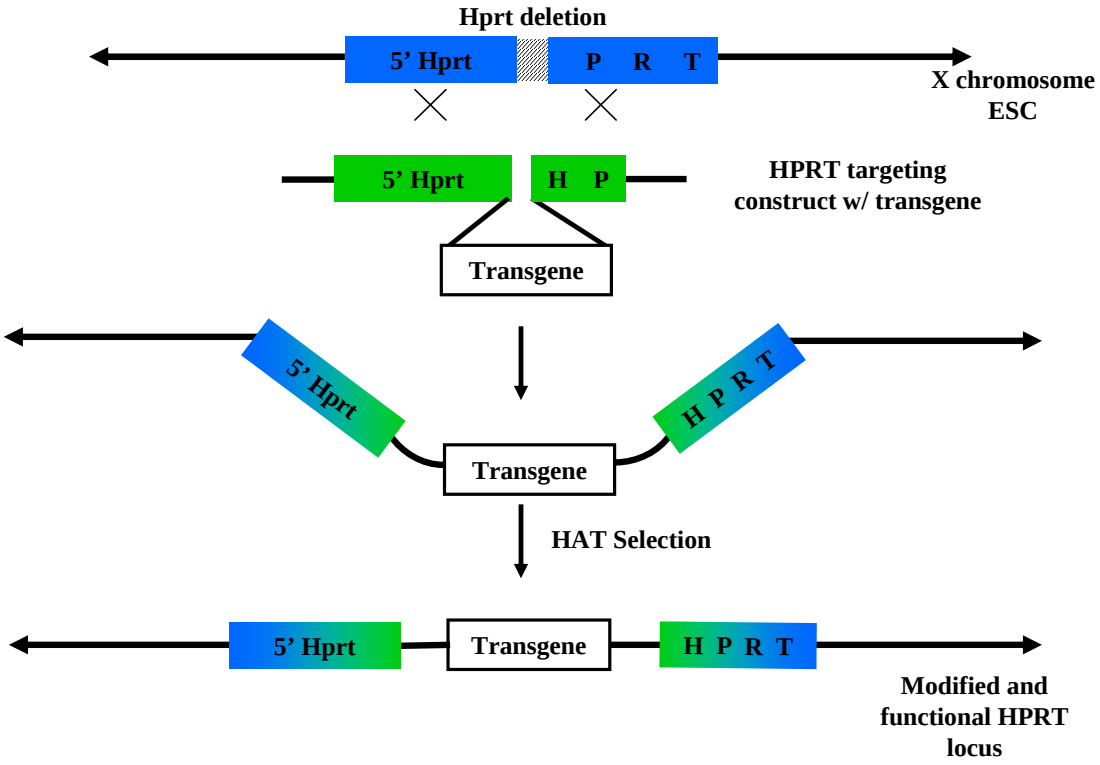

Figure 4.2: General method for targeting transgenes through homologous recombination at the Hprt locus. Figure not to scale. Source: adapted from J.D. Heaney, S.K. Bronson laboratory, unpublished.

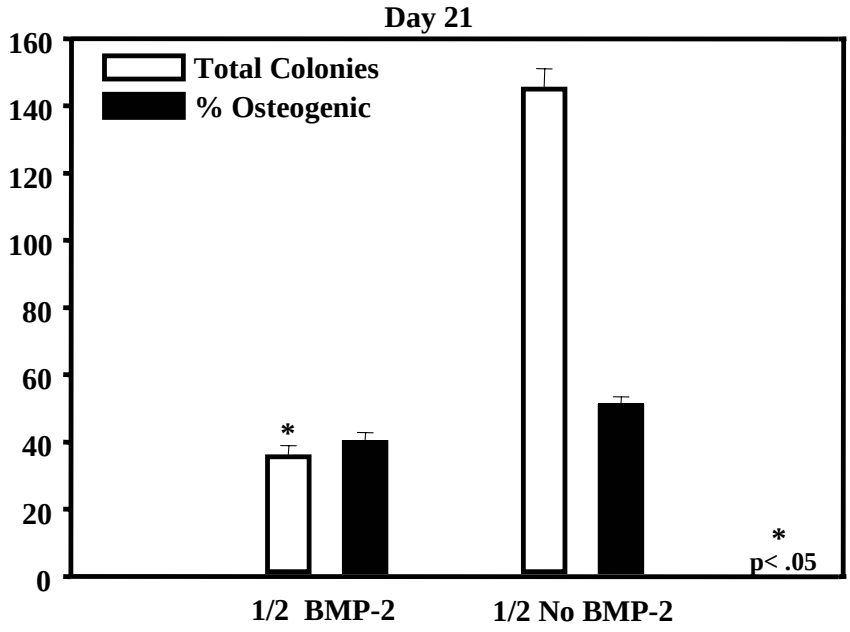

Figure 4.3: Total colony forming units and percentage of colonies with mineralization at day 21 of the osteogenic culture after treatment with or without BMP-2 on days 1 and 2. BMP-2 was added at a final concentration of 80 ng/ml for two hours. See Materials and Methods 2.2.1 for details of procedure. Asterisk represents significant difference when compared to 1/2 No BMP-2 Total Colonies.

A.

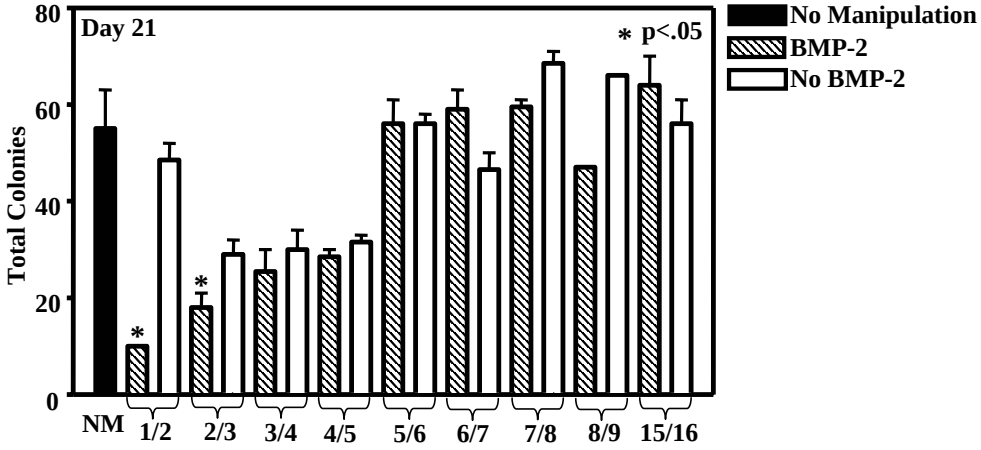

B.

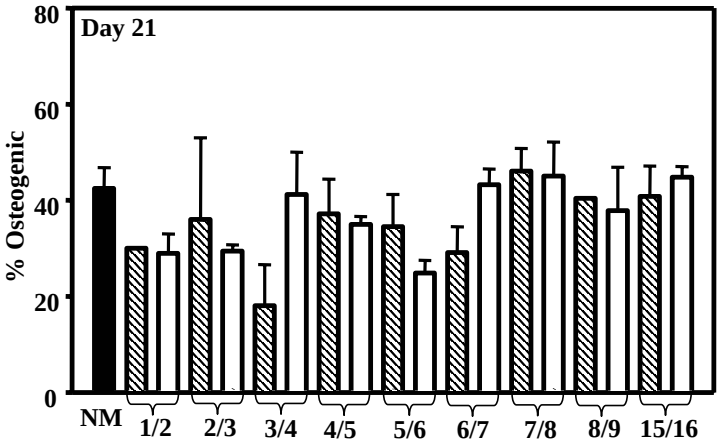

Figure 4.4: Total colonies and percentage of colonies with mineralization at day 21 of the osteogenic culture after treatment with or without BMP-2 for two consecutive days throughout the osteogenic culture. BMP-2 was added at a final concentration of 80 ng/ml for two hours. (**A.**) Total colony formation. Asterisk represents significant difference when compared to No manipulation (NM). (**B.**) Percentage of colonies with mineralization. 1/2 = day 1 and 2 of the osteogenic culture, 2/3 = day 2 and 3 of the osteogenic culture, etc.

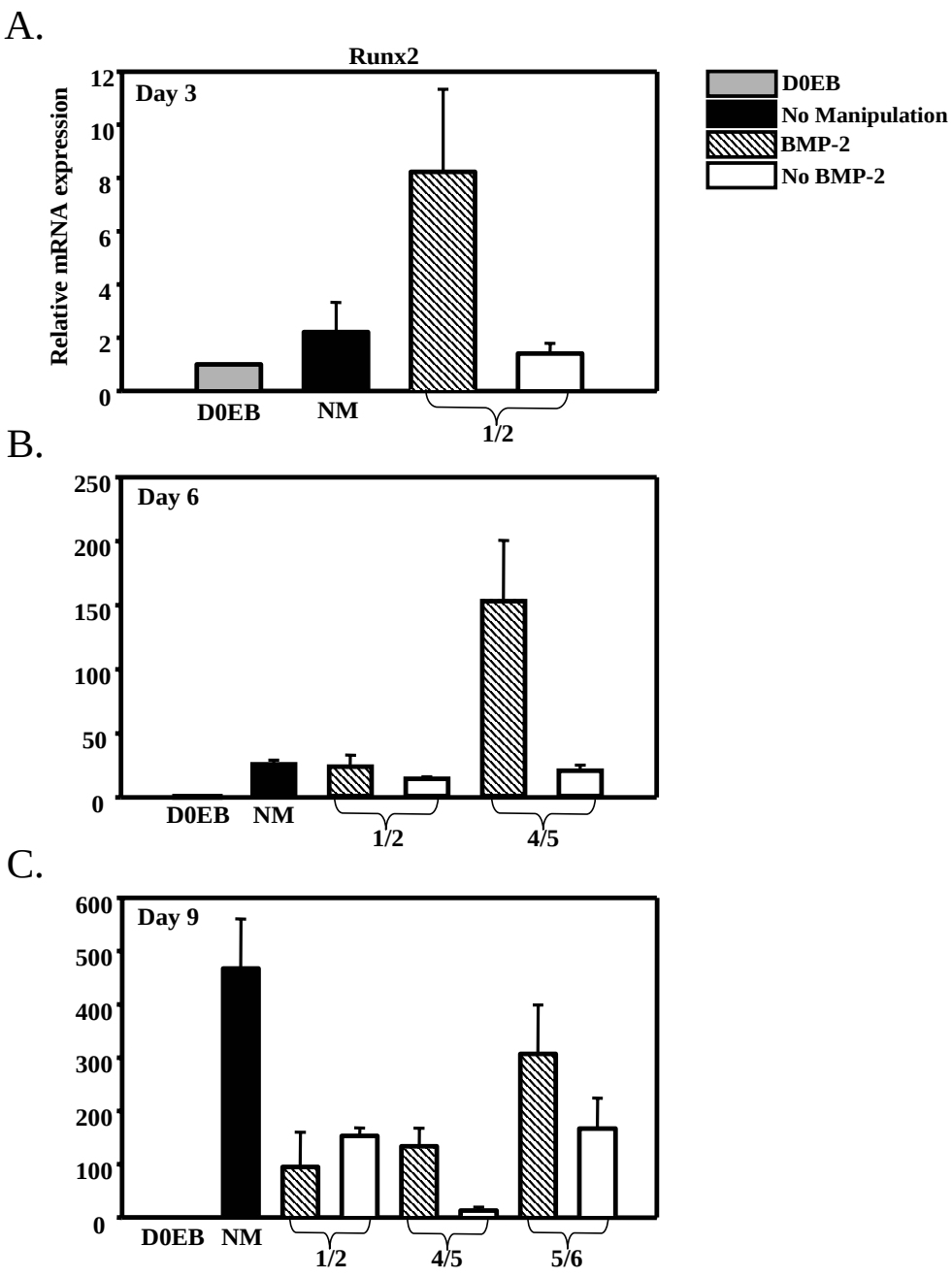

Figure 4.5: QRT-PCR analysis of *Runx2* mRNA expression at (**A**.) day 3, (**B**.) 6, and (**C**.) 9 of the osteogenic culture after treatment with or without BMP-2 for two consecutive days. Each assay was run in duplicate at two different template concentrations. Relative mRNA expression was normalized to ribosomal protein L7 (*Rpl7*) and displayed relative to D0EB. D0EB = day 0 embryoid body, NM = No Manipulation, 1/2 = day 1 and 2 of the osteogenic culture, 4/5 = day 4 and 5 of the osteogenic culture, 5/6 = day 5 and 6 of the osteogenic culture

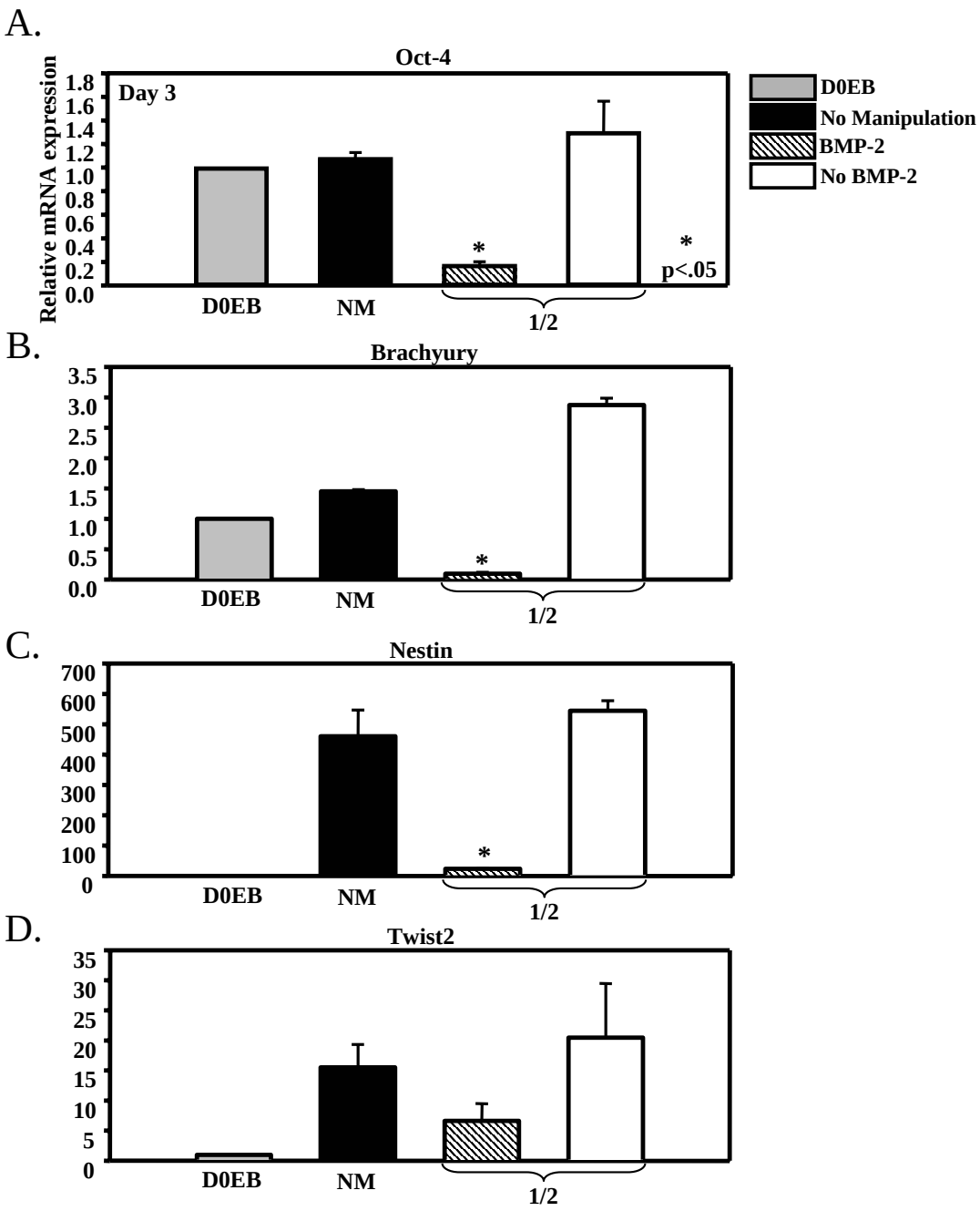

Figure 4.6: QRT-PCR analysis of (**A.**) *Oct-4*, (**B**.) Brachyury, (**C**.) Nestin, and (**D**.) *Twist-2* mRNA expression at day 3 of the osteogenic culture after treatment with or without BMP-2 for two consecutive days. Asterisk represents a significant difference when compared to No BMP-2. Each assay was run in duplicate at two different template concentrations. Relative mRNA expression was normalized to ribosomal protein L7 (*Rpl7*) and displayed relative to D0EB. D0EB = day 0 embryoid body, NM = No Manipulation, 1/2 = day 1 and 2 of the osteogenic culture.

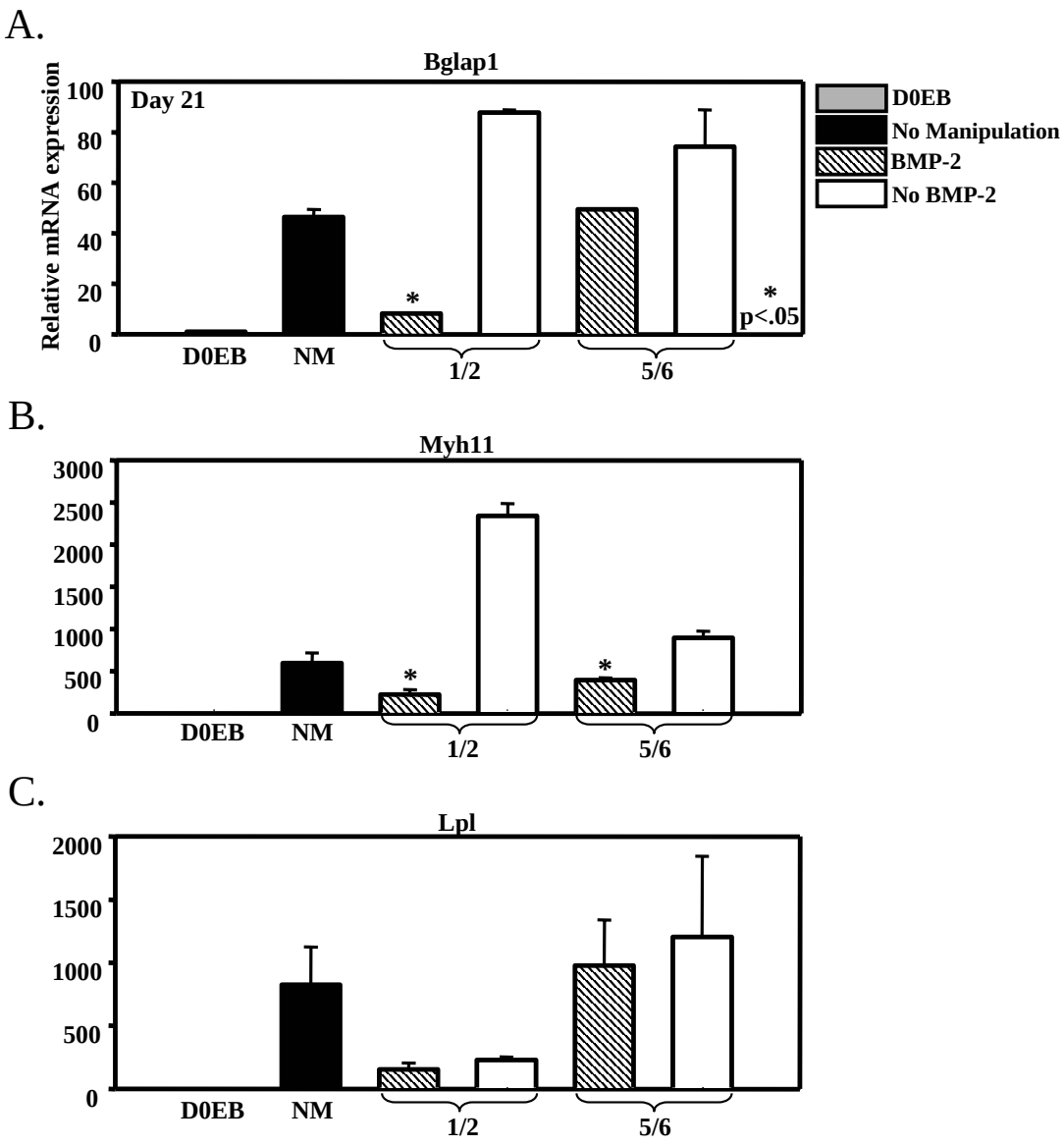

Figure 4.7: QRT-PCR analysis of (**A**.) *Bglap1*, (**B**.) *Myh11*, and (**C**.) *Lpl* mRNA expression at day 21 of the osteogenic culture after treatment with or without BMP-2 on days1/2 and 5/6. Asterisk represents a significant difference when compared to No BMP-2 at the same time points. Each assay was run in duplicate at two different template concentrations. Relative mRNA expression was normalized to ribosomal protein L7 (*Rpl7*) and displayed relative to D0EB. D0EB = day 0 embryoid body, NM = No Manipulation, 1/2 = day 1 and 2 of the osteogenic culture, etc.

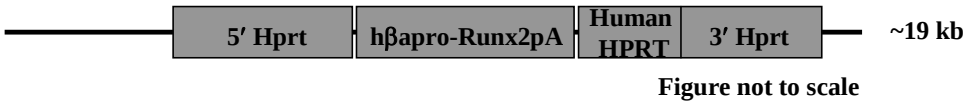

Figure 4.8: Constitutive overexpression of *Runx2* cDNA construct. Diagram of ~19 kb vector containing 5′ Hprt homology (3.75 kb), the human beta-actin promoter (hβapro) and *Runx2* cDNA (8.1 kb), and the human HPRT and 3′ Hprt homology (4.45 kb). The black line represents the remaining vector sequence. This construct was cloned and verified by Kimberly Dunham.

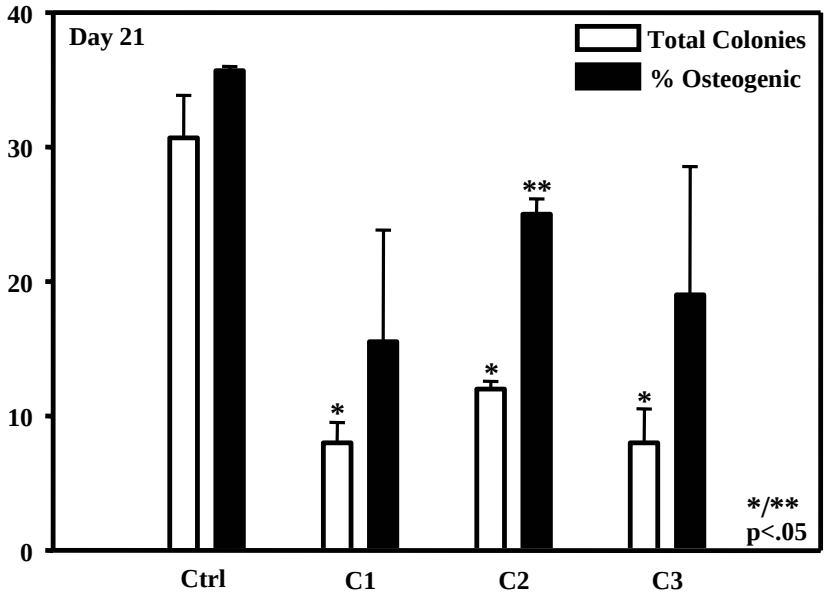

Figure 4.9: Total colony forming units and percentage of colonies with mineralization at day 21 of the osteogenic culture for the parental ESC line (Ctrl) and clones 1, 2, and 3 (C1, 2, and 3) containing a constitutive *Runx2* cDNA. A single asterisk represents a significant difference when compared to Ctrl Total Colonies and a double asterisk represents a significant difference when compared to Ctrl % Osteogenic.

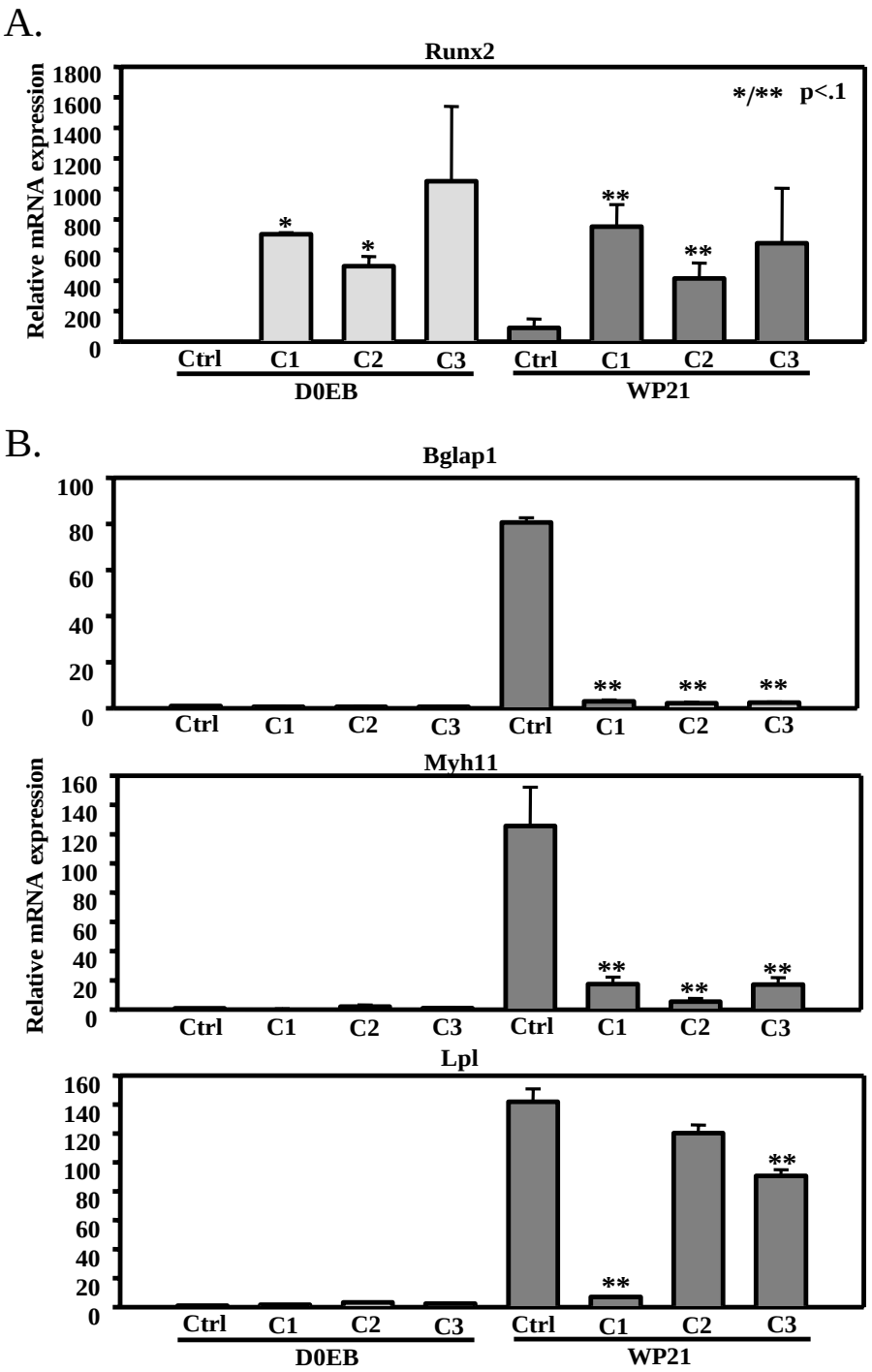

Figure 4.10: QRT-PCR analysis of (**A.**) *Runx2* (**B.**) *Bglap1*, *Myh11*, and *Lpl* mRNA expression at D0EB and WP21 of the osteogenic culture in the parental ESC line (Ctrl) and clones 1, 2, and 3 (C1, 2, and 3) containing a constitutive *Runx2* cDNA. Each assay was run in duplicate at two different template concentrations. Relative mRNA expression was normalized to ribosomal protein L7 (*Rpl7*) and displayed relative to D0EB Ctrl. A single or double asterisk represents a significant difference when compared to D0EB Ctrl or WP21 Ctrl, respectively.

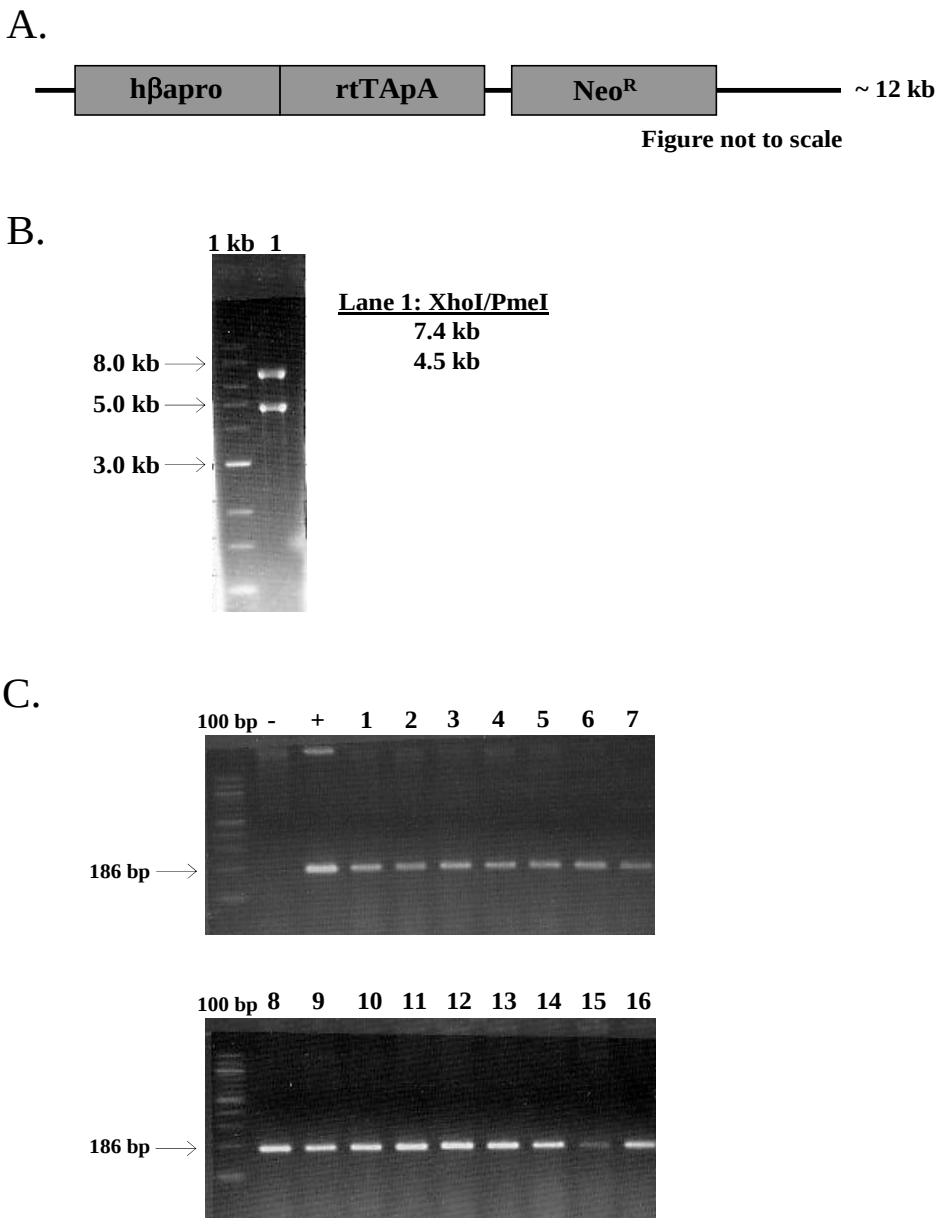

Figure 4.11: Reverse tetracycline-responsive transcriptional activator (rtTA) construct. (**A.**) Diagram of ~ 12 kb vector containing the human beta-actin promoter (hβapro) (4.3 kb), the reverse tetracycline-responsive transcriptional activator (rtTA) (1.5 kb), and the Neo^R gene (1.3 kb) that was electroporated into ESCs. The black line represents the remaining vector sequence. (**B.**) Restriction enzyme digestion of properly cloned vector visualized on a 1% agarose gel. Lane 1 shows vector digested with XhoI and PmeI with expected band sizes listed. (**C.**) RT-PCR analysis of the rtTA in a subset of ESC clones visualized on a 1% agarose gel. The expected product size is 186 bp. Negative control (-) is D0EB = day 0 embryoid body cDNA. Positive control (+) is pKD2 plasmid (see Materials and Methods section 2.2.2 for description).

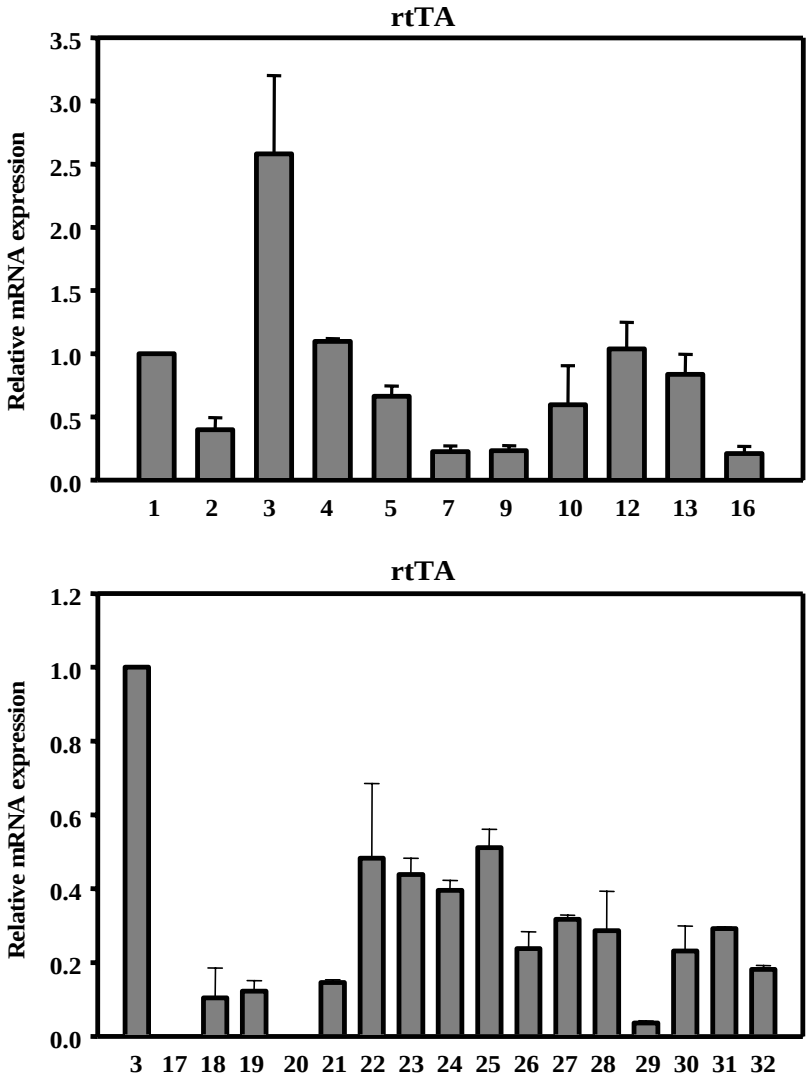

Figure 4.12: QRT-PCR analysis of the reverse tetracycline-responsive transcriptional activator (rtTA) in a subset of ESC clones. Each assay was run in duplicate at two different template concentrations. Relative mRNA expression was normalized to ribosomal protein L7 (*Rpl7*) and displayed relative to clone 1 (top) and clone 3 (bottom). Clone numbers correspond with Figure 4.11. QRT-PCR analysis was not performed on clones 6, 8, 11, 14, and 15 due to poor RNA quality. Clone 3 expresses rtTA at the highest levels of all clones tested and is the ESC line used in the experiments shown in Figure 4.13.

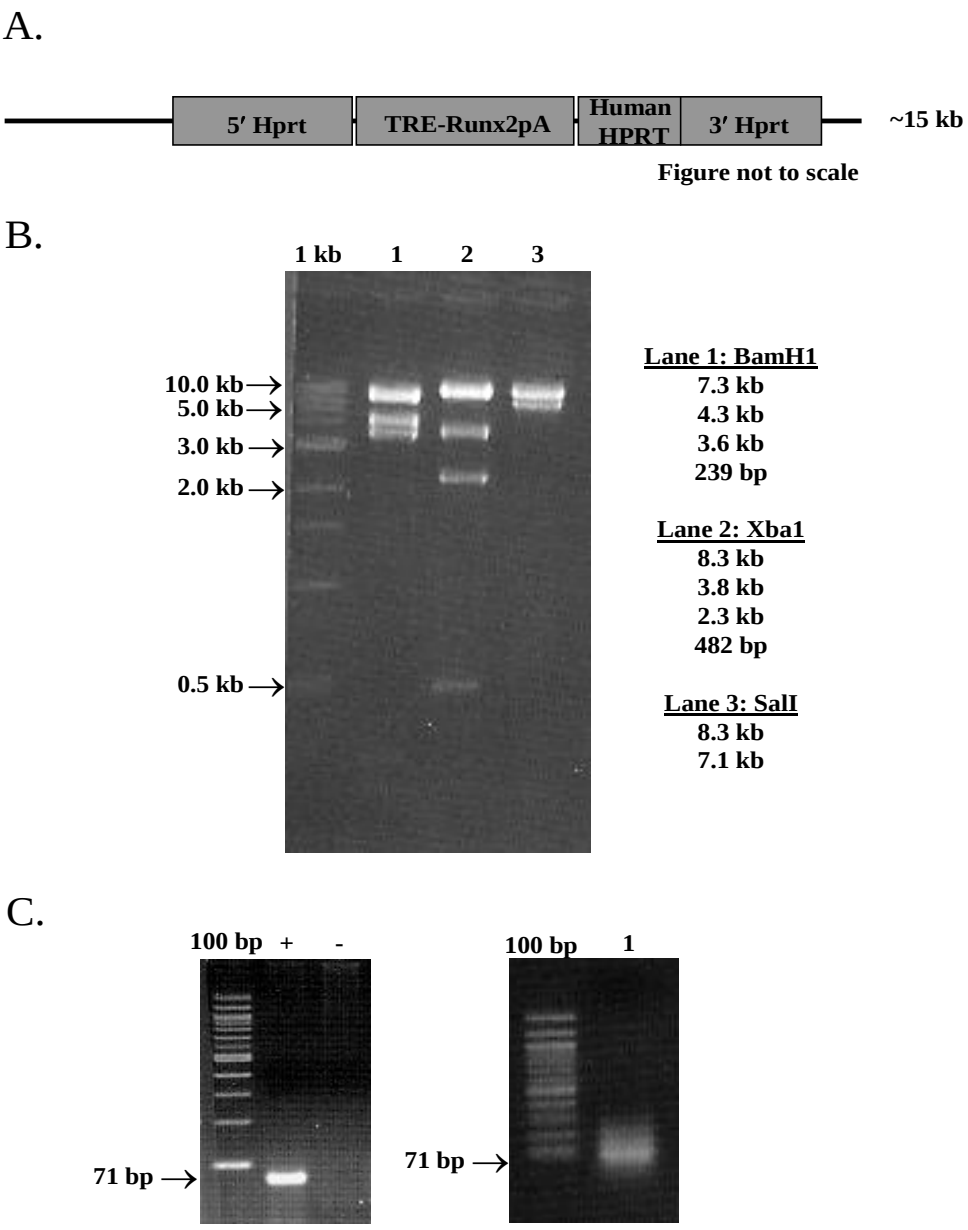

Figure 4.13: Tetracycline-inducible *Runx2* cDNA construct. (**A.**) Diagram of ~15 kb vector containing 5′ Hprt homology (3.75 kb), the tetracycline responsive element (TRE) (containing the tet promoter) and inducible *Runx2* cDNA (4.3 kb), and the human HPRT and 3′ Hprt homology (4.45 kb) that was electroporated into ESCs. The black line represents the remaining vector sequence. (**B.**) Restriction enzyme digests of properly cloned vector visualized on a 1% agarose gel. Lanes 1, 2, and 3 are the same vector clone digested with BamHI, XbaI, and SalI, respectively. Expected fragment sizes for each enzyme digest are listed. (**C**.) RT-PCR analysis of rescued Hprt locus in rtTA clone 3 (Fig. 4.11 and 4.12) containing the targeted inducible *Runx2* cDNA. The expected product size is 71 bp. Primer sequences are listed in Table 2.5. + = targeted ESC line previously verified, - = ESC line with Hprt deletion (left panel), Lane 1 = targeted clone 3 (right panel)

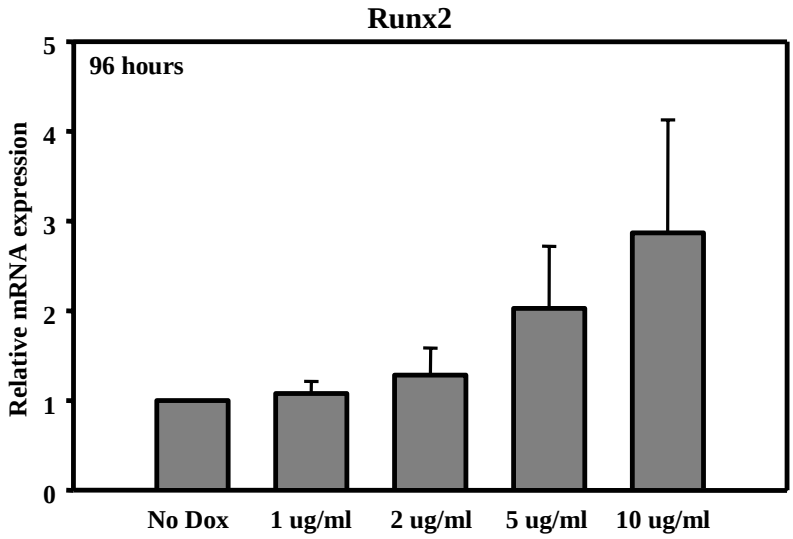

Figure 4.14: QRT-PCR analysis of *Runx2* mRNA expression in ESCs containing a tetracycline-inducible *Runx2* cDNA after treatment with increasing amounts of doxycycline for 96 hours. Each assay was run in triplicate at two different template concentrations. Relative mRNA expression was normalized to ribosomal protein L7 (*Rpl7*) and displayed relative to No Dox. Dox = doxycycline

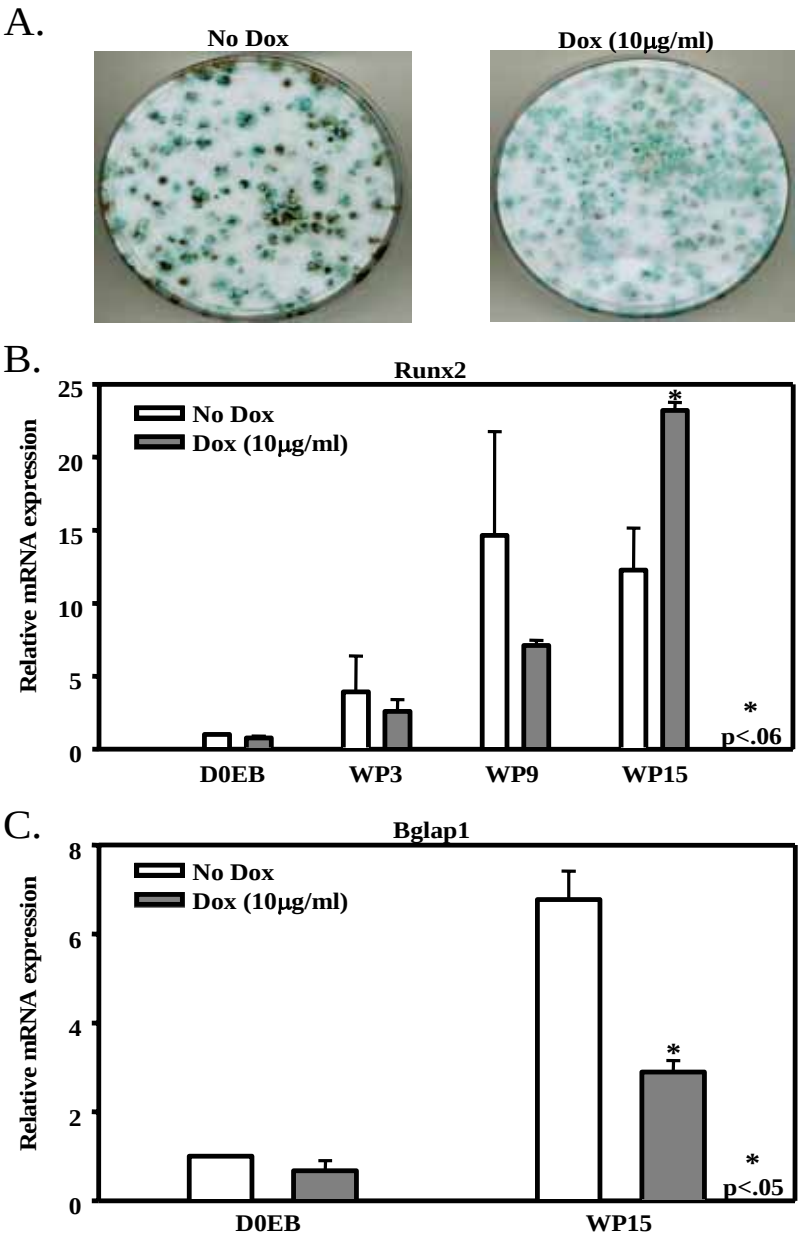

Figure 4.15: Effect of tetracycline-inducible *Runx2* cDNA on the osteogenic culture. (**A.**) Osteogenic culture plates of *in vitro* differentiated ESCs containing a tetracycline-inducible *Runx2* cDNA at day 15 in the absence (left panel) and presence (right panel) of 10 μg/ml of doxycycline. Plates were fixed and stained with silver nitrate (mineralization) and methyl green (counterstain). (**B.**) QRT-PCR analysis of *Runx2* mRNA expression at D0EB, WP3, WP9, and WP15 of the osteogenic culture in the absence (white) and presence (gray) of 10 μg/ml doxycycline. (**C**.) QRT-PCR analysis of *Bglap1* mRNA expression at D0EB and WP15 of the osteogenic culture in the absence (white) and presence (gray) of 10 μg/ml doxycycline. Each assay was run in triplicate at two different template concentrations. Relative mRNA expression was normalized to ribosomal protein L7 (*Rpl7*) and displayed relative to D0EB No Dox. Asterisk represents a significant difference when compared to WP15 No Dox. D0EB = day 0 embryoid body, WP3 = whole plate day 3, WP9 = whole plate day 9, WP15 = whole plate day 15, Dox = doxycycline

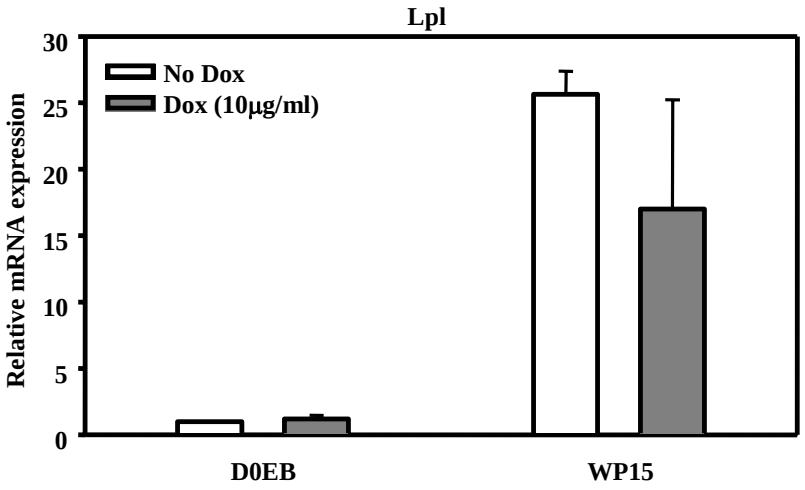

Figure 4.16: QRT-PCR analysis of *Lpl* mRNA expression at D0EB and WP15 of the osteogenic culture in the absence (white) and presence (gray) of 10 μg/ml doxycycline. Each assay was run in triplicate at two different template concentrations. Relative mRNA expression was normalized to ribosomal protein L7 (*Rpl7*) and displayed relative to D0EB No Dox. D0EB = day 0 embryoid body, WP15 = whole plate day 15, Dox = doxycycline

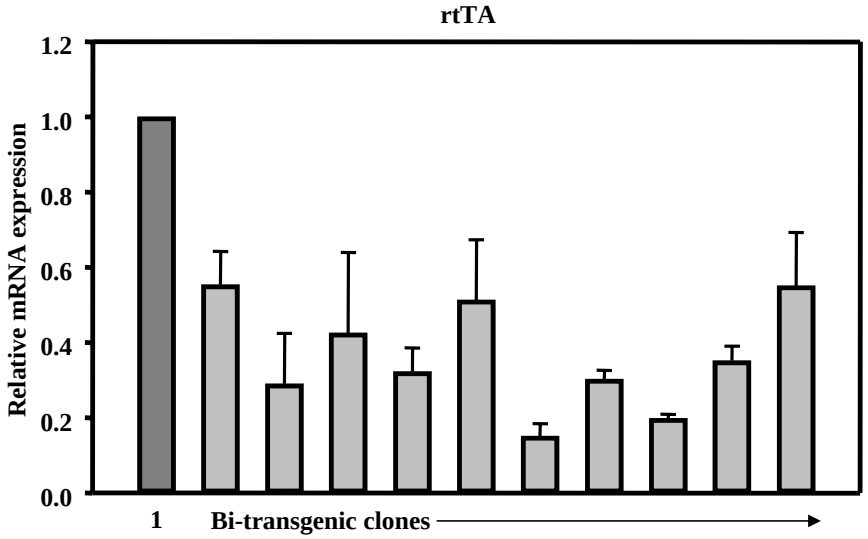

Figure 4.17: QRT-PCR analysis of the reverse tetracycline-responsive transcriptional activator (rtTA) in a subset of bi-transgenic ESC clones containing rtTA and TRE-*Runx2*. Clone 1 is the randomly integrated rtTA ESC clone from Figure 4.12. Each assay was run in duplicate at two different template concentrations. Relative mRNA expression was normalized to ribosomal protein L7 (*Rpl7*) and displayed relative to clone 1.

CHAPTER 5

CONSTITUTIVE AND INDUCIBLE KNOCKDOWN OF EXPRESSION OF RUNX2 IN THE OSTEOGENIC CULTURE SYSTEM

5.1 Introduction

Another technique available to understand the commitment of progenitor cells to the osteogenic lineage is the knockdown or loss-of-function of critical factors. In order to knockdown gene expression in the osteogenic culture and gain a better understanding of osteogenesis as well as commitment of progenitor cells, we have utilized a tetracycline-inducible short hairpin RNA (shRNA) system, which employs components of the pSUPERIOR RNAi System™.

5.1.1 RNA Interference (RNAi)

RNA silencing is the ability to limit the transcript level by either suppressing transcription (transcriptional gene silencing (TGS)) or activating a sequence-specific RNA degradation process (posttranscriptional gene silencing (PTGS) or RNA interference (RNAi)) (204). In several organisms, introduction of double-stranded RNA to induce RNA interference has proven to be a powerful tool to suppress gene expression (205). The term RNAi was first described by Fire and Mello in 1998 when they described the inhibition of gene expression by double-stranded RNAs (dsRNAs) in the nematode worm *Caenorhabditis elegans* (206,207). The first gene they chose to look at was the *unc-22* gene that encodes an abundant but nonessential myofilament protein

(207). They found that double-stranded RNA was more effective at interfering with gene expression than either individual strands alone. Double-stranded RNAs injected into adult animals caused potent and specific interference of gene expression, and only a few molecules of the double-stranded RNA were needed, suggesting an amplification component to this process (207). In 2006, the Nobel Prize in Physiology or Medicine was awarded to Andrew Z. Fire and Craig C. Mello for their discovery of "RNA Interference – gene silencing by double-stranded RNA" (208).

The process of RNA silencing has been found to occur naturally in plants (PTGS), animals (RNAi), and fungi (quelling) and can be virally-induced. All of these processes are based on critical common components (204). The inducer of the process is double-stranded RNA (dsRNA) that targets a specific RNA sequence in a homology-dependent fashion that is then degraded by a set of proteins similar across most organisms (204). The basic mechanism of RNAi involves the processing of long dsRNA into small interfering RNA (siRNA). When the long dsRNA enters into cells, it is cleaved into siRNA by an RNase-III-like enzyme called Dicer. The siRNAs are typically 21-23 nucleotides in length and are bound to a protein complex. The siRNA-protein complex contains helicase activity that unwinds the dsRNA molecules and allows the antisense strand to then bind the targeted RNA sequence. The siRNA-induced silencing complex (RISC) also contains endonuclease activity that degrades the RNA molecules where the antisense strand is bound. The RISC complex is the key step in the process of sequence-specific mRNA degradation (reviewed in (206)). Figure 5.1 depicts the mechanism of RNA interference.

5.1.2 MicroRNA (miRNA)

While siRNAs are one of the most common silencing-related small RNAs, there are other types as well. Another type of silencing RNA that has gained a lot of interest in the past several years is microRNA. It was originally thought that RNAi had a main role in protecting cells from invading nucleic acids or viruses; however, the identification of microRNAs has changed this theory (209). MicroRNAs are a class of noncoding RNAs approximately 22 nucleotides in length that play roles in development by regulating the expression of other genes by targeting the messages of protein-coding genes for cleavage or repressing productive translation. The first miRNA, *lin-4*, was found in *C. elegans* in 1993 by Lee et al. and Wightman et al. (209-211). It was found to repress the expression of the nuclear protein encoding gene *lin-14* as part of the control of developmental timing (209). Several years later the *let-7* mutation was discovered in *C. elegans* and the field of miRNAs began to emerge (212). This mutation was shown to function in a manner similar to *lin-4*.

The processing of miRNAs is similar to that of siRNAs. Pre-miRNAs are converted to mature miRNAs by the enzyme Dicer into approximately the same length as single-stranded siRNAs (209,213,214). The complete pathway also involves another enzyme called Drosha. This RNaseIII-like enzyme first cleaves the stem-loop structure of the original ~70 nucleotide dsRNA that the miRNA originates from. Because the stem-loop structure is imperfectly double-stranded, the miRNA is only partially paired to the other strand (209). miRNAs typically act in a combinatorial manner with several miRNAs binding to a single transcript (209,215).

The mechanism by which miRNAs mediate repression of target genes has been somewhat elusive, but recent studies in human cells have begun to shed light on this topic (216,217). Humphreys et al. showed that miRNAs interfere with the initiation step of translation and suggest that the molecular target is the cap-binding protein eukaryotic initiation factor 4E (eIF-4E) (216). It has also been shown that the accumulation of the targeted mRNA occurs in processing (P) bodies (217). P bodies are discrete cytoplasmic foci in yeast in which mRNA decapping, degradation, and/or storage occur (209,218), which correlates with the molecular target of eIF-4E as well as the involvement of the 7-methylguanosine cap (m^7G cap) (217).

miRNAs have already been shown to be involved in cell fate determination, including the control of cell division and differentiation, and in development, including morphogenesis, neurogenesis, and developmental timing (reviewed in (209)). Along with this comes the consequence of abnormally expressed miRNAs contributing to human diseases and cancer (219). These findings suggest that the field of miRNAs may begin to make contributions to therapeutics, including those for cancer treatment. The identification of miRNAs will also allow for more efficient RNAi systems to be generated and possibly used in human therapeutics. It also sheds light on natural processes that are occurring within the cells that current RNAi technology may potentially interfere with and therefore, lead to harmful side effects. The identification of RNAi and different types of RNAi, such as siRNA and miRNA, has allowed researchers to ask more complex questions about gene regulation and function.

5.1.3 siRNA: Synthesis and Delivery

The natural biology of RNAi in eukaryotic cells offers a defense mechanism against foreign nucleic acids. Recently, this process has been used to gain a better understanding of gene function. One obstacle that has been encountered with this natural process being used as a technology is that there are a number of dsRNA-triggered pathways that mediate non-specific suppression of gene expression (204,220). Fortunately, these nonspecific responses are not triggered if the dsRNA introduced to the cells is shorter than 30 bp, referred to as siRNA, and it has been clearly shown that siRNAs can produce effects similar to that of the long dsRNA (204,221,222). The emergence of siRNA technology has allowed for the study of gene function in what is thought of as a more rapid and inexpensive way (204). For example, since the dawn of this technology, almost all of the approximately 19,000 genes of *C. elegans* have been knocked down with siRNA-directed approaches (204). There are several variables that need to be considered when using siRNA in any model system, including (i) selecting the siRNA sequence in the target gene, (ii) the synthesis of the siRNA or construction of expression vectors containing the DNA sequence which encodes for the siRNA, (iii) optimizing the transfection of the siRNA into the desired cells, and (iv) the ability to monitor the knockdown of gene expression (204).

There are several different parameters that need to be considered when designing the siRNA sequence, such as the length, secondary structure, sugar backbone, and sequence specificity to the target sequence (reviewed in (204)). Although much work has been done to understand what is most essential in the siRNA sequence, the exact parameters are still not known. However, there are some general guidelines that are

typically followed. The target sequence should be 50 to 100 bp downstream of the start codon and the 5′ and 3′ untranslated regions and regions near the start codon should be avoided, and the GC content of the target sequence should be between 30 and 70%.

Once the target sequence has been chosen, there are some general guidelines for the synthesis of the siRNA. One strand should consist of $AA(N_{19})TT$ so that the siRNA has a two nucleotide overhang of uridine residues. This criterion is based on the observation that siRNAs with 3′ overhanging UU dinucleotides are the most effective (223). As mentioned above, the siRNAs should be 21 nucleotides long. The synthesis of siRNAs can be costly and the amount of siRNA can be limited. As a result, researchers have developed methods to synthesize the siRNA *in vitro* (224) and expression vector to synthesize siRNA within the cells. In order to synthesize the siRNA *in vitro*, there are specific promoters necessary to transcribe the sense and antisense strands, specifically the T7 promoter (224). The expression vectors are typically designed with the siRNA template downstream of an RNA polymerase III promoter, which is usually either an RNA U6 or RNase H1 promoter. The expression vector described and used in this chapter is pSUPERIOR™ which contains an H1 promoter and is available from Oligoengine™.

There are several methods for delivering siRNA into cells. Many transfection reagents can be used in order to deliver synthetic siRNA into cells, such as Lipofectamine 2000 or Oligofectamine from Invitrogen, TransIT-TKO from Mirus, and Siport Amine and Siport from Ambion. Along with transfection reagents, electroporation can be used to introduce synthesized siRNAs and expression vectors. The expression vector used in this chapter was introduced to the cells by electroporation. All the methods for siRNA

synthesis and delivery described in this section were tested for use with the HM1 and BK4 ESC lines in the osteogenic culture system and the electroporation of the pSUPERIOR™ system was the most efficient method.

In order to detect gene silencing by siRNA, the specific target mRNA or its protein product needs to be assayed. For target protein knockdown, the typical method is by immunofluorescence or western blotting. For measuring target mRNA knockdown, the preferred methods are QRT-PCR and Northern blot analysis (reviewed in (204)). The mRNA expression of siRNA targeted genes used in this chapter was detected by QRT-PCR.

5.1.4 pSUPERIOR RNAi System™

The pSUPERIOR RNAi System™ is an inducible shRNA system that is tetracycline-regulated and utilizes regulatory elements from the *E. coli* Tn*10*-encoded tetracycline resistance operon (225,226). The regulation is based on the binding of tetracycline to the tetracycline repressor (TetR or Tet repressor) and derepression of the promoter that is controlling expression of the gene of interest (227). The pSUPERIOR RNAi System™ requires several components for the inducible knockdown of targeted genes. The first component of this inducible system is a Tet repressor-expressing vector. The recommended vector for use with the pSUPERIOR RNAi System™ is the pcDNA6/TR© regulatory vector from Invitrogen. This vector expresses high levels of the Tet repressor gene (228) under control of the human cytomegalovirus (CMV) immediate-early promoter (229). The second component is the pSUPERIOR vector containing the siRNA hairpin precursor downstream of an H1 promoter and a tetracycline

operator 2 ($TetO_2$) site. The H1 promoter is a polymerase-III RNA gene promoter that produces a small RNA transcript that lacks a polyadenosine tail. The $TetO_2$ sequence is a binding site for two molecules of the Tet repressor. The final component of this system is tetracycline. Doxycycline is also commonly used as an inducing reagent with this system because it is similar to tetracycline in its mechanism of action, dose response, and induction characteristics, but has a longer half-life than tetracycline (48 hours versus 24 hours) (226).

In the absence of tetracycline, the Tet repressor forms a homodimer that binds to the $TetO_2$ sequence in the H1 promoter and causes transcriptional repression of the siRNA hairpin precursor. In the presence of tetracycline, tetracycline binds to the Tet repressor, causing a conformational change that prevents its binding to the $TetO_2$ sequence, thus allowing transcription of the siRNA hairpin precursor (Fig. 5.2A). The siRNA hairpin precursor contains a unique 19 nucleotide sequence designed to target a gene of interest. The resulting transcript contains both the sense and antisense strands; therefore, it should fold back on itself to form a nine bp stem-loop structure in which the stem-loop is quickly cleaved to form a functional siRNA (Fig. 5.2B) (226).

5.2 Results

5.2.1 Tetracycline Repressor (TetR) and Inducible Short Hairpin RNA (shRNA)

There are two constructs involved in the pSUPERIOR™ RNAi system: (i) one containing the tetracycline repressor and (ii) one containing the inducible short hairpin RNA (shRNA). Figure 5.3A shows a diagram of the TetR vector, which contains the cytomegalovirus (CMV) promoter, globin intervening sequence (IVS), TetR, SV40 poly adenylation signal sequence (poly A), and the Neo^R gene so that G418 resistance can be used to identify ESCs that have randomly and stably integrated the construct. Before integration into ESCs, DNA was prepared from several vector clones, and the proper cloning of the construct was verified by restriction enzyme digestion with NcoI (Fig. 5.3B). Lane 7 of Figure 5.3B depicts a properly cloned construct. From this newly created vector, a 3.8 kb fragment was isolated which contained all the elements listed above. This fragment was isolated, purified, and electroporated into the BK4 ESC line. After random integration, several clones which survived G418 selection were tested by QRT-PCR for the expression level of the TetR (Fig. 5.4). While several clones were used for the targeted integration of the inducible shRNA, clone 7 (from Fig. 5.4) was used for the experiments outlined in this chapter. Since the inducible shRNA system requires the addition of tetracycline (doxycycline) to the osteogenic culture, the impact of doxycycline (a tetracycline analog) on total colony forming units and percentage of colonies that are able to mineralize was tested on an ESC line containing only the TetR (clone 7 discussed above) (Fig. 5.5). The addition of 1 μg/ml doxycycline to the osteogenic culture did not result in a significant difference at day 21 for either total

colonies or percentage of colonies with mineralization in comparison to the no doxycycline control. This indicates that doxycycline alone does not have an impact on these factors.

This ESC line was then used for the targeted integration of tetracycline-inducible *Oct-4* and *Runx2* shRNA constructs. The *Oct-4* shRNA construct was used as a proof of principle for the system. Figure 5.6A shows a diagram of a general tetracycline-inducible shRNA vector, illustrating the components of the transgene, as well as those necessary for the targeted integration of the construct to the Hprt locus. The inducible components of the pSUPERIOR RNAi System™ were cloned into an Hprt targeting vector so that this portion of the system could be targeted in a single copy to the Hprt locus by homologous recombination (Fig. 4.2). The proper cloning of the *Oct-4* and *Runx2* shRNA vectors was verified by restriction enzyme digestion with NcoI and HindIII (Figs. 5.6B, C, respectively). Lanes 6 and 8 of Figure 5.6C represent properly cloned *Runx2* shRNA vectors in a subset of vector clones tested. In both lanes, the fragments seen above 6.9 kb and at 1.5 kb represent undigested DNA. The 433 bp fragment in both B and C are hard to visualize but can be seen on the original 1% agarose gel. The verified *Oct-4* and *Runx2* shRNA vectors shown Figure 5.6B and in lane 8 of Figure 5.6C, respectively, were each electroporated into the BK4 ESC line containing the TetR (clone 7). After targeted integration at the Hprt locus, RNA was isolated from *Oct-4* and *Runx2* shRNA ESC clones that survived HAT selection. RT-PCR analysis was used to verify the presence of the rescued *Hprt* locus, which contains a portion of the human HPRT (Figs. 5.6D, E). The 5′ primer was designed to anneal to the human HPRT and the 3′ primer was designed to anneal to the 3′ mouse Hprt homology, both depicted in Figure 5.6A.

The expected band size for the RT-PCR reaction is 71 bp and was visualized on a 1% agarose gel for both the *Oct-4* shRNA (Fig. 5.6D) and *Runx2* shRNA ESC clones (Fig. 5.6E).

5.2.2 Proof of Principle – Inducible Knockdown of Oct-4 in Murine ESCs

The tetracycline-inducible *Oct-4* shRNA vector was designed to be used as a proof of principle for the inducible system in ESCs. Oct-4 is a transcription factor necessary for maintaining ESC potential and self-renewal capacity (146,147). Therefore, the knockdown of *Oct-4* mRNA would be detrimental to the maintenance of the ESCs (230) and the effectiveness of the system could be assessed before differentiation of the osteogenic culture. Doxycycline was added to the ESCs containing the TetR and inducible *Oct-4* shRNA vector at concentrations ranging from 0.2 μg/ml to 1 μg/ml for 48 hours. RNA was isolated from the ESCs, and the mRNA expression level was analyzed by QRT-PCR (Fig. 5.7). There was a significant ($p<0.05$) decrease in *Oct-4* mRNA expression when 0.2, 0.4, and 0.6 μg/ml doxycycline were added for 48 hours in comparison to the no doxycycline control. This showed that the *Oct-4* shRNA vector was capable of knocking down the *Oct-4* mRNA transcript but only at certain concentrations. While we hoped the *Oct-4* shRNA would be a straightforward proof of principle for the inducible shRNA system, we realized that the characteristics of the ESCs were complex in regards to the use of this system and therefore, not as easily transferable to the osteogenic culture. These factors and other confounding variables will be discussed in further detail in section 5.3.

5.2.3 Inducible Knockdown of Runx2 in the Osteogenic Culture

The tetracycline-inducible *Runx2* shRNA ESC line was differentiated in the osteogenic culture for 21 days. Doxycycline was added to the culture for the first seven or fourteen days at either 0.5 μg/ml or 1 μg/ml. Figure 5.8A shows a timeline schematic of the osteogenic culture indicating the days of doxycycline treatment with a thin black arrow. At day 21 of the osteogenic culture, plates treated with no doxycycline and 0.5 μg/ml or 1 μg/ml doxycycline for seven or fourteen days were evaluated for total colony forming units and percentage of colonies with mineralization (Fig. 5.8B). The results showed no significant difference in total colonies or percentage of colonies with mineralization when doxycycline was added for the first seven or fourteen days at either concentration when compared to the no doxycycline control. The relative *Runx2* mRNA expression was evaluated from D0EB, day 4, day 7, and day 14 of the osteogenic culture for the no doxycycline control, 0.5 μg/ml, and 1 μg/ml doxycycline treatment for seven days (Fig. 5.9). There was a significant ($p<0.05$) decrease in *Runx2* mRNA expression at day 4 of the osteogenic culture when 1 μg/ml doxycycline was added in comparison to the control at day 4. At all other time points and doxycycline concentrations there was no significant difference in *Runx2* mRNA expression. As a result a constitutive *Runx2* shRNA vector was created to test the effectiveness of the siRNA sequence before use in the inducible system.

5.2.4 Constitutive Knockdown of Runx2 in the Osteogenic Culture

In order to create a constitutive *Runx2* shRNA, the tetracycline-inducible *Runx2*

shRNA construct, described in section 5.2.1, was electroporated into a BK4 ESC line that did not contain a randomly integrated TetR. As a result, there should be no inhibition of the *Runx2* shRNA promoter and transcription of the siRNA hairpin should occur constitutively, thus resulting in the creation of a constitutive *Runx2* shRNA ESC line. A constitutive *Runx2* shRNA ESC clone was differentiated using the osteogenic culture. Figure 5.10A shows the total colony forming units and percentage of colonies with mineralization for the parental BK4 ESC line and the constitutive *Runx2* shRNA ESC line. The constitutive *Runx2* shRNA line showed a significant ($p<0.05$) decrease in both total colonies and percentage of colonies with mineralization when compared to the parental BK4 ESC line. RNA was isolated from D0EB, day 10, and day 22 of the osteogenic culture for both the parental BK4 ESC line and the constitutive *Runx2* shRNA line. QRT-PCR analysis showed a significant ($p<0.06$) decrease in *Runx2* mRNA expression at day 10 and 22 when compared to the control at each time point (Fig. 5.10B). This indicates that the *Runx2* siRNA sequence and shRNA vector are able to knockdown expression of *Runx2* in the osteogenic culture and negatively impact the total colony forming units and percentage of colonies that mineralize.

5.2.5 Inducible and Constitutive Knockdown of Runx2 in the Osteogenic Culture: Can the Inducible Mimic the Constitutive?

Since the constitutive *Runx2* shRNA clone tested was able to knockdown the expression of *Runx2* in the osteogenic culture and impact the osteogenic outcome, two other constitutive *Runx2* shRNA clones were tested for reproducibility. Along with this experiment, the inducible *Runx2* shRNA ESC line (from Figures 5.8 and 5.9) was tested

for its ability to mimic the constitutive ESC line if doxycycline was added throughout the entire culture. Doxycycline (0.5 μg/ml) was added to the inducible *Runx2* shRNA ESC line at day -3 (ESC) of the osteogenic culture and maintained in the medium until day 21 (Fig. 5.11A). Day -3 represents two days before trypsinization of ESCs or the beginning of osteogenic manipulation. Therefore, in a sense, the inducible construct should be constitutive. At day 21 of the osteogenic culture, the total colony forming units and percentage of colonies with mineralization were determined for the parental ESC line, inducible *Runx2* shRNA ESC line, and three constitutive *Runx2* shRNA ESC clones (Fig. 5.11B). The inducible shRNA and constitutive shRNA clones 2 and 3 showed a significant ($p<0.05$) decrease in total colonies when compared to the parental ESC line. Clone 1 also showed a decrease in total colonies, but it was not significant. There was also a decrease in percentage of colonies that mineralized for all four lines tested, but it was not significant in comparison to the parental line. This showed that in terms of total colonies and percent of colonies that were osteogenic, the inducible shRNA was able to mimic the constitutive shRNA and the other two constitutive clones performed similarly to clone C3 (Figure 5.10). The *Runx2* mRNA expression was analyzed by QRT-PCR at day 7, day 14, and day 21 of the osteogenic culture (Figs. 5.12A, B, C, respectively) for the parental BK4 ESC line, an inducible shRNA ESC line, and three constitutive shRNA ESC line clones in comparison to the D0EB. This analysis revealed a significant ($p<0.05$) decrease in *Runx2* mRNA expression for the inducible shRNA and three constitutive shRNA clones at day 7, 14, and 21 in comparison to the parental ESC control.

The expression of several mature lineage markers was analyzed by QRT-PCR at day 21 to determine whether the knockdown of *Runx2* expression and the decrease in total colonies correlated with the expression of the mature osteoblast marker, *Bglap1*. Figure 5.13A shows the expression of *Bglap1* at day 21 for the parental ESC line control, inducible *Runx2* shRNA, and three constitutive shRNA ESC clones in comparison to the D0EB. The expression of *Bglap1* was significantly ($p<0.05$) decreased in the inducible and constitutive ESC lines in comparison to the parental ESC line. However, the expression of two other mature lineage markers, *Myh11* (myogenesis) (Fig. 5.13B) and *Lpl* (adipogenesis) (Fig. 5.13C), were not significantly decreased in the inducible or constitutive *Runx2* shRNA clones when compared to the parental ESC line, suggesting the knockdown of *Runx2* mRNA in the osteogenic culture to be specifically detrimental to the osteogenic lineage.

5.3 Discussion

As stated in the Introduction section 5.1.3, several methods of siRNA synthesis and delivery were used in conjunction with the osteogenic culture system but proved to be ineffective. *In vitro* synthesized siRNA was generated for *Runx2* with the Ambion *Silencer*™ siRNA Construction Kit. We first attempted to electroporate the *in vitro* synthesized siRNA into ESCs either prior to the last ESC plating or prior to plating of the osteogenic culture. These time points were chosen because during the EB culture and after plating for the osteogenic culture the cells are adherent to the tissue culture plate no longer suitable for electroporation. In addition to the limited time points for electroporation, the *in vitro* synthesized siRNA was only stable for 72 hours and therefore expression of target genes would need to be most critical at these two time points to see an effect. However, we saw no knockdown of gene expression for *Runx2* (with three different target sequences) or impact on osteogenesis when the siRNA was electroporated at either time point (data not shown). We do know that *Runx2* is not highly expressed in either the ESC or D2EB (Fig. 3.5B) but the results suggested it was too early for siRNA to have an impact or the siRNA was not efficient at knocking down expression.

As a result, we decided to transfect the *in vitro* synthesized siRNA into osteogenic cells at early time points of the osteogenic culture when the cells were adherent. It was also decided to label the siRNA so that delivery into cells could be visualized. The Label IT siRNA Tracker TM-Rhodamine Intracellular Localization Kit (Mirus) was used to label the synthetic siRNA with Rhodamine, a fluorescent dye. The TransIT-TKO transfection reagent (Mirus) was used to deliver the labeled, synthetic siRNA to the cells. Upon transfection the siRNA was visualized within the cells with a

fluorescent microscope (Fig. 5.14); however, the transfection reagent was toxic to the cells during early days of the osteogenic culture. The complex nature of the osteogenic system in regards to siRNA delivery led us to create an inducible siRNA system that could be stably integrated into the ESC genome and subsequently induced before and throughout the osteogenic culture. We hypothesized that this method would circumvent some of the challenges with delivery and would enable us to identify the commitment time point of progenitor cells to the osteogenic lineage.

The *Oct-4* shRNA construct and results described in this chapter were intended as a proof of principle for the inducible siRNA system. It has been shown that murine embryonic stem cells transfected with a plasmid containing an RNA polymerase type III promoter to constitutively express small stem-loop *Oct-4* RNA transcripts showed reduced levels of *Oct-4* mRNA expression and displayed trophectodermal differentiation (230). These results suggested that the *Oct-4* shRNA construct would be a good candidate for validating the system in ESCs before inducing osteogenic differentiation. However, there were many confounding variables with the inducible system in ESCs that made the data obtained from the *Oct-4* shRNA construct difficult to translate in the osteogenic culture. The cell density and doubling time of the ESCs seemed to play a larger role in the knockdown of *Oct-4* mRNA expression levels than expected.

Several TetR ESC lines were used to target the *Oct-4* shRNA because the level of TetR required for the system to function as desired was not known. Since this is a tetracycline derepressible system, too much TetR might require a toxic amount of tetracycline to allow transcription. Conversely, too little of the TetR might result in a "leaky" system. Two separate TetR lines with differing TetR expression levels (Fig. 5.4,

clones 3 and 7) were used to target the *Oct-4* shRNA construct. Subsequently, several of these shRNA clones were tested as well. These electroporations were done in the presence and absence of feeder cells to eliminate any residual tetracycline from the original feeder media. This, however, proved not to have an impact on the outcome of the experiments. In testing the different *Oct-4* shRNA clones, doxycycline from two separate companies, Clontech and Sigma, was used at concentrations varying from 0 to 20 μg/ml. There were also two separate QRT-PCR primer pairs designed to detect knockdown of the mRNA transcript. The first primer pair was anchored upstream of the target siRNA sequence, and the second primer pair was anchored on either side of the target sequence. This was done because it wasn't known how long it took for the transcript to be degraded after siRNA targeting. Once the mRNA is targeted by siRNA it should be cleaved and so the primer pairs anchored on either side of the target sequence would immediately be unable to detect a product making these primers more efficient in detecting transcript loss.

After all the experiments and troubleshooting that was conducted the most straightforward interpretation is that the amount of doxycycline necessary for knockdown was dependent upon the density of the cells. The density of ESCs is much greater than that of the cells plated for the osteogenic culture. A confluent plate of ESCs will yield approximately 3-5 x 10^7 cells as compared to an osteogenic culture plating of 2 x 10^3 cells. As a result of differences in cell density there is also a difference in proliferation or doubling time of the cells. From microscopic analysis, we know that that the more dense a plate of ESCs or osteogenic culture plate, the more rapid the proliferation of the cells. This may explain why in Figure 5.7, the level of *Oct-4* mRNA was reduced with 0.2, 0.4,

and 0.6 μg/ml doxycycline but at 0.8 and 1 μg/ml there was no effect. The cells may also be biphasic so that at certain time points ESCs may be undergoing different phases of doubling times and may require different amounts of doxycycline. For example, if there is a decrease in *Oct-4* expression levels this would slow the growth of the cells. With a decrease in cell growth, the TetR will accumulate beyond the concentration of doxycycline. The doxycycline will no longer be able to activate transcription of the shRNA because the accumulation of the TetR will allow it to repress the H1 promoter. This in turn will increase *Oct-4* expression levels. While these results are still unclear to us, we realized that the inducible shRNA system would probably perform differently in the osteogenic culture and therefore, we decided to move on to the *Runx2* shRNA construct.

While the loss-of-function of *Runx2* has been well characterized in the mouse model and has been investigated in immature osteoblast-like cells, primary rat osteoblasts (231), and bone metastatic cancer cells, the knockdown of this transcription factor with siRNA in ESC-derived osteogenic cultures has not been documented (26,28,135). In the first experiment conducted with inducible *Runx2* shRNA, shown in Figures 5.8 and 5.9, doxycycline was added at 0.5 and 1 μg/ml for the first seven or fourteen days of the osteogenic culture. The results showed no change in total colony forming units, percentage of colonies with mineralization, or *Runx2* mRNA expression. There are several possibilities to explain these results: (i) the doxycycline concentration or addition time points may not be optimal, (ii) the TetR expression level may not be appropriate, (iii) the *Runx2* siRNA sequence may not be effective at knocking down the expression of *Runx2*, or (iv) the endogenous up-regulation of *Runx2* in the osteogenic culture may be

too great for the inducible system to regulate. Since the *Runx2* target sequence was previously published (see Table 2.3) and before testing different doxycycline concentrations and addition time points or TetR ESC lines, a constitutive *Runx2* shRNA vector was created to test the effectiveness of the actual siRNA sequence with the H1 promoter in the absence of an inducible system.

The constitutive *Runx2* shRNA proved to be effective at knocking down *Runx2* mRNA expression and also resulted in a decrease in total colony forming units and percentage of colonies with mineralization, suggesting the decrease in *Runx2* expression was detrimental to osteogenesis (Fig. 5.10). As a result, the inducible *Runx2* shRNA ESC line was tested again but with induction throughout the culture, from the ESC (day -3) to day 21 of the osteogenic culture. This experiment was performed to test the ability of the system to induce shRNA, as well as mimic the constitutive construct. These results (Fig. 5.11, 5.12, and 5.13) showed that the inducible shRNA was able to function and mimicked the constitutive shRNA in terms of knocking down *Runx2* mRNA expression. The knockdown of *Runx2* mRNA expression was seen at day 7, day 14, and day 21, indicating the system could knockdown expression throughout the culture (Fig. 5.12). There was also a significant decrease in total colony forming units and a decrease in mineralization with the inducible and constitutive *Runx2* shRNA, suggesting that the knockdown of *Runx2* in the osteogenic culture is detrimental to osteogenesis (Fig. 5.11). However, the timing of Runx2 activity must be critical because addition of doxycycline from days 0 – 7 or 0 – 14 of the culture (Fig. 5.8) did not have the same impact.

The analysis of mature lineage markers further supported the notion that knockdown of *Runx2* expression is detrimental to osteogenesis because *Bglap1*

expression was significantly diminished at day 21 in the inducible and constitutive *Runx2* shRNA ESC lines (Fig. 5.13A). However, the expression of *Myh11* and *Lpl*, markers of smooth muscle and fat, were not significantly affected by the *Runx2* shRNA, suggesting the knockdown of *Runx2* mRNA in the osteogenic culture to be specifically detrimental to the osteogenic lineage.

The results of this experiment seem to suggest that the induction of *Runx2* shRNA is critical during the time points before the cells are plated for the osteogenic culture, specifically the five days between day -3 and D2EB (see Figure 5.11A or 5.15 for schematic). These were the additional time points added from the first *Runx2* shRNA experiment where no effect was seen (Fig. 5.8). The inducible *Runx2* shRNA ESC line can now be used to narrow this window of *Runx2* expression and determine when the critical decrease in *Runx2* mRNA is occurring. This can be interpreted as the time point when the precursor cells commit to the osteogenic lineage. It will also be necessary to investigate the protein level of Runx2 because we hypothesize that there is a delay between siRNA induction and decreased protein expression, perhaps placing the critical time point during the first several days of the osteogenic culture as the overexpression experiments suggest. This time point may span one or more days due to the heterogeneity of the culture at any stage.

Two experiments were conducted to investigate this time frame in greater detail, but some obstacles were encountered in regards to the size of the experiments. As shown in Figure 3.2, the time in EB formation greatly impacts the total colony forming units, with increased time equaling decreased colony formation. In the experiments conducted, there were several different doxycycline starting points tested (Fig. 5.15) and therefore,

the EBs were split into two plating times separated by at least five hours. This greatly skewed the results of the experiment. However, in the second experiment all EBs were trypsinized at the same time but had to be plated for the osteogenic culture one at a time. This also skewed the results of the experiment because the cells that were plated last remained on ice for at least one hour and inevitably, some cell death occurred. These variables were not originally anticipated and can be difficult to control for, but future experiments should be designed to take these factors into account. One possible solution is to stagger the flushing of ESCs for EB formation for each doxycycline starting point and correlate this with staggered plating for the osteogenic culture. This will alleviate the different time lengths in EB formation and cell death.

The versatility of this inducible shRNA system will allow for the construction of siRNA to target any gene of interest. There are several transcription factors implicated in osteogenesis that would be interesting to investigate with loss-of-function constructs, such as Sox-9, Twist-1, Twist-2, or osterix. We have begun work with a Twist-1 inducible shRNA construct. We would predict that knockdown of *Twist-1* expression would promote osteogenesis because the Twist proteins have been shown to inhibit Runx2 function (47). However, a decrease in Twist-1 expression has not been seen, with either the inducible or constitutive constructs, and therefore, further experiments need to be done. In addition to targeting these transcription factors implicated in osteogenesis, the system would also be useful for other lineages known to be present in the osteogenic culture. For example, the presence of myogenesis and adipogenesis has been seen in the osteogenic culture both in the whole plate (Fig. 3.5C) as well as in individual colonies (Fig. 3.6B). The question remains how these other lineages are affecting the outcome of

the osteogenic culture in terms of mineralized colony formation as well as gene expression in whole plates and individual colonies. We would predict that the knockdown of transcription factors necessary for competing mesenchymal lineages would increase osteogenesis and/or restrict lineage potential. shRNA constructs designed to target MyoD/myogenic or PPARγ/adipogenic may be able to answer some of these questions.

The hypothesis that these manipulation experiments were based on is that a critical decision point involving the mesenchymal lineages occurs sometime before day 3 of the osteogenic culture. The results of these experiments suggest this time frame to be correct, although there are still more experiments that need to be done to narrow this critical juncture and understand when these cells commit to the osteogenic lineage.

In light of the fact that the Twist-1 inducible shRNA construct was unable to induce knockdown of the transcription factor, it is worth reviewing some potential problems of this system as well as experimental design alternatives. As discussed briefly in this section, the level of TetR needed for this system to function properly is still not clear. If there are inadequate amounts of TetR, there may be leakiness of shRNA expression as a result of incomplete repression of the H1 promoter. Although in the case of Twist-1 this does not appear to be the problem. Conversely, if the level of expression of the TetR is too high, after addition of doxycycline there may be a lack of shRNA expression. Eight TetR clones were screened for expression levels and two clones were used in electroporations of the shRNA constructs. The two clones chosen were the highest expressing TetR ESC line and a clone with expression at half that level. It may be beneficial to screen through more clones and target several clones with varying levels

of expression. Also, a lack of mRNA repression may indicate that the chosen siRNA target sequence is inefficient, even though the sequences were previously published. It may be necessary to create multiple shRNA constructs to be tested for a particular gene. Similar to the overexpression constructs, targeting the inducible shRNA constructs in a single copy may not be effective. There is one published example of an effective shRNA targeted in a single copy to the Hprt locus and one targeted in a single copy to the Rosa26 locus (232,233), respectively. However, these are constitutively expressed and there have been no publications of inducible shRNA targeted in a single-copy to the Hprt locus. Therefore, it may be beneficial to randomly integrate the inducible constructs as well.

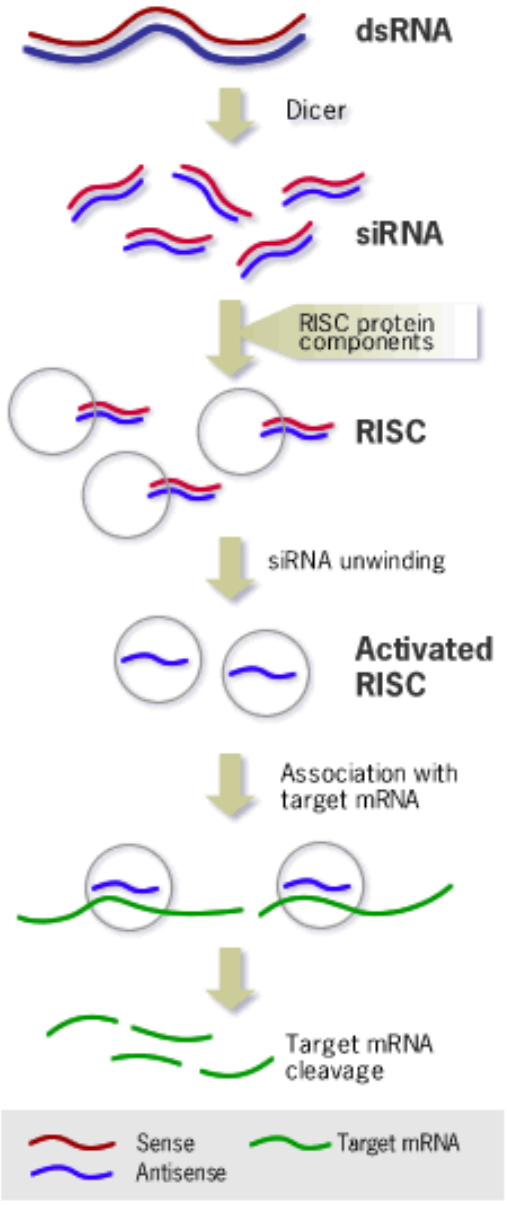

Figure 5.1: Mechanism of RNA Interference (RNAi). Long dsRNAs are cleaved into 20-25 nucleotide small interfering RNAs (siRNAs) by an RNase III-like enzyme called Dicer. The siRNAs assemble into RNA-induced silencing complexes (RISCs). The siRNA strands are then unwound to form activated RISCs and subsequently guided to complementary RNA molecules, where they cleave the target RNA (Figure and legend adapted from source (234)).

A. pSUPERIOR RNAi System™

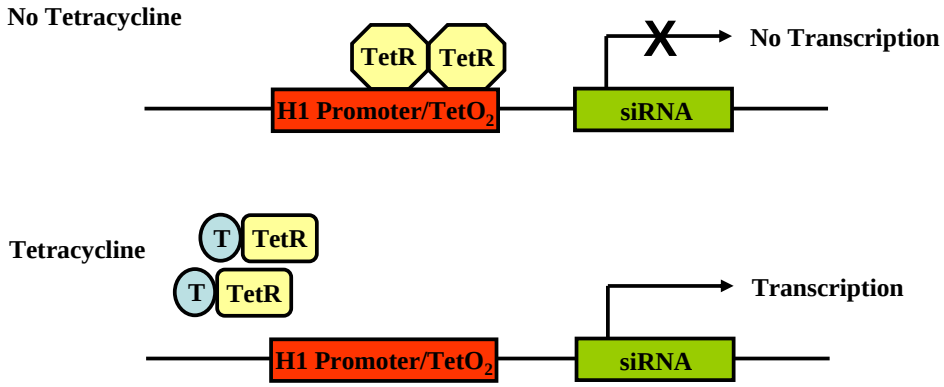

B.

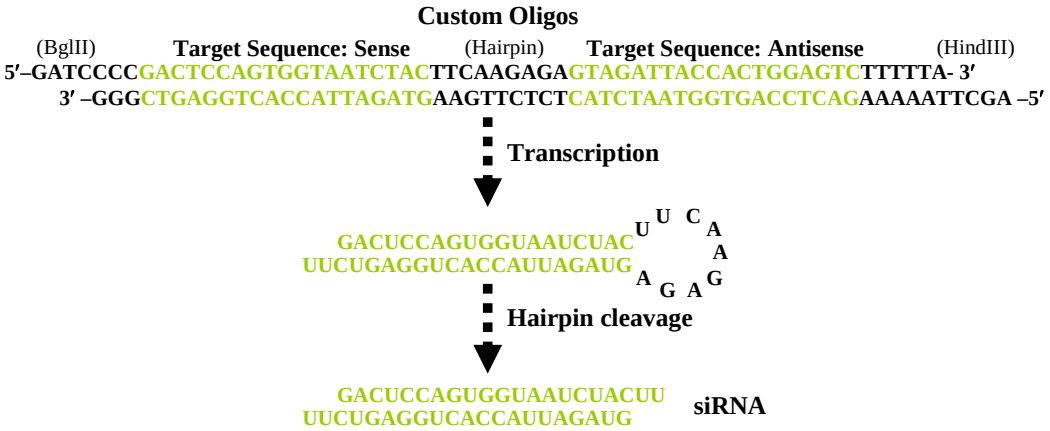

Figure 5.2: pSUPERIOR RNAi System™ and custom oligo design. (**A**.) Schematic of pSUPERIOR RNAi System™. In the absence of tetracycline, the Tet repressor forms a homodimer that binds to the $TetO_2$ sequence in the H1 promoter and causes repression of the siRNA hairpin. In the presence of tetracycline, tetracycline binds to the Tet repressor and causes a conformational change, preventing its binding to the $TetO_2$ sequence, allowing transcription of the siRNA hairpin. (**B**.) Custom oligos of an example siRNA hairpin precursor, which contains a unique 19 nucleotide sequence designed to a target gene of interest. Upon transcription, the resulting transcript contains both sense and antisense strands, allowing fold back of a 9 bp stem-loop structure. The stem-loop is quickly cleaved, resulting in a functional siRNA. TetR = Tet repressor, T = tetracycline (**B**.) Adapted from source (226).

A.

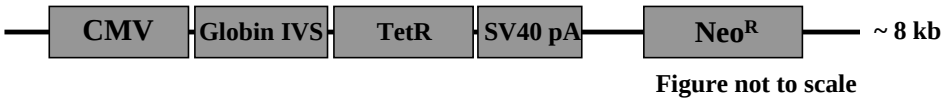

Figure not to scale

B.

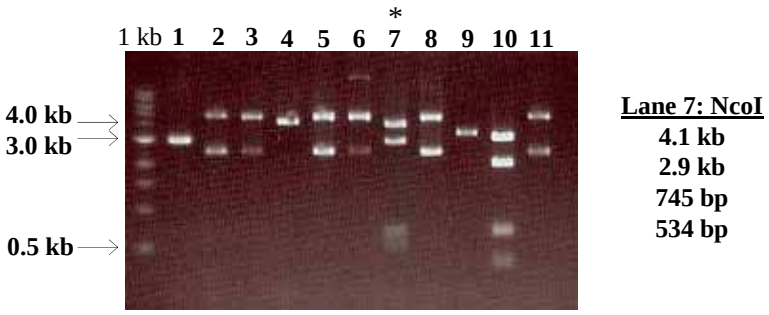

Figure 5.3: Tetracycline repressor (TetR) construct. (**A.**) Diagram of ~8 kb vector containing the CMV promoter, globin IVS, Tet repressor, and SV40pA (2.3 kb) and Neo^R gene (1.3 kb). The black line represents the remaining vector sequence. (**B.**) Restriction enzyme digestion with NcoI of 11 colonies; lane 7 represents properly cloned vector visualized on a 1% agarose gel. Expected band sizes are listed. Proper cloning of lane 7 (asterisk) was also verified by restriction enzyme digestion with BamHI, EcoRI, and HindIII (not shown).

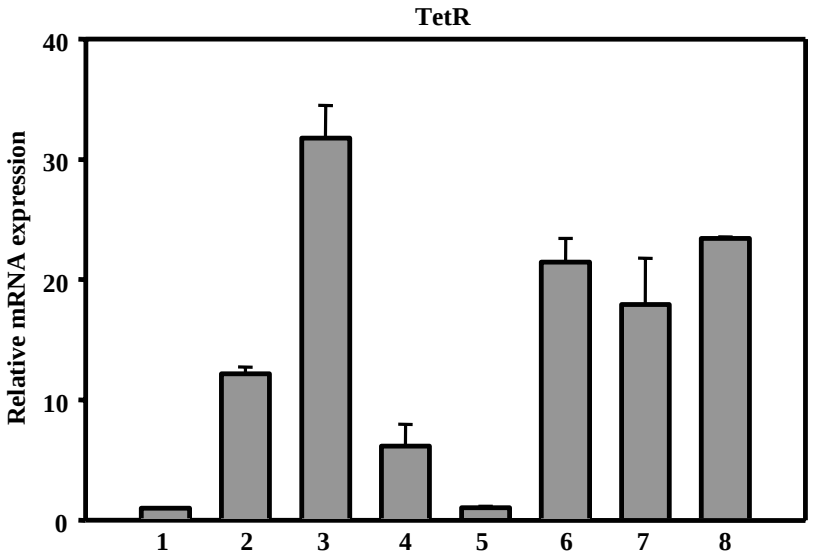

Figure 5.4: QRT-PCR analysis of the Tet repressor (TetR) in a subset of ESC clones. Each assay was run in duplicate at two different template concentrations. Relative mRNA expression was normalized to ribosomal protein L7 (*Rpl7*) and displayed relative to clone 1.

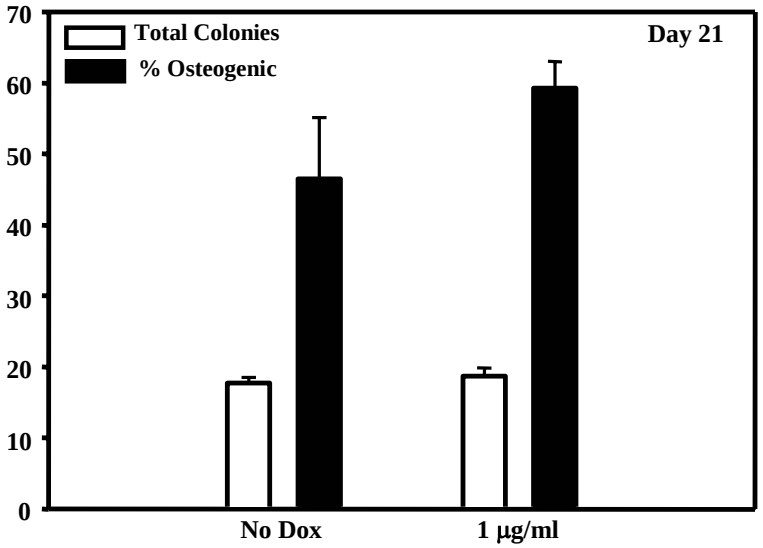

Figure 5.5: Total colony forming units and percentage of colonies with mineralization at day 21 of the osteogenic culture for ESCs containing a TetR (clone 7, Fig. 5.4) in the absence (No Dox) and presence (1 μg/ml) of doxycycline. There was no significant difference between No Dox and 1 μg/ml Dox for either total colonies or % osteogenic.

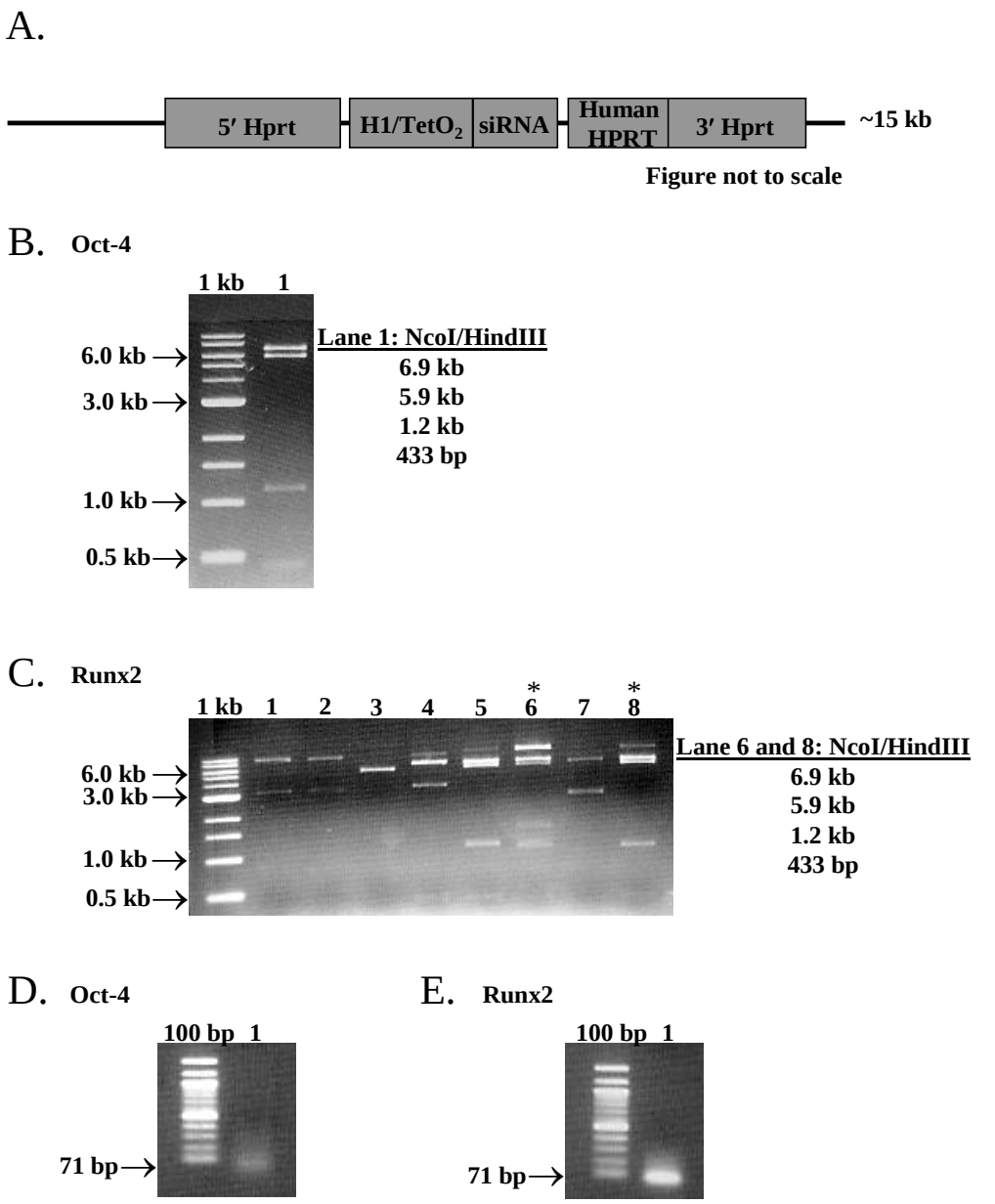

Figure 5.6: Tetracycline-inducible shRNA constructs. (**A**.) Diagram of ~15 kb vector containing 5′ Hprt homology (3.75 kb), the H1 promoter, $TetO_2$ sequence and shRNA (Oct-4 = 315 bp, Runx2 = 350 bp), and the human HPRT and the 3′ Hprt homology (4.45 kb) that was electroporated into ESCs. The black line represents remaining vector sequence. Restriction enzyme digestion with NcoI/HindIII of properly cloned (**B**.) *Oct-4* and (**C**.) *Runx2* shRNA vectors visualized on a 1% agarose gel. Expected fragment sizes are listed. *Runx2* shRNA digestion depicts 8 colonies, lanes 6 and 8 (asterisk) represent properly cloned vectors. Vector shown in lane 8 was used for electroporations. RT-PCR analysis of rescued *Hprt* locus in TetR clone 7 (Fig. 5.4) containing the targeted, inducible (**D**.) *Oct-4* and (**E**.) *Runx2* shRNA. Product size is 71 bp. Primer sequences are listed in Table 2.5. (See Figure 4.13C for positive and negative control reactions with the given primers.)

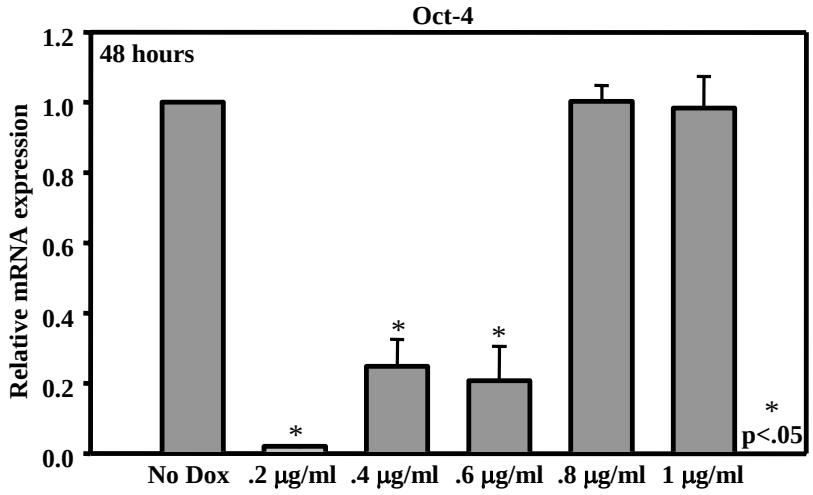

Figure 5.7: QRT-PCR analysis of *Oct-4* mRNA expression in TetR clone 7 ESCs (Fig. 5.4) containing a tetracycline-inducible *Oct-4* shRNA after treatment with increasing amounts of doxycycline for 48 hours. Each assay was run in triplicate at two different template concentrations. Relative mRNA expression was normalized to ribosomal protein L7 (*Rpl7*) and displayed relative to No Dox. Asterisk represents a significant difference when compared to No Dox.

A.

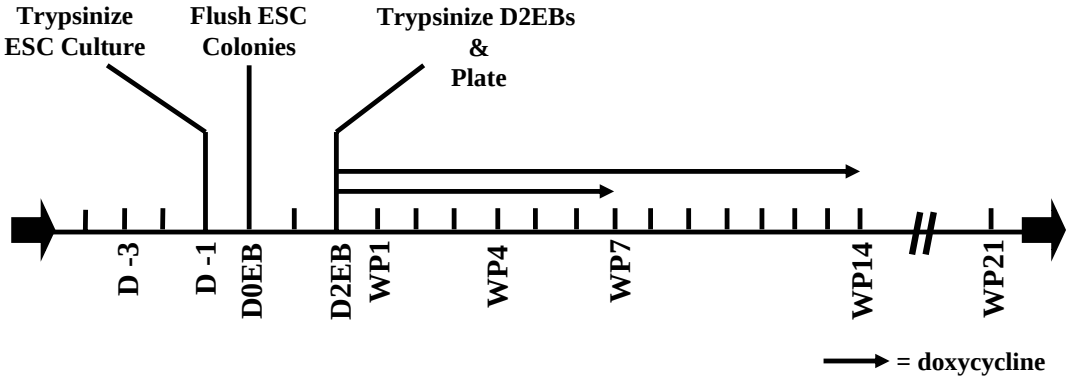

B.

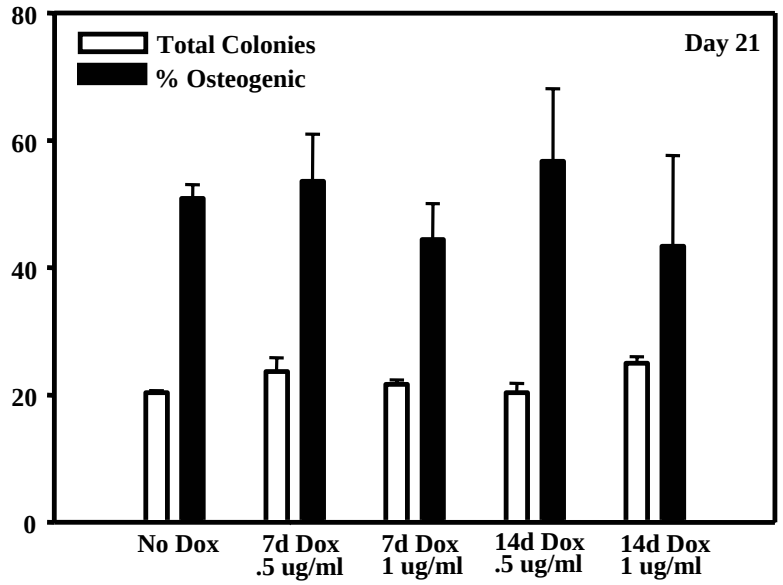

Figure 5.8: Effect of tetracycline-inducible *Runx2* shRNA on the osteogenic culture after treatment with 0.5 μg/ml or 1 μg/ml doxycycline for seven or fourteen days. (**A.**) Timeline of osteogenic differentiation indicating when doxycycline was added to the culture. Tick marks represent days. Thin arrows represent addition of doxycycline to plates (two different lengths of time (seven and fourteen days) were tested). (**B.**) Total colony forming units and percentage of colonies with mineralization at day 21 of the osteogenic culture for ESCs containing a tetracycline-inducible *Runx2* shRNA after treatment for 7 (7d Dox) or 14 (14d Dox) days with 0.5 μg/ml or 1 μg/ml doxycycline. D -1 = day -1, D -3 = day -3 (D -1 and D-3 become more important in later figures.)

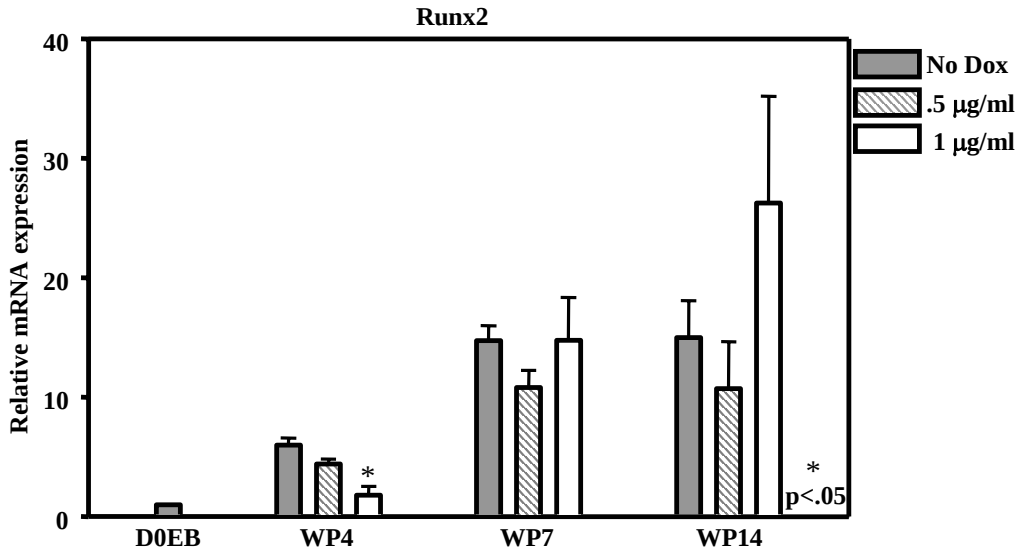

Figure 5.9: QRT-PCR analysis of *Runx2* mRNA expression for D0EB, WP4, WP7, and WP14 of the osteogenic culture for ESCs containing a tetracycline-inducible *Runx2* shRNA after treatment with 0.5 μg/ml or 1 μg/ml doxycycline for seven days. Each assay was run in triplicate at two different template concentrations. Relative mRNA expression was normalized to ribosomal protein L7 (*Rpl7*) and displayed relative to D0EB. Asterisk represents significant difference when compared to No Dox for WP4.

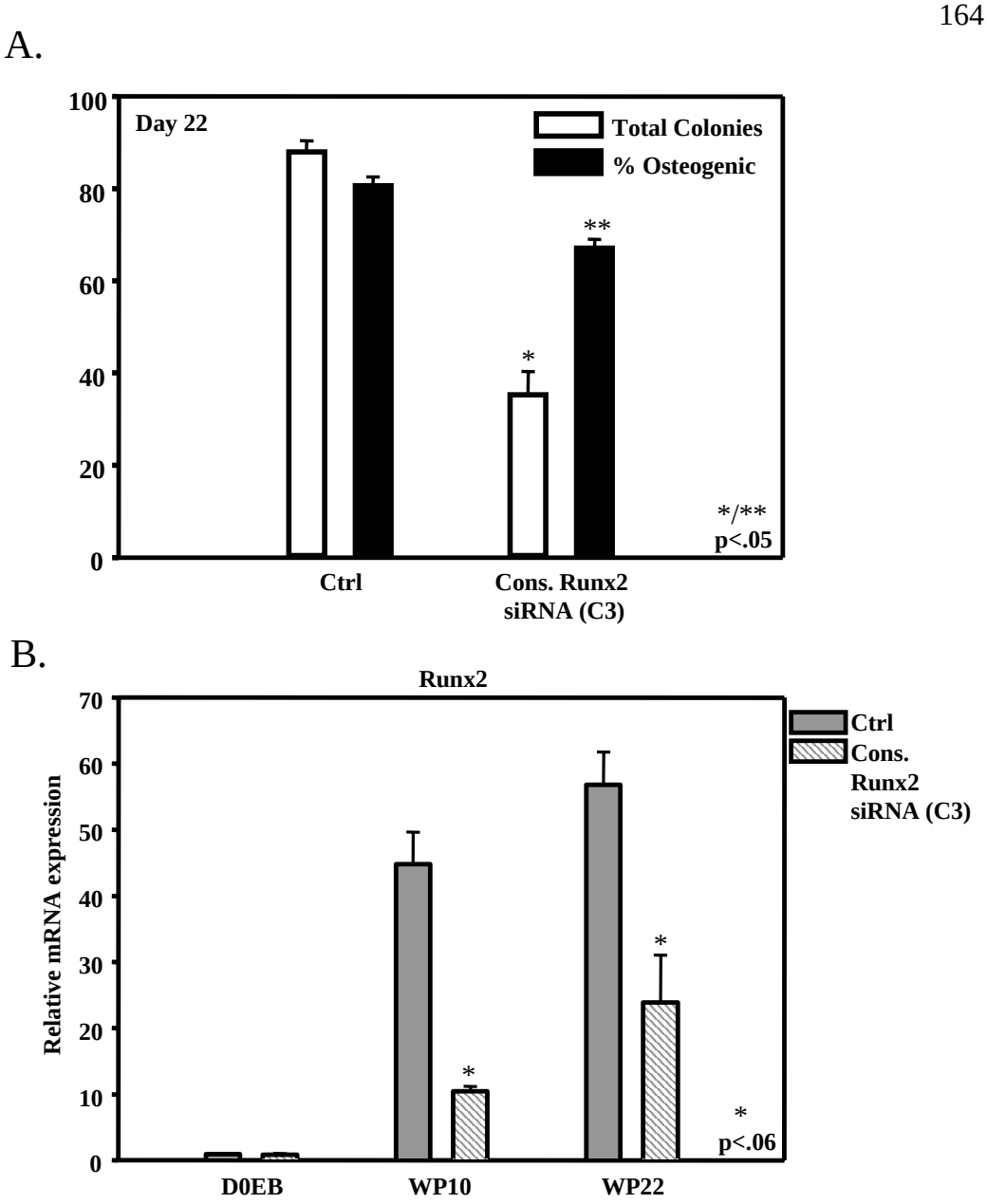

Figure 5.10: Effect of constitutive *Runx2* shRNA on the osteogenic culture. (**A.**) Total colony forming units and percentage of colonies with mineralization at day 22 of the osteogenic culture for the parental ESC line (Ctrl) and a clone containing a constitutive *Runx2* shRNA (C3). A single asterisk represents a significant difference when compared to Ctrl Total Colonies, and a double asterisk represents a significant difference when compared to Ctrl % Osteogenic. (**B.**) QRT-PCR analysis of *Runx2* mRNA expression for D0EB, WP10, and WP22 osteogenic cultures for Ctrl and C3. Each assay was run in triplicate at two different template concentrations. Relative mRNA expression was normalized to ribosomal protein L7 (*Rpl7*) and displayed relative to D0EB Ctrl.

A.

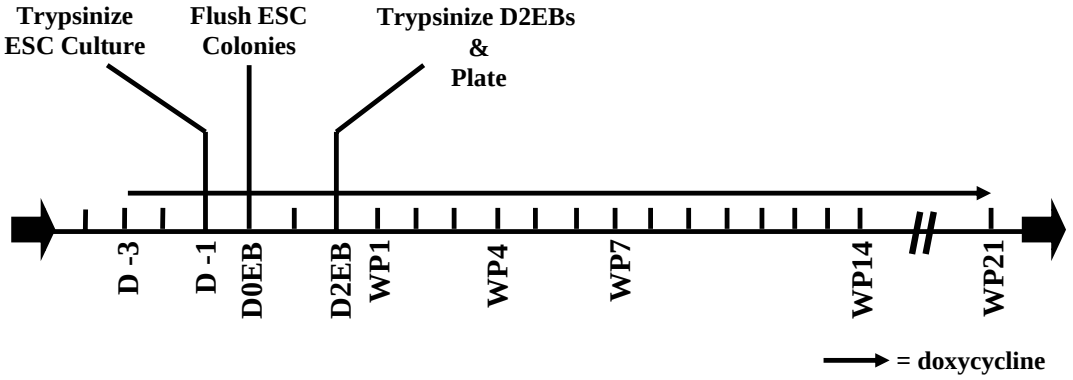

B.

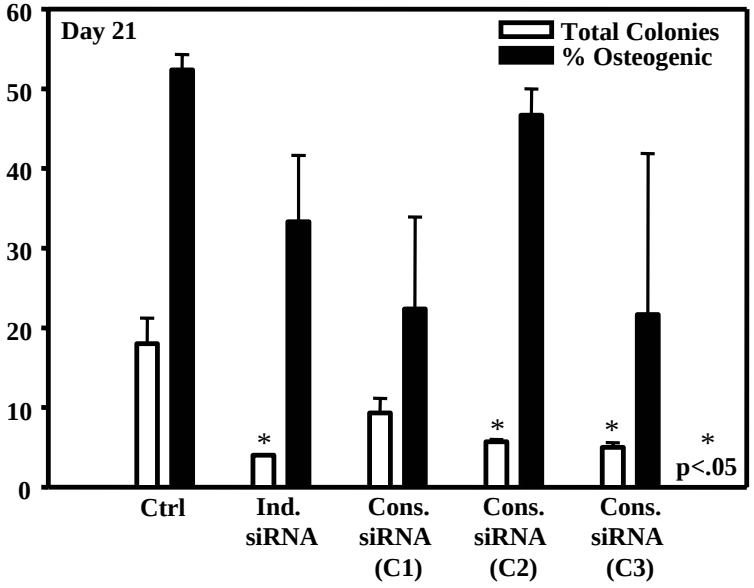

Figure 5.11: Effect of tetracycline-inducible and constitutive *Runx2* shRNA on the osteogenic culture. (**A.**) Timeline of osteogenic differentiation indicating when doxycycline (0.5 μg/ml) was added to the culture for tetracycline-inducible *Runx2* shRNA (Ind. siRNA). Tick marks represent days. Thin arrow represents addition of doxycycline to plates (D -3 to WP21). (**B.**) Total colony forming units and percentage of colonies with mineralization at day 21 of the osteogenic culture for the parental ESC line (Ctrl), an ESC line containing a tetracycline-inducible *Runx2* shRNA (Ind. siRNA) (same ESC line as Fig. 5.8 and 5.9), and ESC clones 1, 2, and 3 (C1, 2, and 3) (C3 is same ESC line as Fig. 5.10) containing a constitutive *Runx2* shRNA. Asterisk represents a significant difference when compared to Ctrl Total Colonies. D -1 = day -1, D -3 = day -3.

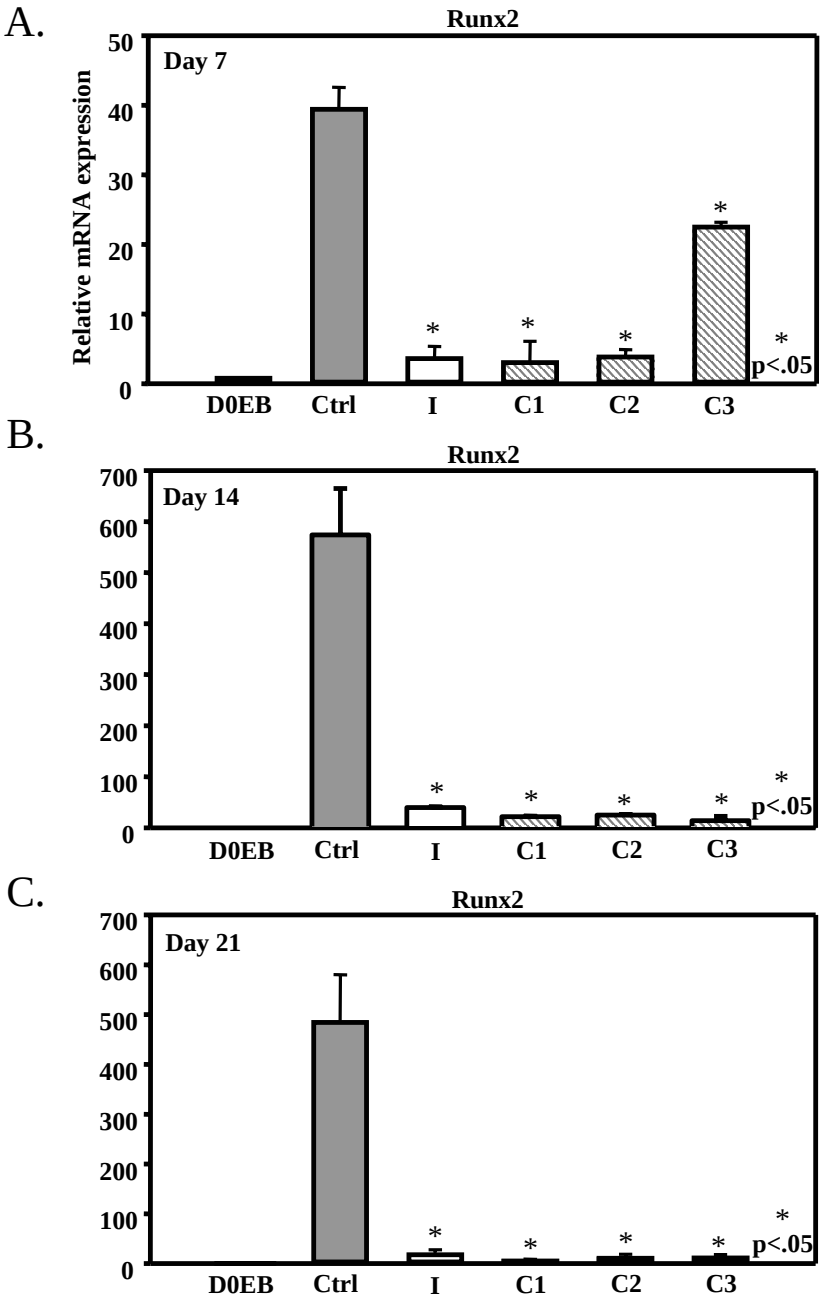

Figure 5.12: QRT-PCR analysis of *Runx2* mRNA expression at (**A**.) day 7, (**B**.) day 14, and (**C**.) day 21 of the osteogenic culture for D0EB, the parental ESC line (Ctrl), an ESC line containing tetracycline-inducible *Runx2* shRNA (I) (0.5 μg/ml from D -3 to WP21), and ESC clones 1, 2, and 3 containing a constitutive *Runx2* shRNA (C1, 2, and 3). Each assay was run in triplicate at two different template concentrations. Relative mRNA expression was normalized to ribosomal protein L7 (*Rpl7*) and displayed relative to D0EB. Asterisk represents a significant difference when compared to Ctrl of same time point.

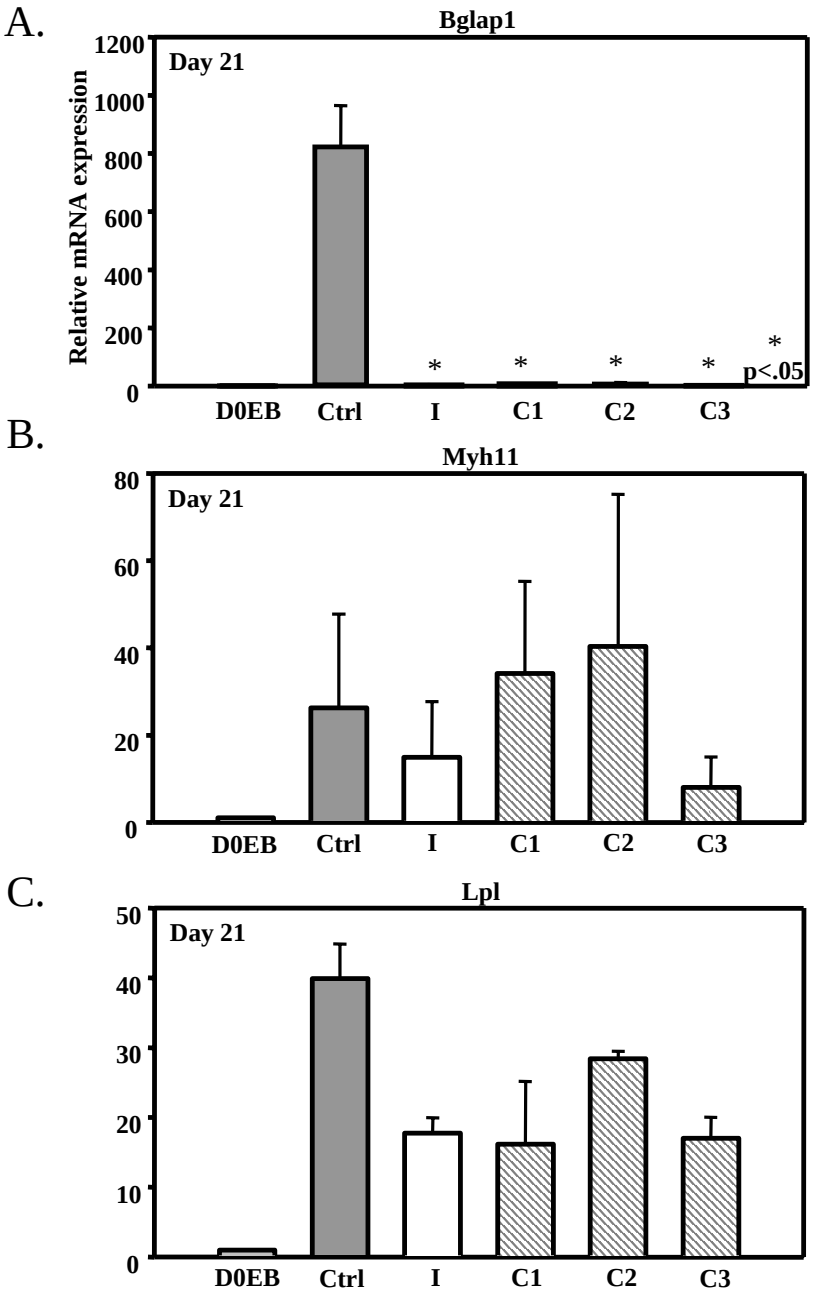

Figure 5.13: QRT-PCR analysis of (**A**.) *Bglap1*, (**B**.) *Myh11*, and (**C**.) *Lpl* mRNA expression at day 21 of the osteogenic culture for D0EB, the parental ESC line (Ctrl), an ESC line containing tetracycline-inducible *Runx2* shRNA (I) (0.5 μg/ml from D -3 to WP21), and ESC clones 1, 2, and 3 containing a constitutive *Runx2* shRNA (C1, 2, and 3). Each assay was run in triplicate at two different template concentrations. Relative mRNA expression was normalized to ribosomal protein L7 (*Rpl7*) and displayed relative to D0EB. Asterisk represents a significant difference when compared to Ctrl.

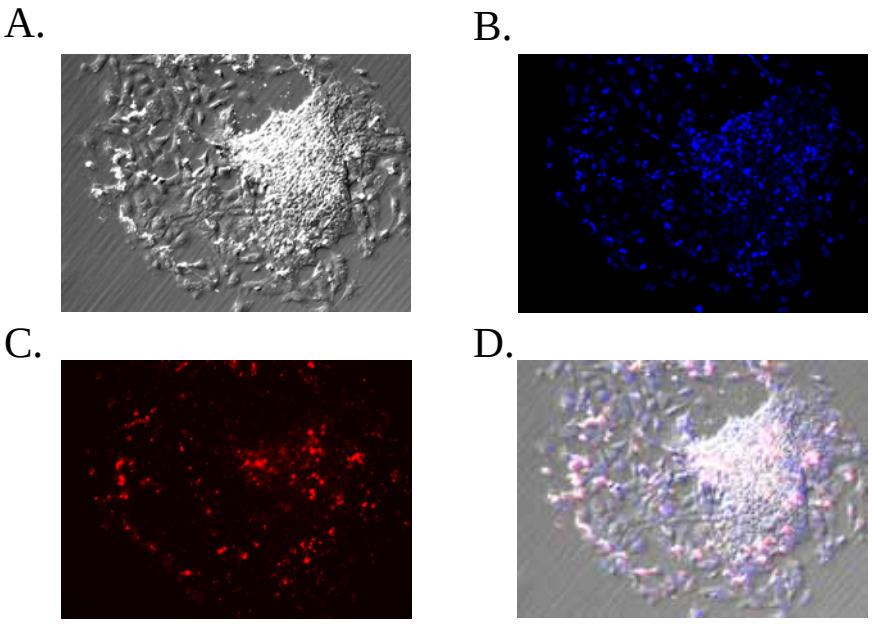

Figure 5.14: Visualization of labeled *Runx2* siRNA in a day 5 individual colony, 26 hours post transfection. (**A**.) Phase contrast microscopy image of colony (10x magnification). (**B**.) Fluorescent microscopy of nuclei identified with a Hoescht stain. (**C**.) Fluorescent microscopy of Rhodamine incorporation into cells of the individual colony. (**D**.) Combined images of A, B, and C. For control plates, Rhodamine image was too low for detection.

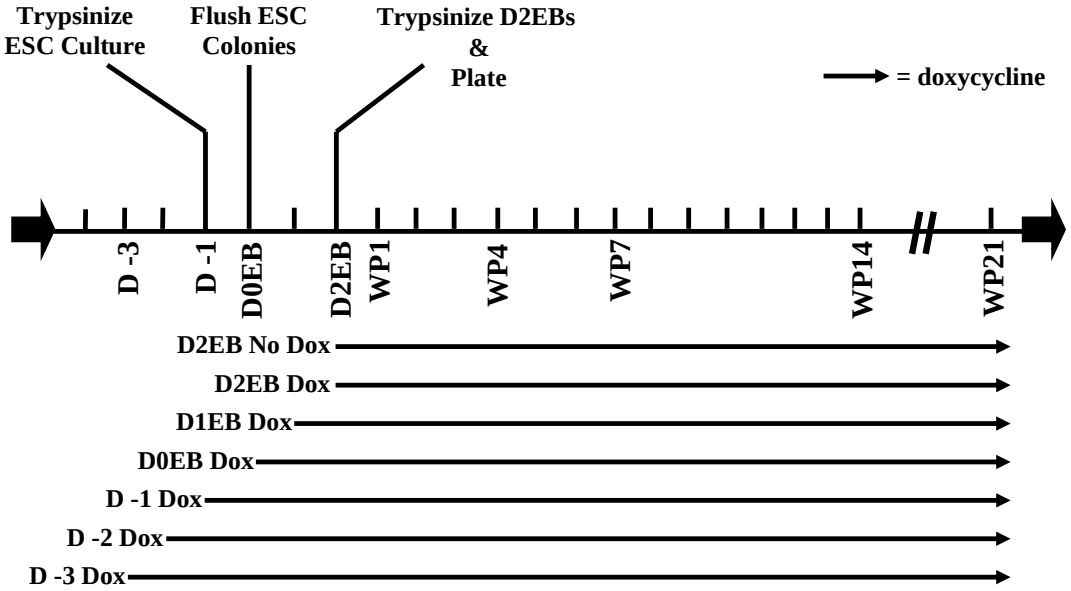

Figure 5.15: Timeline of osteogenic differentiation indicating different doxycycline starting points. Thin black arrow represents doxycycline addition. Dox = doxycycline.

CHAPTER 6

GENERAL DISCUSSION

6.1 Overview

The process of bone formation can be observed *in vitro* in the form of a mineralized nodule. Mesenchymal stem cells (MSCs), the immediate precursors to osteoprogenitors, are found in the marrow, and likely in numerous other sites throughout the organism. Differentiation of these progenitors, when placed into culture under appropriate conditions, proceeds through characteristic stages of commitment, proliferation, matrix secretion, and mineral deposition during a period of 3-4 weeks. We have developed an ESC-derived osteogenic culture system. ESCs are allowed to form embryoid bodies (EBs) that are then disrupted after two days and plated as single cells at densities as low as 25 cells/cm^2. By eight days post plating, a significant percentage of the colonies have morphology characteristic of other types of osteogenic cultures. By three weeks in culture, these colonies go on to form layered nodules. Generally 60% of the colonies are layered, mineralized nodules.

This thesis provides three lines of evidence for osteogenesis in these ESC-derived cultures: (i) cell and colony morphology as revealed by phase contrast microscopy, (ii) mineralization of extracellular matrix as revealed by von Kossa staining, and (iii) QRT-PCR analysis of cDNA from entire plates and individual colonies revealing expression of genes characteristic of, and specific for, osteoblasts. For QRT-PCR analysis, we have isolated RNA from entire plates and individual colonies at different stages of the

differentiation process to investigate the expression of genes characteristic of the osteoblast lineage, as well as genes characteristic of other lineages and stem/progenitor cells. Analysis of gene expression in the first week revealed that brachyury, *Twist-2*, *Runx2*, and *Sox-9* are up-regulated by day 4 of the osteogenic culture, with osterix expression increasing by day 7. *Runx2*, osterix, type I collagen, and *Bglap1*, all important for osteogenesis, are transcriptionally up-regulated by day 14 and continue to increase in expression out to 21 days. QRT-PCR analysis of amplified RNA from individual colonies indicates that it is the morphologically osteogenic colonies that are expressing mRNA characteristic of the osteoblast lineage and allows us to further categorize colonies into hematopoietic, osteogenic, adipogenic, myogenic or a mixture of mesenchymal lineages.

The goal of this project has been to define the timing and molecular basis of commitment in ESC-derived osteogenic cultures. We hypothesize that there is a critical decision point involving the mesenchymal lineages that occurs somewhere before day 3 of the osteogenic culture. Runx2 is necessary for bone formation and is postulated to be the transcriptional switch of osteoblast differentiation (21). In order to investigate the commitment of progenitor cells to the osteogenic lineage in the osteogenic culture system, we have utilized the up-regulation of *Runx2* by BMP-2 and developed overexpression and knockdown of *Runx2* mRNA expression constructs.

We have generated both constitutive and tetracycline-inducible *Runx2* overexpressing ESCs to investigate the effect of *Runx2* overexpression in our osteogenic cultures. The transgenic ESC lines were differentiated and analyzed for *Runx2* mRNA expression, as well as mineralized colony formation. Interestingly, while the QRT-PCR

data revealed a robust increase in *Runx2* mRNA expression for the constitutive overexpression of *Runx2*, the overall colony number and percent of colonies mineralized decreased, suggesting the overexpression of *Runx2* can be detrimental for osteogenesis, as well as other mesenchymal lineages. Although expression was significantly lower than constitutive levels, *Runx2* mRNA overexpression was also detrimental to osteogenesis when it was induced throughout the culture, but in this case seemed to be more specific to the osteogenic lineage. These experiments, along with the BMP-2 data, suggest that overexpression of *Runx2* during early time points in the osteogenic culture before commitment has occurred is detrimental for osteogenesis.

We have also generated ESCs containing constitutive and tetracycline-inducible *Runx2* shRNA constructs to investigate the loss of Runx2 function in our osteogenic cultures, as well as to continue to investigate the commitment of progenitor cells to the osteogenic lineage. The transgenic ESCs were differentiated and analyzed for both *Runx2* mRNA expression and mineralized colony formation. Induction of the inducible shRNA throughout the osteogenic culture mimicked the results of the constitutive *Runx2* shRNA expression experiments. Knockdown of *Runx2* mRNA expression throughout the osteogenic culture was detrimental to osteogenesis but not to other mesenchymal lineages, such as the myogenic and adipogenic lineages. The timing of induction in these experiments suggests that there is a critical decision being made in regards to the osteogenic lineage during early time points in culture.

This method of initiating osteogenesis from murine ESC cultures, where individual EB-derived progenitors are plated at a low density such that the potential and differentiation of a single cell can be determined, is the only described method that

allows for the observation and manipulation of the commitment stage of mesengenesis from single murine embryonic progenitors. It also shows great promise for unraveling the mechanisms of commitment to the osteogenic lineage, as well as exploring the therapeutic potential of cells of this lineage.

6.2 Gene Expression, Osteogenic Commitment, and Therapeutic Populations

The gene expression analysis described in Chapter 3 was critical for the validation of the osteogenic culture system. It allowed us to track the expression of transcription factors and mature markers necessary for proof of osteogenesis in the culture. The gene expression analysis also allowed us to follow the progression of ESCs from multipotential cells to differentiated osteoblasts, as diagramed in the working model (Fig. 3.7). This progression of differentiation and the ability to track transcription factors throughout the culture is key to identifying the commitment of progenitor cells to the osteogenic lineage. Based on the *Runx2* manipulation studies discussed in Chapters 4 and 5, we believe that a critical decision point involving the mesenchymal lineages, and in particular the osteogenic lineage, is occurring before day 3 of the osteogenic culture. Gene expression analysis from early time points in culture revealed that several transcription factors implicated in bone development are transcriptionally up-regulated by day 4 of the osteogenic culture (Fig. 3.4). These include *Twist-2*, *Sox-9*, and *Runx2*, with osterix up-regulation occurring after day 7. Not only does the expression of these factors during these time points support our hypothesis, it also suggests a time frame for the enrichment of a therapeutic population.

A second project in our laboratory investigates the potential for a therapeutic population in the osteogenic culture. This project is being conducted by Jean DeMarco. Because the proliferative capacity of the mature osteoblast is negligible, but ESCs have been demonstrated to form teratomas when transplanted *in vivo*, we also hypothesize that an intermediate cell population with the desired therapeutic qualities of significant

proliferative capacity and restricted lineage potential exists within the ESC-derived osteogenic culture. In order to test this hypothesis, ESC-derived progenitor cells will be used to identify a time point in the *in vitro* osteogenic culture, in which cells can be isolated and transferred *in vivo* for therapeutic capacity. Experiments from this thesis suggest that the time frame will be during early days of the osteogenic culture. This second project will utilize transcription factors, identified by experiments in this thesis, as reporters for hopefully identifying this therapeutic population ESCs have been genetically engineered to contain a yellow fluorescent protein (YFP) transgene constitutively expressed under the control of the CAGGS (CAG promoter (CMV enhancer and chicken β-globin promoter), rabbit β-globin gene sequences including a polyadenylation signal, and an SV40 *ori*) (235) in order to track the donor-derived cells *in vivo*. This construct was randomly integrated so that a second construct could be targeted in a single copy to the Hprt locus. The second construct will be used for enrichment of cells expressing transcription factors implicated in bone formation, *Twist-2*, *Sox-9*, *Runx2*, and osterix. These constructs will utilize mouse bacterial artificial chromosomes (BACs) containing one of our genes of interest. Each BAC will be modified such that green fluorescent protein (GFP) is regulated by the transcription factor of interest and is able to be targeted to the Hprt locus of the YFP-expressing ESCs. With the two constructs properly integrated, this will allow for tracking (through YFP) and enrichment (through GFP) of an intermediate cell population with potential therapeutic capacity. The enriched cells will be tested for their ability to engraft synthetic scaffolds and adult bone subcutaneously in mice. The long term goal of this project is to transfer

the enriched progenitors capable of engrafting synthetic scaffolds and adult bone into oim mice (mouse model of osteogenesis imperfecta) and test for improved bone formation.

6.3 Importance of the Osteogenic Culture System and Implications for Stem Cell-Based Therapeutics

Stem cell-based therapies have the potential to treat several different bone disorders, including severe bone fractures, osteoporosis, and osteogenesis imperfecta (OI), a genetic disorder also known as brittle bone disease. The number of people affected with OI in the United States is still unknown, but the best estimates suggest between 20,000 and 50,000 (Osteogenesis Imperfecta Foundation (OIF)) (236). OI is characterized most widely by bone fragility, although other phenotypes do arise, including osteoporosis, dentigenesis imperfecta, blue sclera, easy bruising, and scoliosis. There are seven types of OI that are largely based on there clinical characteristics. Most cases are caused by mutations that affect the genes that encode the proα1 and proα2 polypeptide chains that comprise the type I collagen molecule, although OI types V, VI, and VII are not thought to be directly associated with type I collagen mutations but other unidentified molecules. Type I collagen, as stated earlier, is the major protein of bone, comprising 95% of its entire collagen content. It is composed of two identical α1 polypeptide chains (COL1A1) and one α2 polypeptide chain (COL1A2). These three chains twist around each other to form a rope-like structure. Mutations in either of the polypeptide chains that affect the helical domain of one of the proα chains will result in the improper formation or lack of type I collagen production and, in turn, OI (237,238). The bone fragility, therefore, is most likely a result of insufficient matrix production or accumulation of defective collagen molecules (reviewed in (238)).

The current treatment of OI aims to increase function while at the same time decreasing the occurrence of fractures. There are several types of treatments that can be grouped into either orthopedic management or pharmacological agents. Currently, the use of the pharmacological agent pamidronate, a bisphosphonate, in the treatment of OI has shown some beneficial effects (238-244). Bisphosphonates are compounds that inhibit the resorption of bone by binding to the bone matrix and inhibiting osteoclast activity. While the bisphosphonates have begun to improve the lifestyle of patients with OI, they do not correct for the mutations in collagen synthesis and therefore, are not a cure (238). Cell therapy approaches have been designed to address the collagen mutations in OI. These therapies would supply cells that would replace the mutant osteoblasts that make abnormal collagen chains. The idea for this cell therapy is that as mutant osteoblasts turn over or become quiescent, they can be replaced by normal osteoblasts introduced from transplanted progenitors (238).

MSCs have been used in cell therapy approaches to treat OI. The MSC has the potential to treat bone disorders because it is the parental cell of the bone-forming osteoblast. They are found in the bone marrow and therefore, bone marrow transplants or purified MSCs would be good candidates for use in stem cell-based bone disorder therapies, where replacement or supplementation of the number of bone forming cells is desired. However, even though the use of MSCs in treating bone related disorders has shown some promise, it has not been as successful as hoped. The first human clinical trials were conducted by Horwitz and colleagues, after some initial success using murine and primate models (238,245). They conducted allogeneic bone marrow transplantation in five children with OI using whole marrow harvested from leukocyte antigen (HLA)

matched or single-antigen-mismatched siblings. After three months, three of the five children showed donor osteoblast engraftment and new dense bone formation in representative specimens of trabecular bone (245). After six months, there was a 7.5 cm increase in body length compared to a 1.25 cm increase in control patients. There was also an increase in total body bone mineral content (TBBMC) determined with X-ray absorptiometry in comparison to baseline values. With further follow ups, the patient's growth rates slowed or reached a plateau, and the number of cells that engrafted was very low (246). After three months, it was estimated that only 1.5–2% of the cells in the trabecular bone of recipients were donor derived (245). Indicating that while there was improvement in bone formation there was extremely low engraftment of donor cells. In a follow up treatment, Horwitz et al. used gene-marked, donor marrow-derived mesenchymal cells to treat six children who had previously undergone bone marrow transplantation. While there was an increase in growth velocity after six months, there was only a 1% detection of donor cell engraftment at any site, including bone and never a detection of the marker gene (247). The authors conclude that allogeneic mesenchymal cells offer a feasible posttransplantation therapy; however, the question remains whether these few engrafted cells from whole marrow transplantation or mesenchymal cell infusion are long-living osteogenic precursors or committed osteoblasts with a short half-life (248).

In the bone marrow, the frequency of MSCs has been estimated to be about 10 MSCs per one million of all bone marrow cells; however, due to the lack of definitive markers for this cell, it is not possible to determine the exact proportion of MSCs in the marrow (78,249). At present, MSCs are identified by a combination of physical,

phenotypic and functional properties (248). The inability to definitively identify the MSC and calculate its frequency in the bone marrow may be one reason these cells have not been as useful in stem cell-based therapies. While the use of MSCs to treat OI has met some success, there is still a need for further research and more efficient methods to increase the number and engraftment of therapeutic progenitor cells. There is also the possibility to generate bone forming cells from adult tissues, such as fat, but the therapeutic efficacy of these cells is still unclear (250).

ESCs are one other potential source of therapeutic cells and have several advantages over MSCs and other adult stem cells. ESCs can form all cell and tissue types and are, therefore, not only useful in bone related disorders, but other diseases/disorders as well. These cells can be maintained in culture indefinitely and can be easily identified with several marker genes, such as Oct-4 and Nanog (71,72,146). There has been a lot of progress in directing the differentiation of ESCs to specific cell types in culture, as well as the ability to enrich or purify specific cell types from a mixed population. This promises to increase the number of therapeutic cells that can be transplanted in comparison to the limiting number of MSCs found within the bone marrow. With the use of nuclear transfer, the possibility of a patient's immune response rejecting the donor cells is eliminated. In nuclear transfer, the patient's DNA would be transferred into an enucleated oocyte and used to generate ESCs matched to the patient. For these several reasons, the use of ESCs in cell replacement therapy may soon be a more promising and valuable tool in treating many different diseases. We are hopeful that the progress made with our osteogenic culture system will one day be beneficial for patients with diseases such as osteogenesis imperfecta.

Reference List

1. **Marks, S. C. and P. R. Odgren**. 2002. Structure and Development of the Skeleton, p. 3-15. *In* J. P. Bilezikian, L. G. Raisz, and G. A. Rodan (ed.), Principles of Bone Biology. Academic Press.

2. **Karsenty, G.** 1999. The genetic transformation of bone biology. Genes & Development **13**:3037-3051.

3. **Ducy, P., T. Schinke, and G. Karsenty**. 2000. The osteoblast: A sophisticated fibroblast under central surveillance. Science **289**:1501-1504.

4. **Franz-Odendaal, T. A., B. K. Hall, and P. E. Witten**. 2006. Buried alive: How osteoblasts become osteocytes. Developmental Dynamics **235**:176-190.

5. **Aubin, J. E., J. B. Lian, and G. S. Stein**. 2006. Bone Formation: Maturation and Functional Activities of Osteoblast Lineage Cells, p. 20-29. *In* J. B. Lian and S. R. Goldring (ed.), Primer on the Metabolic Bone Diseases and Disorders of Mineral Metabolism. The American Society of Bone and Mineral Research, Washingtion, D.C.

6. **Li, Z. P., K. M. Kong, and W. L. Qi**. 2006. Osteoclast and its roles in calcium metabolism and bone development and remodeling. Biochemical and Biophysical Research Communications **343**:345-350.

7. **Nijweide, P. J., E. H. Burger, and J. Klein-Nulend**. 2002. The Osteocyte, p. 93-107. *In* J. P. Bilezikian, L. G. Raisz, and G. A. Rodan (ed.), Principles of Bone Biology. Academic Press.

8. **Palumbo, C.** 1986. A 3-Dimensional Ultrastructural-Study of Osteoid-Osteocytes in the Tibia of Chick-Embryos. Cell and Tissue Research **246**:125-131.

9. **Noble, B. S. and J. Reeve**. 2000. Osteocyte function, osteocyte death and bone fracture resistance. Molecular and Cellular Endocrinology **159**:7-13.

10. **Doty, S. B.** 1981. Morphological Evidence of Gap-Junctions Between Bone-Cells. Calcified Tissue International **33**:509-512.

11. **Palumbo, C., S. Palazzini, and G. Marotti**. 1990. Morphological-Study of Intercellular-Junctions During Osteocyte Differentiation. Bone **11**:401-406.

12. **Yellowley, C. E., Z. Y. Li, Z. Y. Zhou, C. R. Jacobs, and H. J. Donahue**. 2000. Functional gap junctions between osteocytic and osteoblastic cells. Journal of Bone and Mineral Research **15**:209-217.

13. **Manolagas, S. C.** 2000. Birth and death of bone cells: Basic regulatory mechanisms and implications for the pathogenesis and treatment of osteoporosis. Journal of Aging and Physical Activity **8**:248.

14. **Chung, U. I., H. Kawaguchi, T. Takato, and K. Nakamura**. 2004. Distinct osteogenic mechanisms of bones of distinct origins. Journal of Orthopaedic Science **9**:410-414.

15. **Karp, J. M.** 2002. Embryonic Development of Bone and the Molecular Regulation of Intramembranous and Endochondral Bone Formation, p. 33-58. *In* J. P. Bilezikian, L. G. Raisz, and G. A. Rodan (ed.), Principles of Bone Biology. Academic Press.

16. **Nakashima, K. and B. de Crombrugghe**. 2003. Transcriptional mechanisms in osteoblast differentiation and bone formation. Trends in Genetics **19**:458-466.

17. **Olsen, B. R.** 2006. Bone Embryology, p. 2-6. *In* J. B. Lian and S. R. Goldring (ed.), Primer on the Metabolic Bone Diseases and Disorders of Mineral Metabolism. American Society of Bone and Mineral Research, Washington, D.C.

18. **Hill, T. P., D. Spater, M. M. Taketo, W. Birchmeier, and C. Hartmann**. 2005. Canonical Wnt/beta-catenin signaling prevents osteoblasts from differentiating into chondrocytes. Developmental Cell **8**:727-738.

19. **Day, T. F., X. Z. Guo, L. Garrett-Beal, and Y. Z. Yang**. 2005. Wnt/beta-catenin signaling in mesenchymal progenitors controls osteoblast and chondrocyte differentiation during vertebrate skeletogenesis. Developmental Cell **8**:739-750.

20. www.dictionary.com . 2007.

21. **Shroeder, T. M., E. D. Jensen, and J. J. Westendorf**. 2005. Runx2: A master organizer of gene transcription in developing and maturing osteoblasts. Birth Defects Research (Part C) **75**:213-225.

22. **Ducy, P., C. Desbois, B. Boyce, G. Pinero, B. Story, C. Dunstan, E. Smith, J. Bonadio, S. Goldstein, C. Gundberg, A. Bradley, and G. Karsenty**. 1996. Increased bone formation in osteocalcin-deficient mice. Nature **382**:448-452.

23. **Glowacki, J., C. Rey, M. J. Glimcher, K. A. Cox, and J. Lian**. 1991. A Role for Osteocalcin in Osteoclast Differentiation. Journal of Cellular Biochemistry **45**:292-302.

24. **Desbois, C., D. A. Hogue, and G. Karsenty**. 1994. The Mouse Osteocalcin Gene-Cluster Contains 3 Genes with 2 Separate Spatial and Temporal Patterns of Expression. Journal of Biological Chemistry **269**:1183-1190.

25. **Ducy, P. and G. Karsenty**. 1995. 2 Distinct Osteoblast-Specific Cis-Acting Elements Control Expression of A Mouse Osteocalcin Gene. Molecular and Cellular Biology **15**:1858-1869.

26. **Otto, F., A. P. Thornell, T. Crompton, A. Denzel, K. C. Gilmour, I. R. Rosewell, G. W. H. Stamp, R. S. P. Beddington, S. Mundlos, B. R. Olsen, P. B. Selby, and M. J. Owen**. 1997. Cbfa1, a candidate gene for cleidocranial dysplasia syndrome, is essential for osteoblast differentiation and bone development. Cell **89**:765-771.

27. **Ducy, P., R. Zhang, V. Geoffroy, A. L. Ridall, and G. Karsenty**. 1997. Osf2/Cbfa1: A transcriptional activator of osteoblast differentiation. Cell **89**:747-754.

28. **Komori, T., H. Yagi, S. Nomura, A. Yamaguchi, K. Sasaki, K. Deguchi, Y. Shimizu, R. T. Bronson, Y. H. Gao, M. Inada, M. Sato, R. Okamoto, Y. Kitamura, S. Yoshiki, and T. Kishimoto**. 1997. Targeted disruption of Cbfa1 results in a complete lack of bone formation owing to maturational arrest of osteoblasts. Cell **89**:755-764.

29. **Banerjee, C., A. Javed, J. Y. Choi, J. Green, V. Rosen, A. J. van Wijnen, J. L. Stein, J. B. Lian, and G. S. Stein**. 2001. Differential regulation of the two principal Runx2/Cbfa1 N-terminal isoforms in response to bone morphogenetic protein-2 during development of the osteoblast phenotype. Endocrinology **142**:4026-4039.

30. **Lengner, C. J., H. Drissi, J. Y. Choi, A. J. van Wijnen, J. L. Stein, G. S. Stein, and J. B. Lian**. 2002. Activation of the bone-related Runx2/Cbfa1 promoter in mesenchymal condensations and developing chondrocytes of the axial skeleton. Mechanisms of Development **114**:167-170.

31. **Xiao, Z. S., A. B. Hjelmeland, and L. D. Quarles**. 2004. Selective deficiency of the "bone-related" Runx2-II unexpectedly preserves osteoblast-mediated skeletogenesis. Journal of Biological Chemistry **279**:20307-20313.

32. **Drissi, H., Q. Luc, R. Shakoori, S. Chuva de Sousa Lopes, J. Y. Choi, A. Terry, M. Hu, A. J. van Wijnen, and G. S. Stein**. 2000. Transcriptional Autoregulation of the Bone Related CBFA1/RUNX2 Gene. Journal of Cellular Physiology **184**:341-350.

33. **Nakashima, K., X. Zhou, G. Kunkel, Z. P. Zhang, J. M. Deng, R. R. Behringer, and B. de Crombrugghe**. 2002. The novel zinc finger-containing transcription factor Osterix is required for osteoblast differentiation and bone formation. Cell **108**:17-29.

34. **Kim, Y. J., H. N. Kim, E. K. Park, B. H. Lee, H. M. Ryoo, S. Y. Kim, I. S. Kim, J. L. Stein, J. B. Lian, G. S. Stein, A. J. van Wijnen, and J. Y. Choi**. 2006. The bone-related Zn finger transcription factor Osterix promotes proliferation of mesenchymal cells. Gene **366**:145-151.

35. **Ng, L. J., S. Wheatley, G. E. O. Muscat, J. Conway Campbell, J. Bowles, E. Wright, D. M. Bell, P. P. L. Tam, K. S. E. Cheah, and P. Koopman**. 1997. Sox9 binds DNA, activates transcription, and coexpresses with type II collagen during chondrogenesis in the mouse. Developmental Biology **183**:108-121.

36. **Wright, E., M. R. Hargrave, J. Christiansen, L. Cooper, J. Kun, T. Evans, U. Gangadharan, A. Greenfield, and P. Koopman**. 1995. The Sry-Related Gene Sox9 Is Expressed During Chondrogenesis in Mouse Embryos. Nature Genetics **9**:15-20.

37. **Zhao, Q., H. Eberspaecher, V. Lefebvre, and B. Decrombrugghe**. 1997. Parallel expression of Sox9 and Col2a1 in cells undergoing chondrogenesis. Developmental Dynamics **209**:377-386.

38. **Bi, W. M., W. D. Huang, D. J. Whitworth, J. M. Deng, Z. P. Zhang, R. R. Behringer, and B. de Crombrugghe**. 2001. Haploinsufficiency of Sox9 results in defective cartilage primordia and premature skeletal mineralization. Proceedings of the National Academy of Sciences of the United States of America **98**:6698-6703.

39. **Bi, W. M., J. M. Deng, Z. P. Zhang, R. R. Behringer, and B. de Crombrugghe**. 1999. Sox9 is required for cartilage formation. Nature Genetics **22**:85-89.

40. **Akiyama, H., M. C. Chaboissier, J. F. Martin, A. Schedl, and B. de Crombrugghe**. 2002. The transcription factor Sox9 has essential roles in successive steps of the chondrocyte differentiation pathway and is required for expression of Sox5 and Sox6. Journal of Bone and Mineral Research **17**:S142.

41. **Akiyama, H., J. E. Kim, K. Nakashima, G. Balmes, N. Iwai, J. M. Deng, Z. P. Zhang, J. F. Martin, R. R. Behringer, T. Nakamura, and B. de Crombrugghe**. 2005. Osteo-chondroprogenitor cells are derived from Sox9 expressing precursors. Proceedings of the National Academy of Sciences of the United States of America **102**:14665-14670.

42. **Chen, Z. F. and R. R. Behringer**. 1995. Twist Is Required in Head Mesenchyme for Cranial Neural-Tube Morphogenesis. Genes & Development **9**:686-699.

43. **Sosic, D., J. A. Richardson, K. Yu, D. M. Ornitz, and E. N. Olson**. 2003. Twist regulates cytokine gene expression through a negative feedback loop that represses NF-kappa B activity. Cell **112**:169-180.

44. **Bourgeois, P., A. L. Bolcato-Bellemin, J. M. Danse, A. Bloch-Zupan, K. Yoshiba, C. Stoetzel, and F. Perrin-Schmitt**. 1998. The variable expressivity and incomplete penetrance of the twist-null heterozygous mouse phenotype resemble those of human Saethre-Chotzen syndrome. Human Molecular Genetics **7**:945-957.

45. **El Ghouzzi, V., M. LeMerrer, F. Perrinschmitt, E. Lajeunie, P. Benit, D. Renier, P. Bourgeois, A. L. BolcatoBellemin, A. Munnich, and J. Bonaventure**. 1997. Mutations of the TWIST gene in the Saethre-Chotzen syndrome. Nature Genetics **15**:42-46.

46. **Howard, T. D., W. A. Paznekas, E. D. Green, L. C. Chiang, N. Ma, R. I. O. Deluna, C. G. Delgado, M. GonzalezRamos, A. D. Kline, and E. W. Jabs**. 1997. Mutations in TWIST, a basic helix-loop-helix transcription factor, in Saethre-Chotzen syndrome. Nature Genetics **15**:36-41.

47. **Bialek, P., B. Kern, X. L. Yang, M. Schrock, D. Sosic, N. Hong, H. Wu, K. Yu, D. M. Ornitz, E. N. Olson, M. J. Justice, and G. Karsenty**. 2004. A twist code determines the onset of osteoblast differentiation. Developmental Cell **6**:423-435.

48. **Yang, X. G., K. Matsuda, P. Bialek, S. Jacquot, H. C. Masuoka, T. Schinke, L. Z. Li, S. Brancorsini, P. Sassone-Corsi, T. M. Townes, A. Hanauer, and G. Karsenty**. 2004. ATF4 is a substrate of RSK2 and an essential regulator of osteoblast biology: Implication for Coffin-Lowry syndrome. Cell **117**:387-398.

49. **Yang, X. L. and G. Karsenty**. 2004. ATF4, the osteoblast accumulation of which is determined post-translationally, can induce osteoblast-specific gene expression in non-osteoblastic cells. Journal of Biological Chemistry **279**:47109-47114.

50. **Cavaleri, F. and H. R. Scholer**. 2003. Nanog: A new recruit to the embryonic stem cell orchestra. Cell **113**:551-552.

51. **Keller, G.** 2005. Embryonic stem cell differentiation: emergence of a new era in biology and medicine. Genes & Development **19**:1129-1155.

52. **Smith, A. G.** 2001. Embryo-derived stem cells: Of mice and men. Annual Review of Cell and Developmental Biology **17**:435-462.

53. **Evans, M. J. and M. H. Kauffman**. 1981. Establishment in culture of pluripotent cells from the mouse embryo. Nature **292**:154-156.

54. **Friel, R., S. van der Sar, and P. J. Mee**. 2005. Embryonic stem cells: Understanding their history, cell biology and signalling. Advanced Drug Delivery Reviews **57**:1894-1903.

55. **Bradley, A., M. Evans, M. H. Kaufman, and E. Robertson**. 1984. Formation of Germ-Line Chimeras from Embryo-Derived Teratocarcinoma Cell-Lines. Nature **309**:255-256.

56. **Brook, F. A. and R. L. Gardner**. 1997. The origin and efficient derivation of embryonic stem cells in the mouse. Proceedings of the National Academy of Sciences of the United States of America **94**:5709-5712.

57. **Thomson, J. A., J. Itskovitz-Eldor, S. S. Shapiro, M. A. Waknitz, J. J. Swiergiel, V. S. Marshall, and J. M. Jones**. 1998. Embryonic stem cell lines derived from human blastocysts. Science **282**:1145-1147.

58. **Thomson, J. A. and V. S. Marshall**. 1998. Primate embryonic stem cells. Current Topics in Developmental Biology, Vol 38 **38**:133-165.

59. **Smith, A. G., J. K. Heath, D. D. Donaldson, G. G. Wong, J. Moreau, M. Stahl, and D. Rogers**. 1988. Inhibition of Pluripotential Embryonic Stem-Cell Differentiation by Purified Polypeptides. Nature **336**:688-690.

60. **Williams, R. L., D. J. Hilton, S. Pease, T. A. Willson, C. L. Stewart, D. P. Gearing, E. F. Wagner, D. Metcalf, N. A. Nicola, and N. M. Gough**. 1988. Myeloid-Leukemia Inhibitory Factor Maintains the Developmental Potential of Embryonic Stem-Cells. Nature **336**:684-687.

61. **Gough, N. M., R. L. Williams, D. J. Hilton, S. Pease, T. A. Willson, J. Stahl, D. P. Gearing, N. A. Nicola, and D. Metcalf**. 1989. Lif - A Molecule with Divergent Actions on Myeloid Leukemic-Cells and Embryonic Stem-Cells. Reproduction Fertility and Development **1**:281-288.

62. **Davis, S., T. H. Aldrich, N. Stahl, L. Pan, T. Taga, T. Kishimoto, N. Y. Ip, and G. D. Yancopoulos**. 1993. Lifr-Beta and Gp-130 As Heterodimerizing Signal Transducers of the Tripartite Cntf Receptor. Science **260**:1805-1808.

63. **Niwa, H., T. Burdon, I. Chambers, and A. Smith**. 1998. Self-renewal of pluripotent embryonic stem cells is mediated via activation of STAT3. Genes & Development **12**:2048-2060.

64. **Ying, Q. L., J. Nichols, I. Chambers, and A. Smith**. 2003. BMP induction of Id proteins suppresses differentiation and sustains embryonic stem cell self-renewal in collaboration with STAT3. Cell **115**:281-292.

65. **Boyer, L. A., D. Mathur, and R. Jaenisch**. 2006. Molecular control of pluripotency. Current Opinion in Genetics & Development **16**:455-462.

66. **Nichols, J., B. Zevnik, K. Anastassiadis, H. Niwa, D. Klewe-Nebenius, I. Chambers, H. Scholer, and A. Smith**. 1998. Formation of pluripotent stem cells in the mammalian embryo depends on the POU transcription factor Oct4. Cell **95**:379-391.

67. **Niwa, H.** 2001. Molecular mechanism to maintain stem cell renewal of ES cells. Cell Structure and Function **26**:137-148.

68. **Pesce, M. and H. R. Scholer**. 2001. Oct-4: Gatekeeper in the beginnings of mammalian development. Stem Cells **19**:271-278.

69. **Niwa, H., J. Miyazaki, and A. G. Smith**. 2000. Quantitative expression of Oct-3/4 defines differentiation, dedifferentiation or self-renewal of ES cells. Nature Genetics **24**:372-376.

70. **Avilion, A. A., S. K. Nicolis, L. H. Pevny, L. Perez, N. Vivian, and R. Lovell-Badge**. 2003. Multipotent cell lineages in early mouse development depend on SOX2 function. Genes & Development **17**:126-140.

71. **Chambers, I., D. Colby, M. Robertson, J. Nichols, S. Lee, S. Tweedie, and A. Smith**. 2003. Functional expression cloning of Nanog, a pluripotency sustaining factor in embryonic stem cells. Cell **113**:643-655.

72. **Mitsui, K., Y. Tokuzawa, H. Itoh, K. Segawa, M. Murakami, K. Takahashi, M. Maruyama, M. Maeda, and S. Yamanaka**. 2003. The homeoprotein Nanog is required for maintenance of pluripotency in mouse epiblast and ES cells. Cell **113**:631-642.

73. **Keller, G. M.** 1995. In-Vitro Differentiation of Embryonic Stem-Cells. Current Opinion in Cell Biology **7**:862-869.

74. **Nakano, T., H. Kodama, and T. Honjo**. 1994. Generation of Lymphohematopoietic Cells from Embryonic Stem-Cells in Culture. Science **265**:1098-1101.

75. **Nishikawa, S., S. Nishikawa, M. Hirashima, N. Matsuyoshi, and H. Kodama**. 1998. Progressive lineage analysis by cell sorting and culture identifies FLK1(+)VE-cadherin(+) cells at a diverging point of endothelial and hemopoietic lineages. Development **125**:1747-1757.

76. **Doss, M. X., C. I. Koehler, C. Gissel, J. Hescheler, and A. Sachinidis**. 2004. Embryonic stem cells: a promising tool for cell replacement therapy. Journal of Cellular and Molecular Medicine **8**:465-473.

77. **McNeish, J.** 2004. Embryonic stem cells in drug discovery. Nature Reviews Drug Discovery **3**:70-80.

78. **Vaananen, H. K.** 2005. Mesenchymal stem cells. Annals of Medicine **37**:469-479.

79. **Aubin, J. E. and J. T. Triffitt**. 2002. Mesenchymal Stem Cells and Osteoblast Differentiation, p. 59-81. *In* J. P. Bilezikian, L. G. Raisz, and G. A. Rodan (ed.), Principles of Bone Biology. Academic Press.

80. **Prockop, D. J.** 1997. Marrow stromal cells as stem cells for nonhematopoietic tissues. Science **276**:71-74.

81. **Friedenstein, A. J., R. K. Chailakhyan, and U. V. Gerasimov**. 1987. Bone-Marrow Osteogenic Stem-Cells - Invitro Cultivation and Transplantation in Diffusion-Chambers. Cell and Tissue Kinetics **20**:263-272.

82. **Stewart, K., P. Monk, S. Walsh, C. M. Jefferiss, J. Letchford, and J. N. Beresford**. 2003. Stro-1, Hop-26 (Cd63), Cd49A and Sb-10 (Cd166) As Markers of Primitive Human Marrow Stromal Cells and Their More Differentiated Progeny: A Comparative Investigation in Vitro. Cell and Tissue Research **313**:281-290.

83. **Stein, G. S., J. B. Lian, J. L. Stein, A. J. van Wijnen, B. Frenkel, and M. Montecino**. 1996. Mechanisms Regulating Osteoblast Proliferation and Differentiation, p. 69-86. *In* J. P. Bilezikian, L. G. Raisz, and G. A. Rodan (ed.), Principles of Bone Biology. Academic Press, San Diego.

84. **McCulloch, C. A. G., M. Struguresc**u, **F. Hughes, A. H. Melcher, and J. E. Aubin**. 1991. Osteogenic Progenitor Cells in Rat Bone-Marrow Stromal Populations Exhibit Self-Renewal in Culture. Blood **77**:1906-1911.

85. **Ecarotcharrier, B., F. H. Glorieux, M. Vanderrest, and G. Pereira**. 1983. Osteoblasts Isolated from Mouse Calvaria Initiate Matrix Mineralization in Culture. Journal of Cell Biology **96**:639-643.

86. **Bellows, C. G., J. E. Aubin, J. N. M. Heersche, and M. E. Antosz**. 1986. Mineralized Bone Nodules Formed in vitro from Enzymatically Released Rat Calvaria Cell-Populations. Calcified Tissue International **38**:143-154.

87. **Beresford, J. N., S. E. Graves, and C. A. Smoothy**. 1993. Formation of Mineralized Nodules by Bone Derived Cells-In vitro - A Model of Bone-Formation. American Journal of Medical Genetics **45**:163-178.

88. **Buttery, L. D. K., S. Bourne, J. D. Xynos, H. Wood, F. J. Hughes, S. P. F. Hughes, V. Episkopou, and J. M. Polak**. 2001. Differentiation of osteoblasts and in vitro bone formation from murine embryonic stem cells. Tissue Engineering **7**:89-99.

89. **zur Nieden, N. I., G. Kempka, and H. J. Ahr**. 2003. In vitro differentiation of embryonic stem cells into mineralized osteoblasts. Differentiation **71**:18-27.

90. **Kawaguchi, J., P. J. Mee, and A. G. Smith**. 2005. Osteogenic and chondrogenic differentiation of embryonic stem cells in response to specific growth factors. Bone **36**:758-769.

91. **Sottile, V., A. Thomson, and J. Mcwhir**. 2003. In vitro osteogenic differentiation of human ES cells. Cloning and Stem Cells **5**:149-155.

92. **Bielby, R. C., A. R. Boccaccini, J. M. Polak, and L. D. K. Buttery**. 2004. In vitro differentiation and in vivo mineralization of osteogenic cells derived from human embryonic stem cells. Tissue Engineering **10**:1518-1525.

93. **Karp, J. M., L. S. Ferreira, A. Khademhosseini, A. H. Kwon, J. Yeh, and R. S. Langer**. 2006. Cultivation of human embryonic stem cells without the embryoid body step enhances osteogenesis in vitro. Stem Cells **24**:835-843.

94. **Caplan, A. I. and S. P. Bruder**. 2001. Mesenchymal stem cells: building blocks for molecular medicine in the 21st century. Trends in Molecular Medicine **7**:259-264.

95. **Byers, B. A. and A. J. Garcia**. 2004. Exogenous Runx2 expression enhances in vitro osteoblastic differentiation and mineralization in primary bone marrow stromal cells. Tissue Engineering **10**:1623-1632.

96. **Byers, B. A., G. K. Pavlath, T. J. Murphy, G. Karsenty, and A. J. Garcia**. 2002. Cell-type-dependent up-regulation of in vitro mineralization after overexpression of the osteoblast-specific transcription factor Runx2/Cbfa1. Journal of Bone and Mineral Research **17**:1931-1944.

97. **Liu, W. G., S. Toyosawa, T. Furuichi, N. Kanatani, C. Yoshida, Y. Liu, M. Himeno, S. Narai, A. Yamaguchi, and T. Komori**. 2001. Overexpression of Cbfa1 in osteoblasts inhibits osteoblast maturation and causes osteopenia with multiple fractures. Journal of Cell Biology **155**:157-166.

98. **Geoffroy, V., M. Kneissel, B. Fournier, A. Boyde, and P. Matthias**. 2002. High bone resorption in adult aging Transgenic mice overexpressing Cbfa1/Runx2 in cells of the osteoblastic lineage. Molecular and Cellular Biology **22**:6222-6233.

99. **Tsuchiya, H., H. Kitoh, F. Sugiura, and N. Ishiguro**. 2003. Chondrogenesis enhanced by overexpression of sox9 gene in mouse bone marrow-derived mesenchymal stem cells. Biochemical and Biophysical Research Communications **301**:338-343.

100. **Kim, J. H., H. J. Do, H. M. Yang, J. H. Oh, S. J. Choi, D. K. Kim, K. Y. Cha, and H. M. Chung**. 2005. Overexpression of SOX9 in mouse embryonic stem cells directs the immediate chondrogenic commitment. Experimental and Molecular Medicine **37**:261-268.

101. www.informatics.jax.org . 2007.

102. **Oshima, A., H. Tanabe, T. Yan, G. N. Lowe, C. A. Glackin, and A. Kudo**. 2002. A novel mechanism for the regulation of osteoblast differentiation: Transcription of periostin, a member of the fasciclin I family, is regulated by the bHLH transcription factor, Twist. Journal of Cellular Biochemistry **86**:792-804.

103. **Satokata, I. and R. Maas**. 1994. Msx1 Deficient Mice Exhibit Cleft-Palate and Abnormalities of Craniofacial and Tooth Development. Nature Genetics **6**:348-356.

104. **Komori, T.** 2006. Regulation of osteoblast differentiation by transcription factors. Journal of Cellular Biochemistry **99**:1233-1239.

105. **Satokata, I., L. Ma, H. Ohshima, M. Bei, I. Woo, K. Nishizawa, T. Maeda, Y. Takano, M. Uchiyama, S. Heaney, H. Peters, Z. Q. Tang, R. Maxson, and R. Maas**. 2000. Msx2 deficiency in mice causes pleiotropic defects in bone growth and ectodermal organ formation. Nature Genetics **24**:391-395.

106. **Levi, G., P. Topilko, S. SchneiderMaunoury, M. Lasagna, S. Mantero, R. Cancedda, and P. Charnay**. 1996. Defective bone formation in Krox-20 mutant mice. Development **122**:113-120.

107. **Gollner, H., C. Dani, B. Phillips, S. Philipsen, and G. Suske**. 2001. Impaired ossification in mice lacking the transcription factor Sp3. Mechanisms of Development **106**:77-83.

108. **Doetschman, T. C., H. Eistetter, M. Katz, W. Schmidt, and R. Kemler**. 1985. The Invitro Development of Blastocyst-Derived Embryonic Stem-Cell Lines - Formation of Visceral Yolk-Sac, Blood Islands and Myocardium. Journal of Embryology and Experimental Morphology **87**:27-44.

109. **Nakano, T., H. Kodama, and T. Honjo**. 1996. In vitro development of primitive and definitive erythrocytes from different precursors. Science **272**:722-724.

110. **Wiles, M. V. and G. Keller**. 1991. Multiple Hematopoietic Lineages Develop from Embryonic Stem (Es) Cells in Culture. Development **111**:259-267.

111. **Potocnik, A. J., P. J. Nielsen, and K. Eichmann**. 1994. In-Vitro Generation of Lymphoid Precursors from Embryonic Stem-Cells. Embo Journal **13**:5274-5283.

112. **Tsai, M., J. Wedemeyer, S. Ganiatsas, S. Y. Tam, L. I. Zon, and S. J. Galli**. 2000. In vivo immunological function of mast cells derived from embryonic stem cells: An approach for the rapid analysis of even embryonic lethal mutations in adult mice in vivo. Proceedings of the National Academy of Sciences of the United States of America **97**:9186-9190.

113. **Fairchild, P. J., F. A. Brook, R. L. Gardner, L. Graca, V. Strong, Y. Tone, M. Tone, K. F. Nolan, and H. Waldmann**. 2000. Directed differentiation of dendritic cells from mouse embryonic stem cells. Current Biology **10**:1515-1518.

114. **Risau, W., H. Sariola, H. G. Zerwes, J. Sasse, P. Ekblom, R. Kemler, and T. Doetschman**. 1988. Vasculogenesis and Angiogenesis in Embryonic-Stem-Cell-Derived Embryoid Bodies. Development **102**:471-478.

115. **Yamashita, J., H. Itoh, M. Hirashima, M. Ogawa, S. Nishikawa, T. Yurugi, M. Naito, K. Nakao, and S. Nishikawa**. 2000. Flk1-positive cells derived from embryonic stem cells serve as vascular progenitors. Nature **408**:92-96.

116. **Maltsev, V. A., J. Rohwedel, J. Hescheler, and A. M. Wobus**. 1993. Embryonic Stem-Cells Differentiate In-Vitro Into Cardiomyocytes Representing Sinusnodal, Atrial and Ventricular Cell-Types. Mechanisms of Development **44**:41-50.

117. **Rohwedel, J., V. Maltsev, E. Bober, H. H. Arnold, J. Hescheler, and A. M. Wobus**. 1994. Muscle-Cell Differentiation of Embryonic Stem-Cells Reflects Myogenesis In-Vivo - Developmentally-Regulated Expression of Myogenic Determination Genes and Functional Expression of Ionic Currents. Developmental Biology **164**:87-101.

118. **Dani, C., A. G. Smith, S. Dessolin, P. Leroy, L. Staccini, P. Villageois, C. Darimont, and G. Ailhaud**. 1997. Differentiation of embryonic stem cells into adipocytes in vitro. Journal of Cell Science **110**:1279-1285.

119. **Kramer, J., C. Hegert, K. M. Guan, A. M. Wobus, P. K. Muller, and J. Rohwedel**. 2000. Embryonic stem cell-derived chondrogenic differentiation in vitro: activation by BMP-2 and BMP-4. Mechanisms of Development **92**:193-205.

120. **Bagutti, C., A. M. Wobus, R. Fassler, and F. M. Watt**. 1996. Differentiation of embryonal stem cells into keratinocytes: Comparison of wild-type and beta(1) integrin-deficient cells. Developmental Biology **179**:184-196.

121. **Bain, G., D. Kitchens, M. Yao, J. E. Huettner, and D. I. Gottlieb**. 1995. Embryonic Stem-Cells Express Neuronal Properties In-Vitro. Developmental Biology **168**:342-357.

122. **Strubing, C., G. Ahnerthilger, J. Shan, B. Wiedenmann, J. Hescheler, and A. M. Wobus**. 1995. Differentiation of Pluripotent Embryonic Stem-Cells Into the Neuronal Lineage In-Vitro Gives Rise to Mature Inhibitory and Excitatory Neurons. Mechanisms of Development **53**:275-287.

123. **Fraichard, A., O. Chassande, G. Bilbaut, C. Dehay, P. Savatier, and J. Samarut**. 1995. In-Vitro Differentiation of Embryonic Stem-Cells Into Glial-Cells and Functional-Neurons. Journal of Cell Science **108**:3181-3188.

124. **Brustle, O., K. N. Jones, R. D. Learish, K. Karram, K. Choudhary, O. D. Wiestler, I. D. Duncan, and R. D. G. Mckay**. 1999. Embryonic stem cell-derived glial precursors: A source of myelinating transplants. Science **285**:754-756.

125. **Liu, S., Y. Qu, T. J. Stewart, M. J. Howard, S. Chakrabortty, T. F. Holekamp, and J. W. McDonald**. 2000. Embryonic stem cells differentiate into

oligodendrocytes and myelinate in culture and after spinal cord transplantation. Proceedings of the National Academy of Sciences of the United States of America **97**:6126-6131.

126. **Magin, T. M., J. Mcwhir, and D. W. Melton**. 1992. A New Mouse Embryonic Stem-Cell Line with Good Germ Line Contribution and Gene Targeting Frequency. Nucleic Acids Research **20**:3795.

127. **Hooper, M., K. Hardy, A. Handyside, S. Hunter, and M. Monk**. 1987. Hprt-Deficient (Lesch-Nyhan) Mouse Embryos Derived from Germline Colonization by Cultured-Cells. Nature **326**:292-295.

128. **Bronson, S. K.** 2003. Bone nodule formation via in vitro differentiation of murine embryonic stem cells. Methods Enzymol. **365**:241-251.

129. **Woll, N. L. and S. K. Bronson**. 2006. Analysis of Embryonic Stem Cell-Derived Osteogenic Cultures, p. 149-160. *In* K. Turksen (ed.), Embryonic Stem Cells-II, Nonhuman ES cells, vol. 2. Humana Press, Totowa.

130. **Bronson, S. K., E. G. Plaehn, K. D. Kluckman, J. R. Hagaman, N. Maeda, and O. Smithies**. 1996. Single-copy transgenic mice with chosen-site integration. Proceedings of the National Academy of Sciences of the United States of America **93**:9067-9072.

131. **Gunning, P., J. Leavitt, G. Muscat, S. Y. Ng, and L. Kedes**. 1987. A Human Beta-Actin Expression Vector System Directs High-Level Accumulation of Antisense Transcripts. Proceedings of the National Academy of Sciences of the United States of America **84**:4831-4835.

132. **Misra, R., S. Bronson, Q. Xiao, W. Garrison, J. Li, R. Zhao, and S. Duncan**. 2001. Generation of single-copy transgenic mouse embryos directly from ES cells by tetraploid embryo complementation. BMC Biotechnol **1**.

133. **Heaney, J. D., A. N. Rettew, and S. K. Bronson**. 2004. Tissue-specific expression of a BAC transgene targeted to the Hprt locus in mouse embryonic stem cells. Genomics **83**:1072-1082.

134. **Velkey, J. M. and K. S. O'Shea**. 2003. Oct4 RNA interference induces trophectoderm differentiation in mouse embryonic stem cells. Genesis **37**:18-24.

135. **Pratap, J., A. Javed, L. R. Languino, A. J. van Wijnen, J. L. Stein, G. S. Stein, and J. B. Lian**. 2005. The Runx2 osteogenic transcription factor regulates matrix metalloproteinase 9 in bone metastatic cancer cells and controls cell invasion. Molecular and Cellular Biology **25**:8581-8591.

136. **Yang, J., S. A. Mani, J. L. Donaher, S. Ramaswamy, R. A. Itzykson, C. Come, P. Savagner, I. Gitelman, A. Richardson, and R. A. Weinberg**. 2004.

Twist, a master regulator of morphogenesis, plays an essential role in tumor metastasis. Cell **117**:927-939.

137. **Olsen, B. R., A. M. Reginato, and W. F. Wang**. 2000. Bone development. Annual Review of Cell and Developmental Biology **16**:191-220.

138. **McCulloch, C. A., M. Struguresc u, F. Hughes, A. H. Melcher, and J. E. Aubin**. 1991. Osteogenic progenitor cells in rat bone marrow stromal populations exhibit self-renewal in culture. Blood **77**:1906-1911.

139. **Schinke, T. and G. Karsenty**. 2002. Transcriptional control of osteoblast differentiation and function, p. 83-91. *In* J. P. Bilezikian, L. G. Raisz, and G. A. Rodan (ed.), Principles of Bone Biology. Academic Press, San Diego.

140. **Wozney, J. M. and V. Rosen**. 1998. Bone morphogenetic protein and bone morphogenetic protein gene family in bone formation and repair. Clinical Orthopaedics and Related Research. **346**:26-37.

141. **Centrella, M., V. Rosen, J. M. Wozney, S. R. Casinghino, and T. L. McCarthy**. 1997. Opposing effects by glucocorticoid and bone morphogenetic protein-2 in fetal rat and bone cell cultures. Journal of Cellular Biochemistry **67**:528-540.

142. **Seibel, M. J., R. Eastell, C. M. Gundberg, G. Hargus, and H. A. Pols**. 2002. Biochemical Markers of Bone Metabolism, p. 1543-1571. *In* J. P. Bilezikian, L. G. Raisz, and G. A. Rodan (ed.), Principles of Bone Biology, vol. 2. Academic Press.

143. **Preston, S. L., M. R. Alison, S. J. Forbes, N. C. Direkze, R. Poulsom, and N. A. Wright**. 2003. The new stem cell biology: something for everyone. Journal of Clinical Pathology-Molecular Pathology **56**:86-96.

144. **Shimko, D. A., C. A. Burks, K. C. Dee, and E. A. Nauman**. 2004. Comparison of in vitro mineralization by murine embryonic and adult stem cells cultured in an osteogenic medium. Tissue Engineering **10**:1386-1398.

145. **Hegert, C., J. Kramer, G. Hargus, J. Muller, K. Guan, A. M. Wobus, P. K. Muller, and J. Rohwedel**. 2002. Differentiation plasticity of chondrocytes derived from mouse embryonic stem cells. Journal of Cell Science **115**:4617-4628.

146. **Scholer, H. R., S. Ruppert, N. Suzuki, K. Chowdhury, and P. Gruss**. 1990. New Type of Pou Domain in Germ Line-Specific Protein Oct-4. Nature **344**:435-439.

147. **Scholer, H. R., G. R. Dressler, R. Balling, H. Rohdewohld, and P. Gruss**. 1990. Oct-4 - A Germline-Specific Transcription Factor Mapping to the Mouse T-Complex. Embo Journal **9**:2185-2195.

148. **Wilkinson, D. G., S. Bhatt, and B. G. Herrmann**. 1990. Expression Pattern of the Mouse T-Gene and Its Role in Mesoderm Formation. Nature **343**:657-659.

149. **Lendahl, U., L. B. Zimmerman, and R. D. G. Mckay**. 1990. CNS Stem-Cells Express A New Class of Intermediate Filament Protein. Cell **60**:585-595.

150. **Zimmerman, L., U. Lendahl, M. Cunningham, R. Mckay, B. Parr, B. Gavin, J. Mann, G. Vassileva, and A. Mcmahon**. 1994. Independent Regulatory Elements in the Nestin Gene Direct Transgene Expression to Neural Stem-Cells Or Muscle Precursors. Neuron **12**:11-24.

151. **Sutton, J., R. Costa, M. Klug, L. Field, D. W. Xu, D. A. Largaespada, C. F. Fletcher, N. A. Jenkins, N. G. Copeland, M. Klemsz, and R. Hromas**. 1996. Genesis, a winged helix transcriptional repressor with expression restricted to embryonic stem cells. Journal of Biological Chemistry **271**:23126-23133.

152. **Hromas, R., H. G. Ye, M. Spinella, E. Dmitrovsky, D. W. Xu, and R. H. Costa**. 1999. Genesis, a Winged Helix transcriptional repressor, has embryonic expression limited to the neural crest, and stimulates proliferation in vitro in a neural development model. Cell and Tissue Research **297**:371-382.

153. **Dottori, M., M. K. Gross, P. Labosky, and M. Goulding**. 2001. The winged-helix transcription factor Foxd3 suppresses interneuron differentiation and promotes neural crest cell fate. Development **128**:4127-4138.

154. **Mori-Akiyama, Y., H. Akiyama, D. H. Rowitch, and B. de Crombrugghe**. 2003. Sox9 is required for determination of the chondrogenic cell lineage in the cranial neural crest. Proceedings of the National Academy of Sciences of the United States of America **100**:9360-9365.

155. **Rossert, J. and B. de Crombrugghe**. 2002. Type I collagen, p. 189-209. *In* J. P. Bilezikian, L. G. Raisz, and G. A. Rodan (ed.), Principles of Bone Biology. Academic Press, San Diego.

156. **Kirchgessner, T. G., K. L. Svenson, A. J. Lusis, and M. C. Schotz**. 1987. The Sequence of Cdna-Encoding Lipoprotein-Lipase - A Member of A Lipase Gene Family. Journal of Biological Chemistry **262**:8463-8466.

157. **Huntington, N. D. and D. M. Tarlinton**. 2004. CD45: direct and indirect government of immune regulation. Immunology Letters **94**:167-174.

158. **Elima, K., I. Eerola, R. Rosati, M. Metsaranta, S. Garofalo, M. Perala, B. Decrombrugghe, and E. Vuorio**. 1993. The Mouse Collagen-X Gene - Complete

Nucleotide-Sequence, Exon Structure and Expression Pattern. Biochemical Journal **289**:247-253.

159. **Albelda, S. M., P. D. Oliver, L. H. Romer, and C. A. Buck**. 1990. Endocam - A Novel Endothelial-Cell Cell-Adhesion Molecule. Journal of Cell Biology **110**:1227-1237.

160. **Albelda, S. M., W. A. Muller, C. A. Buck, and P. J. Newman**. 1991. Molecular and Cellular Properties of Pecam-1 (Endocam/Cd31) - A Novel Vascular Cell Cell-Adhesion Molecule. Journal of Cell Biology **114**:1059-1068.

161. **Toyosawa, S., S. Shintani, T. Fujiwara, T. Ooshima, A. Sato, N. Ijuhin, and T. Komori**. 2001. Dentin matrix protein 1 is predominantly expressed in chicken and rat osteocytes but not in osteoblasts. Journal of Bone and Mineral Research **16**:2017-2026.

162. **Kiani, C., L. Chen, Y. J. Wu, A. J. Yee, and B. B. Yang**. 2002. Structure and function of aggrecan. Cell Research **12**:19-32.

163. **McAlinden, A., N. Havlioglu, L. Liang, S. R. Davies, and L. J. Sandell**. 2005. Alternative splicing of type II procollagen Exon 2 is regulated by the combination of a weak 5 ' splice site and an adjacent intronic stem-loop Cis element. Journal of Biological Chemistry **280**:32700-32711.

164. **Jones, E. A., S. E. Kinsey, A. English, R. A. Jones, L. Straszynski, D. M. Meredith, A. F. Markham, A. Jack, P. Emery, and D. McGonagle**. 2002. Isolation and characterization of bone marrow multipotential mesenchymal progenitor cells. Arthritis and Rheumatism **46**:3349-3360.

165. **Wolf, C., C. Thisse, C. Stoetzel, B. Thisse, P. Gerlinger, and F. Perrinschmitt**. 1991. The M-Twist Gene of Mus Is Expressed in Subsets of Mesodermal Cells and Is Closely Related to the Xenopus X-Twi and the Drosophila-Twist Genes. Developmental Biology **143**:363-373.

166. **Li, L., P. Cserjesi, and E. N. Olson**. 1995. Dermo-1 - A Novel Twist-Related Bhlh Protein Expressed in the Developing Dermis. Developmental Biology **172**:280-292.

167. **Zelzer, E., W. McLean, Y. S. Ng, N. Fulkai, A. M. Reginato, S. Lovejoy, P. A. D'Amore, and B. R. Olsen**. 2002. Skeletal defects in VEGF(120/120) mice reveal multiple roles for VEGF in skeletogenesis. Development **129**:1893-1904.

168. **Phillips, B. W., N. Belmonte, C. Vernochet, G. Ailhaud, and C. Dani**. 2001. Compactin enhances osteogenesis in murine embryonic stem cells. Biochemical and Biophysical Research Communications **284**:478-484.

169. **Woll, N. L., J. D. Heaney, and S. K. Bronson**. 2006. Osteogenic Nodule Formation From Single Embryonic Stem Cell-Derived Progenitors. Stem Cells and Development **15**:865-879.

170. **Chen, D., M. Zhao, and G. R. Mundy**. 2004. Bone morphogenetic proteins. Growth Factors **22**:233-241.

171. **Wozney, J. M.** 1992. The Bone Morphogenetic Protein Family and Osteogenesis. Molecular Reproduction and Development **32**:160-167.

172. **Urist, M. R.** 1965. Bone - Formation by Autoinduction. Science **150**:893-899.

173. **Wozney, J. M., V. Rosen, A. J. Celeste, L. M. Mitsock, M. J. Whitters, R. W. Kriz, R. M. Hewick, and E. A. Wang**. 1988. Novel Regulators of Bone-Formation - Molecular Clones and Activities. Science **242**:1528-1534.

174. **Luyten, F. P., N. S. Cunningham, S. Ma, N. Muthukumaran, R. G. Hammonds, W. B. Nevins, W. I. Wood, and A. H. Reddi**. 1989. Purification and Partial Amino-Acid Sequence of Osteogenin, A Protein Initiating Bone Differentiation. Journal of Biological Chemistry **264**:13377-13380.

175. **Wang, E. A., V. Rosen, J. S. Dalessandro, M. Bauduy, P. Cordes, T. Harada, D. I. Israel, R. M. Hewick, K. M. Kerns, P. Lapan, D. P. Luxenberg, D. Mcquaid, I. K. Moutsatsos, J. Nove, and J. M. Wozney**. 1990. Recombinant Human Bone Morphogenetic Protein Induces Bone-Formation. Proceedings of the National Academy of Sciences of the United States of America **87**:2220-2224.

176. **Lee, M. H., A. Javed, H. J. Kim, H. I. Shin, S. Gutierrez, J. Y. Choi, V. Rosen, J. L. Stein, A. J. van Wijnen, G. S. Stein, J. B. Lian, and H. M. Ryoo**. 1999. Transient upregulation of CBFA1 in response to bone morphogenetic protein-2 and transforming growth factor beta 1 in C2C12 myogenic cells coincides with suppression of the myogenic phenotype but is not sufficient for osteoblast differentiation. Journal of Cellular Biochemistry **73**:114-125.

177. **Lee, K. S., H. J. Kim, Q. L. Li, X. Z. Chi, C. Ueta, T. Komori, J. M. Wozney, E. G. Kim, J. Y. Choi, H. M. Ryoo, and S. C. Bae**. 2000. Runx2 is a common target of transforming growth factor beta 1 and bone morphogenetic protein 2, and cooperation between Runx2 and Smad5 induces osteoblast-specific gene expression in the pluripotent mesenchymal precursor cell line C2C12. Molecular and Cellular Biology **20**:8783-8792.

178. **Phimphilai, M., Z. R. Zhoa, H. Boules, H. Roca, and R. T. Franceschi**. 2006. BMP signaling is required for RUNX2-dependent induction of the osteoblast phenotype. Journal of Bone and Mineral Research **21**:637-646.

179. **Lee, M. H., Y. J. Kim, H. J. Kim, H. D. Park, A. R. Kang, H. M. Kyung, J. H. Sung, J. M. Wozney, H. J. Kim, and H. M. Ryoo**. 2003. BMP-2-induced Runx2

expression is mediated by Dlx5, and TGF-beta 1 opposes the BMP-2-induced osteoblast differentiation by suppression of Dlx5 expression. Journal of Biological Chemistry **278**:34387-34394.

180. **Ryoo, H. M., M. H. Lee, and Y. J. Kim**. 2006. Critical molecular switches involved in BMP-2-induced osteogenic differentiation of mesenchymal cells. Gene **366**:51-57.

181. **Ryoo, H. M., H. M. Hoffmann, B. Frenkel, A. vanWijnen, T. Beumer, J. L. Stein, G. S. Stein, and J. B. Lian**. 1996. Stage specific expression of DLX-5 during osteoblast differentiation and its role in osteocalcin gene expression. Journal of Bone and Mineral Research **11**:152.

182. **Acampora, D., G. R. Merlo, L. Paleari, B. Zerega, M. P. Postiglione, S. Mantero, E. Bober, O. Barbieri, A. Simeone, and G. Levi**. 1999. Craniofacial, vestibular and bone defects in mice lacking the Distal-less-related gene Dlx5. Development **126**:3795-3809.

183. **Lee, M. H., Y. J. Kim, W. J. Yoon, J. I. Kim, B. G. Kim, Y. S. Hwang, J. M. Wozney, X. Z. Chi, S. C. Bae, K. Y. Choi, J. Y. Cho, J. Y. Choi, and H. M. Ryoo**. 2005. Dlx5 specifically regulates Runx2 type II expression by binding to homeodomain-response elements in the Runx2 distal promoter. Journal of Biological Chemistry **280**:35579-35587.

184. **Byers, B. A., R. E. Guldberg, and A. J. Garcia**. 2004. Synergy between genetic and tissue engineering: Runx2 overexpression and in vitro construct development enhance in vivo mineralization. Tissue Engineering **10**:1757-1766.

185. **Zhang, X., M. Yang, L. Lin, P. Chen, K. T. Ma, C. Y. Zhou, and Y. F. Ao**. 2006. Runx2 overexpression enhances osteoblastic differentiation and mineralization in adipose - derived stem cells in vitro and in vivo. Calcified Tissue International **79**:169-178.

186. **Gersbach, C. A., J. M. Le Doux, R. E. Guldberg, and A. J. Garcia**. 2006. Inducible regulation of Runx2-stimulated osteogenesis. Gene Therapy **13**:873-882.

187. **Goverdhana, S., M. Puntel, W. Xiong, J. M. Zirger, C. Barcia, J. F. Curtin, E. B. Soffer, S. Mondkar, G. D. King, J. Hu, S. A. Sciascia, M. Candolfi, D. S. Greengold, P. R. Lowenstein, and M. G. Castro**. 2005. Regulatable gene expression systems for gene therapy applications: Progress and future challenges. Molecular Therapy **12**:189-211.

188. **Gossen, M. and H. Bujard**. 1992. Tight Control of Gene-Expression in Mammalian-Cells by Tetracycline-Responsive Promoters. Proceedings of the National Academy of Sciences of the United States of America **89**:5547-5551.

189. **Gossen, M., S. Freundlieb, G. Bender, G. Muller, W. Hillen, and H. Bujard**. 1995. Transcriptional Activation by Tetracyclines in Mammalian-Cells. Science **268**:1766-1769.

190. **Mizuguchi, H. and T. Hayakawa**. 2002. The tet-off system is more effective than the tet-on system for regulating transgene expression in a single adenovirus vector. Journal of Gene Medicine **4**:240-247.

191. **Wilson, C., H. J. Bellen, and W. J. Gehring**. 1990. Position Effects on Eukaryotic Gene-Expression. Annual Review of Cell Biology **6**:679-714.

192. **Lloyd, V. K., D. Dyment, D. A. R. Sinclair, and T. A. Grigliatti**. 2003. Different patterns of gene silencing in position-effect variegation. Genome **46**:1104-1117.

193. **Muller, H. J.** 1930. Types of visible variations induced by x-rays in Drosophila. Journal of Genetics **22**:299-2U7.

194. **Dillon, N. and R. Festenstein**. 2002. Unravelling heterochromatin: competition between positive and negative factors regulates accessibility. Trends in Genetics **18**:252-258.

195. **Kioussis, D. and R. Festenstein**. 1997. Locus control regions: overcoming heterochromatin-induced gene inactivation in mammals. Current Opinion in Genetics & Development **7**:614-619.

196. **Grosveld, F., G. B. Vanassendelft, D. R. Greaves, and G. Kollias**. 1987. Position-Independent, High-Level Expression of the Human Beta-Globin Gene in Transgenic Mice. Cell **51**:975-985.

197. **Greaves, D. R., F. D. Wilson, G. Lang, and D. Kioussis**. 1989. Human Cd2 3'-Flanking Sequences Confer High-Level, T-Cell-Specific, Position-Independent Gene-Expression in Transgenic Mice. Cell **56**:979-986.

198. **Garrick, D., S. Fiering, D. I. K. Martin, and E. Whitelaw**. 1998. Repeat-induced gene silencing in mammals. Nature Genetics **18**:56-59.

199. **Kim, S. H., J. C. Moores, D. David, J. G. Respess, D. J. Jolly, and T. Friedmann**. 1986. The Organization of the Human Hprt Gene. Nucleic Acids Research **14**:3103-3118.

200. **Balk, M. L., J. Bray, C. Day, M. Epperly, J. Greenberger, C. H. Evans, and C. Niyibizi**. 1997. Effect of rhBMP-2 on the osteogenic potential of bone marrow stromal cells from an osteogenesis imperfecta mouse (oim). Bone **21**:7-15.

201. **Shea, C. M., C. M. Edgar, T. A. Einhorn, and L. C. Gerstenfeld**. 2003. BMP treatment of C3H10T1/2 mesenchymal stem cells induces both chondrogenesis and osteogenesis. Journal of Cellular Biochemistry **90**:1112-1127.

202. **zur Nieden, N. I., G. Kempka, D. E. Rancourt, and H. J. Ahr**. 2005. Induction of chondro-, osteo- and adipogenesis in embryonic stem cells by bone morphogenetic protein-2: Effect of cofactors on differentiating lineages. Bmc Developmental Biology **5**.

203. **Urlinger, S., U. Baron, M. Thellmann, M. T. Hasan, H. Bujard, and W. Hillen**. 2000. Exploring the sequence space for tetracycline-dependent transcriptional activators: Novel mutations yield expanded range and sensitivity. Proceedings of the National Academy of Sciences of the United States of America **97**:7963-7968.

204. **Agrawal, N., P. V. N. Dasaradhi, A. Mohmmed, P. Malhotra, R. K. Bhatnagar, and S. K. Mukherjee**. 2003. RNA interference: Biology, mechanism, and applications. Microbiology and Molecular Biology Reviews **67**:657-685.

205. **Sharp, P. A.** 1999. RNAi and double-stranded RNA. Genes & Development **13**:139-141.

206. **Zou, G. M. and M. C. Yoder**. 2005. Application of RNA interference to study stem cell function: current status and future perspectives. Biology of the Cell **97**:211-219.

207. **Fire, A., S. Q. Xu, M. K. Montgomery, S. A. Kostas, S. E. Driver, and C. C. Mello**. 1998. Potent and specific genetic interference by double-stranded RNA in Caenorhabditis elegans. Nature **391**:806-811.

208. www.nobelprize.org . 2007.

209. **Fjose, A. and O. Drivenes**. 2006. RNAi and MicroRNAs: From Animal Models to Disease Therapy. Birth Defects Research (Part C) **78**:150-171.

210. **Lee, R. C., R. L. Feinbaum, and V. Ambros**. 1993. The C-Elegans Heterochronic Gene Lin-4 Encodes Small Rnas with Antisense Complementarity to Lin-14. Cell **75**:843-854.

211. **Wightman, B., I. Ha, and G. Ruvkun**. 1993. Posttranscriptional Regulation of the Heterochronic Gene Lin-14 by Lin-4 Mediates Temporal Pattern-Formation in C-Elegans. Cell **75**:855-862.

212. **Reinhart, B. J., F. J. Slack, M. Basson, A. E. Pasquinelli, J. C. Bettinger, A. E. Rougvie, H. R. Horvitz, and G. Ruvkun**. 2000. The 21-nucleotide let-7 RNA regulates developmental timing in Caenorhabditis elegans. Nature **403**:901-906.

213. **Ketting, R. F., S. E. J. Fischer, E. Bernstein, T. Sijen, G. J. Hannon, and R. H. A. Plasterk**. 2001. Dicer functions in RNA interference and in synthesis of

small RNA involved in developmental timing in C-elegans. Genes & Development **15**:2654-2659.

214. **Knight, S. W. and B. L. Bass**. 2001. A role for the RNase III enzyme DCR-1 in RNA interference and germ line development in Caenorhabditis elegans. Science **293**:2269-2271.

215. **Du, T. T. and P. D. Zamore**. 2005. microPrimer: The biogenesis and function of microRNA. Development **132**:4645-4652.

216. **Humphreys, D. T., B. J. Westman, D. I. K. Martin, and T. Preiss**. 2005. MicroRNAs control translation initiation by inhibiting eukaryotic initiation factor 4E/cap and poly(A) tail function. Proceedings of the National Academy of Sciences of the United States of America **102**:16961-16966.

217. **Pillai, R. S., S. N. Bhattacharyya, C. G. Artus, T. Zoller, N. Cougot, E. Basyuk, E. Bertrand, and W. Filipowicz**. 2005. Inhibition of translational initiation by Let-7 microRNA in human cells. Science **309**:1573-1576.

218. **Sheth, U. and R. Parker**. 2003. Decapping and decay of messenger RNA occur in cytoplasmic processing bodies. Science **300**:805-808.

219. **Hammond, S. M.** 2006. MicroRNAs as oncogenes. Current Opinion in Genetics & Development **16**:4-9.

220. **McManus, M. T. and P. A. Sharp**. 2002. Gene silencing in mammals by small interfering RNAs. Nature Reviews Genetics **3**:737-747.

221. **Elbashir, S. M., W. Lendeckel, and T. Tuschl**. 2001. RNA interference is mediated by 21-and 22-nucleotide RNAs. Genes & Development **15**:188-200.

222. **Yang, D., H. Lu, and J. W. Erickson**. 2000. Evidence that processed small dsRNAs may mediate sequence-specific mRNA degradation during RNAi in Drosophila embryos. Current Biology **10**:1191-1200.

223. **Elbashir, S. M., J. Martinez, A. Patkaniowska, W. Lendeckel, and T. Tuschl**. 2001. Functional anatomy of siRNAs for mediating efficient RNAi in Drosophila melanogaster embryo lysate. Embo Journal **20**:6877-6888.

224. **Donze, O. and D. Picard**. 2002. RNA interference in mammalian cells using siRNAs synthesized with T7 RNA polymerase. Nucleic Acids Research **30**.

225. **Hillen, W. and C. Berens**. 1994. Mechanisms Underlying Expression of Tn10 Encoded Tetracycline Resistance. Annual Review of Microbiology **48**:345-369.

226. www.oligoengine.com . 2007.

227. **Yao, F., T. Svensjo, T. Winkler, M. Lu, C. Eriksson, and E. Eriksson**. 1998. Tetracycline repressor, tetR, rather than the tetR-mammalian cell transcription factor fusion derivatives, regulates inducible gene expression in mammalian cells. Human Gene Therapy **9**:1939-1950.

228. **Postle, K., T. T. Nguyen, and K. P. Bertrand**. 1984. Nucleotide-Sequence of the Repressor Gene of the Tn10 Tetracycline Resistance Determinant. Nucleic Acids Research **12**:4849-4863.

229. www.invitrogen.com . 2007.

230. **Velkey, J. M. and K. S. O'Shea**. 2003. Oct4 RNA interference induces trophectoderm differentiation in mouse embryonic stem cells. Genesis **37**:18-24.

231. **Banerjee, C., L. R. Mccabe, J. Y. Choi, S. W. Hiebert, J. L. Stein, G. S. Stein, and J. B. Lian**. 1997. Runt homology domain proteins in osteoblast differentiation: AML3/CBFA1 is a major component of a bone-specific complex. Journal of Cellular Biochemistry **66**:1-8.

232. **Zheng, G. D., K. Hidaka, and T. Morisaki**. 2005. Stable and uniform gene suppression by site-specific integration of siRNA expression cassette in murine embryonic stem cells. Stem Cells **23**:1028-1034.

233. **Seibler, J., B. Kuter-Luks, H. Kern, S. Streu, L. Plum, J. Mauer, R. Kuhn, J. C. Bruning, and F. Schwenk**. 2005. Single copy shRNA configuration for ubiquitous gene knockdown in mice. Nucleic Acids Research **33**.

234. www.ambion.com . 2007.

235. **Niwa, H., K. Yamamura, and J. Miyazaki**. 1991. Efficient Selection for High-Expression Transfectants with A Novel Eukaryotic Vector. Gene **108**:193-199.

236. www.oif.org . 2007.

237. **Prockop, D. J., A. Colige, H. Helminen, J. S. Khillan, R. Pereira, and P. Vandenberg**. 1993. Mutations in Type-1 Procollagen That Cause Osteogenesis Imperfecta - Effects of the Mutations on the Assembly of Collagen Into Fibrils, the Basis of Phenotypic Variations, and Potential Antisense Therapies. Journal of Bone and Mineral Research **8**:S489-S492.

238. **Niyibizi, C., S. Wang, Z. Mi, and P. D. Robbins**. 2004. Gene therapy approaches for osteogenesis imperfecta. Gene Therapy **11**:408-416.

239. **Glorieux, F. H., N. J. Bishop, H. Plotkin, G. Chabot, G. Lanoue, and R. Travers**. 1998. Cyclic administration of pamidronate in children with severe osteogenesis imperfecta. New England Journal of Medicine **339**:947-952.

240. **Goksen, D., M. Coker, S. Darcan, T. Kose, and S. Kara**. 2006. Low-dose intravenous pamidronate treatment in osteogenesis imperfecta. Turkish Journal of Pediatrics **48**:124-129.

241. **Land, C., F. Rauch, K. Montpetit, J. Ruck-Gibis, and F. H. Glorieux**. 2006. Effect of intravenous pamidronate therapy on functional abilities and level of ambulation in children with osteogenesis imperfecta. Journal of Pediatrics **148**:456-460.

242. **Munns, C. F. J., F. Rauch, R. Travers, and F. H. Glorieux**. 2005. Effects of intravenous pamidronate treatment in infants with osteogenesis imperfecta: Clinical and histomorphometric outcome. Journal of Bone and Mineral Research **20**:1235-1243.

243. **Zacharin, M. and S. Kanumakala**. 2004. Pamidronate treatment of less severe forms of osteogenesis imperfecta in children. Journal of Pediatric Endocrinology & Metabolism **17**:1511-1517.

244. **Plotkin, H., F. Rauch, N. J. Bishop, K. Montpetit, J. Ruck-Gibis, R. Travers, and F. H. Glorieux**. 2000. Pamidronate treatment of severe osteogenesis imperfecta in children under 3 years of age. Journal of Clinical Endocrinology and Metabolism **85**:1846-1850.

245. **Horwitz, E. M., D. J. Prockop, L. A. Fitzpatrick, W. W. K. Koo, P. L. Gordon, M. Neel, M. Sussman, P. Orchard, J. C. Marx, R. E. Pyeritz, and M. K. Brenner**. 1999. Transplantability and therapeutic effects of bone marrow-derived mesenchymal cells in children with osteogenesis imperfecta. Nature Medicine **5**:309-313.

246. **Horwitz, E. M., D. J. Prockop, P. L. Gordon, W. W. K. Koo, L. A. Fitzpatrick, M. D. Neel, M. E. McCarville, P. J. Orchard, R. E. Pyeritz, and M. K. Brenner**. 2001. Clinical responses to bone marrow transplantation in children with severe osteogenesis imperfecta. Blood **97**:1227-1231.

247. **Horwitz, E. M., P. L. Gordon, W. K. K. Koo, J. C. Marx, M. D. Neel, R. Y. Mcnall, L. Muul, and T. Hofmann**. 2002. Isolated allogeneic bone marrow-derived mesenchymal cells engraft and stimulate growth in children with osteogenesis imperfecta: Implications for cell therapy of bone. Proceedings of the National Academy of Sciences of the United States of America **99**:8932-8937.

248. **Giordano, A., U. Galderisi, and I. Marino**. 2007. From the Laboratory Bench to the Patient's Bedside: An Update on Clinical Trials With Mesenchymal Stem Cells. Journal of Cellular Physiology **211**:27-35.

249. **Baksh, D., L. Song, and R. S. Tuan**. 2004. Adult mesenchymal stem cells: characterization, differentiation, and application in cell and gene therapy. Journal of Cellular and Molecular Medicine **8**:301-316.

250. **Hicok, K. C., T. V. Du Laney, Y. S. Zhou, Y. D. C. Halvorsen, D. C. Hitt, L. F. Cooper, and J. M. Gimble**. 2004. Human adipose-derived adult stem cells produce osteoid in vivo. Tissue Engineering **10**:371-380.

Curriculum Vitae
Nicole Leanor Woll

BORN:

August 30, 1978 – Danville, Pennsylvania

EDUCATION:

2001-2007
The Pennsylvania State University
College of Medicine
Intercollege Graduate Degree Program in Genetics
Ph.D. in Genetics expected May 2007

1996-2000
Bucknell University
B.Sc. in Biology – May 2000
Minor in Spanish – May 2000

AWARDS AND SCHOLARSHIPS:

2002-2006	NIH R01 Supplement for Underrepresented Minorities
2005	FASEB MARC Program Travel Award, The American Society for Bone and Mineral Research, Nashville Tennessee
2005	NIH Travel Scholarship, Keystone Symposia Molecular Regulation of Stem Cells, Banff Canada
2004	Graduate Alumni Endowment Scholarship
2001-2002, 2004-2005	Bunton Waller Graduate Award, The Pennsylvania State University
1998	David Burpee Foundation Grant, Bucknell University

PROFESSIONAL EXPERIENCE:

1999-2000
Bucknell University, Undergraduate Teaching Assistant
Human Physiology, Population and Community Biology

1999
The Sigfried and Janet Weis Center for Research, Research Assistant
David Carey, Ph.D.

1998
Bucknell University, Laboratory Technician
Richard Ellis, Ph.D.

PUBLICATIONS:

1. **Woll, NL**, Bronson, SK. Analysis of Embryonic Stem Cell-Derived Osteogenic Cultures. Methods Mol. Biol. 330, 149-159 (2006).
2. **Woll, NL**, Heaney, JD, Bronson, SK. Osteogenic Nodule Formation from Single Embryonic Stem Cell-Derived Progenitors. Stem Cells and Development 15(6), 865-879 (2006).